The functional analysis of Upf1 in S-phase progression and genome stability

David Turton

Thesis submitted for the Degree

of Doctor of Philosophy at the

Department of Biomedical Science,

University of Sheffield

January 2014

This thesis is dedicated to my parents,

for giving me so much.

Table of contents

List of figures

List of tables

Abbreviations

3-AT	3-Amino-1,2,4-triazole
AAA	Upf1 amino acids T28/S1096/S1116 mutated to alanine
APS	Ammonium persulphate
ATM	Ataxia-telangiectasia mutated
ATP	Adenosine triphosphate
ATPase	Adenosine triphosphatase
ATR	ATM and Rad3 related
BSA	Bovine serum albumin
CBC	Cap binding complex CBP80-20
cDNA	Complementary DNA
CH domain	Upf1 domain required for interaction with Upf2
CK2	Casein kinase 2
DAPI	4',6-Diamidino-2-Phenylindole, Dihydrochloride
DECID	Decay inducing complex
ddH_2O	Double distilled water
DMEM	Dulbecco's minimum essential medium
DMSO	Dimethyl sulphoxide
DNA	Deoxyribonucleic acid
DNA-PK	DNA-dependent protein kinase
DTT	Dithiothreitol
ECL	Enhanced chemiluminescence

EDTA	Ethylenediaminetetraacetic acid
eGFP	Enhanced green fluorescent protein
EGTA	Ethylene glycol tetraacetic acid
eIF4E	Eukaryotic initiation factor 4E
EJC	Exon junction complex
FBS	Fetal bovine serum
FISH	Fluorescent *in situ* hybridisation
GFP	Green fluorescent protein
HBP/SLBP	Hairpin-binding protein/Stem-loop binding protein
HD	Replication dependent histone mRNA decay pathway
HEPES	4-(2-hydroxyethyl)-1-piperazineethanesulfonic acid
HU	Hydroxyurea
IgG	Immunoglobulin G
kDa	Dalton
LB	Luria-Bertani
lncRNA	Long non-coding RNA
MMS	Methyl methanesulfonate
mRNA	Messenger RNA
mRNP	Messenger ribonucleoprotein
NMD	Nonsense mediated mRNA decay
ONPG	*ortho*-Nitrophenyl-β-galactoside
ORC2	Origin recognition complex subunit 2
p50	DNA polymerase δ p50 subunit

p66	DNA polymerase δ p66 subunit
p125	DNA polymerase δ p125 subunit
PBS	Phosphate-buffered saline
PCNA	Proliferating cell nuclear antigen
PIKK	Phosphatidylinositol 3-kinase-related kinases
PMSF	Phenylmethanesulfonylfluoride
PNA	Protein nucleic acid
polδ	DNA polymerase δ
polε	DNA polymerase ε
PP2A	Protein phosphatase 2A
PRD	Proline/glycine rich domain in the Upf1 N-terminus
PTC	Premature termination codon
Rent-1	Regulator of nonsense transcripts 1
RNA	Ribonucleic acid
RPA	Replication protein A
S42	Upf1 amino acid - serine 42
SDS	Sodium dodecyl sulphate
SDS-PAGE	Sodium dodecyl sulphate poly acrylamide gel electrophoresis
siRNA	Small interfering RNA
SMD	Staufen mediated mRNA decay
SMG (1-9)	Suppressor with morphogenetic effects on genitalia (1-9)
SOC	Super optimal broth with catabolite repression
SQ domain	Upf1 C-terminal S/T-Q motif rich region

ssDNA	Single-stranded DNA
ssRNA	Single-stranded RNA
SURF	SMG1:Upf1:eRF1-3 complex
T28	Upf1 amino acid – threonine 28
TBS	Tris-buffered saline
TEMED	1,2-bis (dimethylamino)-ethane
TERRA	Telomeric repeat-containing RNA
TFE	Telomere free end
Upf (1-3)	Up-frameshift suppressor (1-3)
UTR	Untranslated region
YPD	Yeast Extract Peptone Dextrose media
γH2AX	Phosphorylated histone 2AX

Acknowledgements

I would like to deeply thank my supervisor Professor Carl Smythe for his outstanding guidance and support, his trust in my abilities and gifting me the freedom to pursue my own research. I also thank him for his patience, belief in me and reassurances during times when it was much needed.

This thesis would also have not been possible without funding from the MRC, and I am grateful to my advisors Professor Steve Winder and Professor Walter Marcotti for their critical thinking and valuable feedback.

For providing me with insight and technical experience, I would like to thank all the past and present members of the Smythe lab for their invaluable advice and work discussions. I particularly thank Dr Richard Beniston, not only for his Upf1 phosphorylation studies, but for taking the time to teach me many of the skills I now possess. I would also like to thank the Ayscough lab, Dr Emma Warbrick, Professor Joachim Lingner, Dr Lynne Maquat and Dr Helen Bryant for providing reagents. For assistance in setting up the Fluorescent *In situ* hybridisation (FISH) experiments, I thank Dr Polly Talley at the Sheffield Children's Hospital Cytogenetics Unit and Dr Darren Robinson in the Light Microscope Facility for their generosity and expertise.

Finally it is a pleasure to unreservedly thank my parents, John and Julie, for blessing me with so many opportunities, for their unfailing encouragement and for supporting me always. I am eternally grateful to Bridie for her unconditional support, understanding and love. Thank you to my family for their belief in me and a special mention to my nephews, for all the fun, smiles and colouring-in that helped to keep me sane.

Summary

Upf1 is an RNA helicase discovered as a component in RNA surveillance pathways, specifically nonsense mediated decay. Recently it has been implicated in cell cycle progression and roles within S-phase, where it was reported to bind to chromatin and associate with DNA polymerase δ. The objective of this thesis was to investigate roles of Upf1 in S-phase progression and genome stability.

Initially I attempted to set up a yeast two-hybrid system that would allow me to identify, at a molecular level, motifs responsible for the association between Upf1 and the p66 DNA polymerase δ subunit. Although I was able to demonstrate interactions between chromatin associated proteins, I was unable to detect significant levels of interaction between Upf1 and p66, and concluded that the system would not be useful for the detailed molecular analysis required.

In a second approach, I utilized FLP recombinase technology to generate a library of isogenic HeLa cell lines capable of inducibly expressing tagged, siRNA resistant forms of wild-type Upf1. I generated and investigated a series of mutants in which amino acid residues within motifs, identified as potential targets of the PIKK family of protein kinases, were altered to non-phosphorylatable forms. Using this approach, I identified Ser42 as a residue important for the recruitment of Upf1 to chromatin, and provided data indicating that this residue is not involved directly in the canonical nonsense mediated decay function of Upf1.

Thirdly I investigated the role of this mutant, as well as other phosphorylation site mutants in the maintenance of genome stability and telomere integrity. Loss of Upf1 recruitment to chromatin resulted in the appearance of double strand breaks, as determined by the proxy marker γH2AX, and a significant increase in telomere loss. Analysis of a mutant lacking known phosphorylation sites required for RNA decay indicated that while this mutant retained the capability of associating with chromatin, it also was unable to prevent genomic instability and telomere loss.

My data are consistent with a model in which Upf1 is recruited to chromatin in a Ser42 dependent manner and requires additional PIKK motif phosphorylation site residues to operate at telomeres to prevent TERRA-induced telomere loss.

Chapter 1 Introduction

1.1 The maintenance of genomic stability is essential for cellular survival

Cells employ a diverse array of cellular surveillance mechanisms to monitor genome integrity and limit the loss of genetic information resulting from damage inflicted on the genome, and the consequences of such loss. Failure to do so results not only in cellular malfunction but is a predisposition for many cancers (Negrini et al., 2010). Understanding the role of cellular surveillance pathways and how they integrate signals from the cell cycle, DNA damage repair, pro- and anti-apoptotic pathways in the response to genomic instability is critical for a rational approach to developing novel therapies as well as diagnostic and prognostic tools.

Insults to genomic integrity may arise as a consequence of external or environmental factors such as ultraviolet or gamma radiation, chemically induced DNA damage including alkylation, oxidation, cross-linking and intercalating mutagens (Sancar et al., 2004). Challenges to the integrity of the genome also arise as a consequence of normal cellular metabolism. Replication fork collapse during DNA synthesis can generate DNA double strand breaks, generation of reactive oxygen species cause oxidative damage to DNA and regions of sequence non-complexity or repetitive sequences provide opportunities for mismatch errors giving rise to mutations (De Bont and van Larebeke, 2004).

1.2 Cellular checkpoints are surveillance mechanisms that operate to recognise and resolve genomic instability

Complex signalling pathways exist within cells to respond to such events that, if not resolved, would compromise the genomic integrity of the cell. These systems initiate three critical steps, a) the arrest of on-going DNA replication to allow time for

DNA repair b) the transcription of DNA repair genes and c) integration of pro and anti-apoptotic signals arising from the severity of the genotoxic insult and the opportunity for recovery via DNA damage response and thus cellular viability. Many of the components of these pathways have been identified and characterised as DNA damage sensors (eg. Rad9/Rad1/Hus1), signal mediators (MDC1), signal transducers (e.g. Chk1/Chk2) and effectors (eg. P53/Cdc25) (Dean et al., 1998; Freire et al., 1998; Matsuoka et al., 1998; Sadhu et al., 1990; Stewart et al., 2003; Zakut-Houri et al., 1985). However, there is clearly overlap in aspects of these functions, for example, the human analogues of Rad9 (Claspin/Brca1) have both sensor and mediator functions (Kumagai and Dunphy, 2000; Miki et al., 1994)

1.3 Phosphatidylinositol 3-kinase-related kinases (PIKK) kinases engaged in checkpoint regulation

The family of phosphatidylinositol 3-kinase-related kinase (PIKK) proteins operate as both damage sensors and signal transducers in the recognition and resolution of genomic instability (Falck et al., 2005; Hall-Jackson et al., 1999; Lees-Miller et al., 1992; Smith et al., 1999). They consist of Ataxia-telangiectasia mutated (ATM), ATM and Rad3 related (ATR), DNA-dependent protein kinase catalytic subunit (DNA-PK), Suppressor with morphogenetic effects on genitalia (SMG1) and transformation/transcription domain-associated protein (TRRAP). The PIKK Mammalian target of rapamycin (mTOR) is not involved in genome stability but functions in cellular growth and G_1 progression (Gingras et al., 2001). ATR is an essential gene required for the viability of both human and mouse cells (Brown and Baltimore, 2000; Cortez et al., 2001; de Klein et al., 2000) and while ATM is non-essential, carriers of ATM mutations have increased cancer risk and a complete loss of

ATM function causes ataxia-telangiectasia, a condition characterised by chromosomal instability, cancer predisposition, radiation sensitivity, and cell cycle abnormalities (Savitsky et al., 1995).

These kinases, with the exception of mTOR, preferentially phosphorylate serine/threonine-glutamine (S/T-Q) motifs within target proteins in response to a range of genomic insults (Reviewed in Abraham, 2004). ATM, DNA-PK and TRRAP are involved in the resolution of DNA double-strand breaks, ATR is recruited to, and activated by, stretches of replication protein A (RPA)-coated single-stranded DNA (ssDNA) and ATM, together with SMG1 is involved in the response to ionizing radiation (Brumbaugh et al., 2004; Canman et al., 1998; Cimprich and Cortez, 2008; Jazayeri et al., 2006; Khanna and Lavin, 1993).

PIKKs also regulate intrinsic cellular processes essential for DNA replication, evidenced in the tightly controlled activation of ATR, ATM and DNA-PK at the end of S-phase, essential for the completion of telomeric DNA replication and end processing (Verdun and Karlseder, 2006). Replication forks can slow or stall if they encounter physical constraints on DNA replication (Labib and Hodgson, 2007) and ATR stabilises these forks until the replication stress is resolved, thus preventing fork collapse and double strand break generation (Lopez-Contreras and Fernandez-Capetillo, 2010). ATR also functions to maintain the stability of genomic fragile sites, specific chromosomal regions susceptible to replication stress induced DNA damage and chromosomal breaks (Glover et al., 1984). These late replicating, AT-rich DNA sequences are thought to form DNA secondary structures that present physical barriers to approaching replication forks (Reviewed in Glover et al., 2005). Replication of these regions requires

the coordinated activation of ATR and Werner syndrome helicase (WRN) to resolve these structures and allow replication fork progression (Casper et al., 2002; Pirzio et al., 2008).

1.4 The Nonsense Mediated mRNA Decay pathway

A loss of genomic integrity resulting in mutation can pose substantial challenges for the cell. Once established, mutations are for the most part not recognised as such, and may generate alterations in protein function and regulation with significant implications for cellular survival. Some mutations manage to evade the surveillance pathways described above. However, cells can recognise and mitigate against at least one such mutation, namely the emergence of a premature termination codon (PTC). Inherited in-frame mutations, incorrectly rearranged immunoglobulin and T-cell receptor genes or transcriptional/splicing errors can all give rise to a PTC within an mRNA (Gudikote and Wilkinson, 2002; Wittmann et al., 2006). If undetected, translation of a PTC-containing mRNA results in C-terminal truncation of the protein. In proteins which contain multiple domains or which engage multiple interacting partners for overall function, truncation may generate dominant-negative effects with often powerful phenotypic consequences. Even where a dominant-negative protein is not generated, undetected PTCs can render the resultant protein non-functional, such as in the inherited predisposition to BRCA1-mediated breast cancer (Szabo et al., 2004; Vallon-Christersson et al., 2001). These 'nonsense' mutations are present in one third of all mutant mRNA transcripts linked to human diseases (Frischmeyer and Dietz, 1999) and underlie many physiological conditions including β-thalassemia, Duchenne Muscular Dystrophy, Cystic fibrosis, Charcot-Marie-Tooth Disease type 2, Ullrich's

disease and hereditary Elliptocytosis (Blake et al., 2002; Chang and Kan, 1979; Moriniere et al., 2010; Usuki et al., 2004; Xu et al., 2012). Nonsense Mediated mRNA Decay (NMD) is a surveillance mechanism which operates to recognise and degrade PTC-containing mRNAs to prevent these genomic mutations manifesting as altered protein function (Isken and Maquat, 2007; Lykke-Andersen et al., 2000; Mendell et al., 2002).

1.4.1 EJCs mark the location of splice sites on processed mRNA molecules

In the current model, as newly transcribed mRNAs are processed and subjected to intron splicing (Figure 1.1a), a large exon-junction complex (EJC) containing Y14, Btz, Magoh, eIF4AIII, Upf2, Upf3a or Upf3b proteins is deposited ~20-24 nucleotides upstream of the exon-exon boundary (Figure 1.1b) (Chamieh et al., 2008; Fang et al., 2013; Gehring et al., 2003; Kataoka et al., 2001; Kataoka and Dreyfuss, 2004; Kim et al., 2001; Le Hir et al., 2000; Lejeune et al., 2002; Lykke-Andersen et al., 2001; Singh et al., 2007). EJCs provide a 'memory' of splicing during additional processing steps in the generation of a mature mRNA capable of steady state translation. The 5' cap structures of immature transcripts, bound by the cap-binding protein (CBP) heterodimer CBP80-CBP20 (CBC), support the loading of ribosomes and a 'pioneer round' of translation, during which, EJC proteins are displaced from an mRNA (Chiu et al., 2004; Dostie and Dreyfuss, 2002; Lejeune et al., 2002; Lejeune et al., 2004; Maquat et al., 2010). Replacement of the CBP80-20 cap with eukaryotic translation initiation factor 4E (eIF4E) after pioneer round completion indicates that an mRNA is, in principle PTC free and subsequently renders mRNAs insensitive to NMD (Hosoda et al., 2005; Ishigaki et al., 2001; Lejeune et al., 2002).

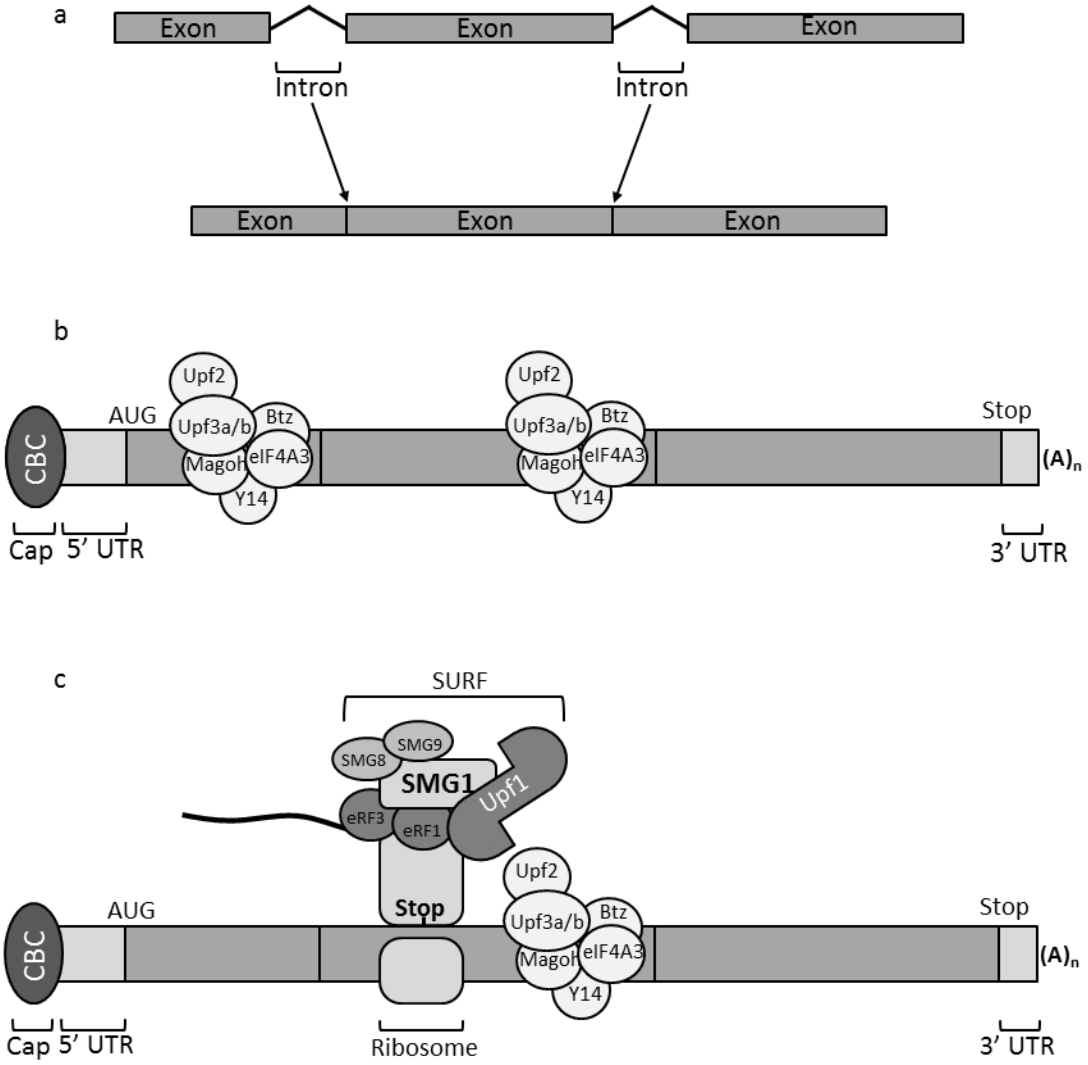

Figure 1.1 The exon junction complex (EJC) highlights the position of premature termination codons (PTCs)

a) Intron splicing during mRNA processing brings neighbouring exons into contact, forming exon-exon junctions. b) The exon-junction complex (EJC) proteins Y14, Btz, Magoh, eIF4AIII, Upf2, Upf3a or Upf3b are deposited ~20-24 nucleotides upstream of the exon-exon boundary on CBP80-20 cap-binding complex (CBC) bound mRNAs. c) Translation termination causes the formation of the SURF complex (SMG1, Upf1, SMG8, SMG9, eRF1 and eRF3) on the termination codon.

The subcellular location of pioneer round translation and exact mechanism of PTC recognition is under some debate however. Newly synthesised mRNAs are transcribed upon export to the cytoplasm and indeed the majority of CBP80 bound mRNAs are cytoplasmic (Lejeune et al., 2002) and degradation of nonsense transcripts has been shown to occur in cytoplasmic perinuclear regions (Chen and Shyu, 2003; Trcek et al., 2013). However, translation has also been observed in discrete nuclear foci (Iborra et al., 2001) and both EIF4E bound mRNAs (Lejeune et al., 2002) and decay of nonsense transcripts have been identified in the nucleus (Cheng and Maquat, 1993; de Turris et al., 2011; Humphries et al., 1984), suggesting PTC recognition can occur in both locations. A recent report by Rufener and Muhlemann., 2013, has demonstrated that both CBP80- *and* eIF4E-bound PTC containing mRNA transcripts are equally degraded within the cell, similar as observed in *S.cerevisiae* (Gaba et al., 2005; Gao et al., 2005; Maderazo et al., 2003). Upf1 was also shown to interact with eIF4E, in addition to CBP80 (Rufener and Muhlemann, 2013) suggesting NMD may be initiated by a premature termination event on any mRNA, even after pioneer round completion. It is clear that while evidence exists for multiple circumstances in which NMD can be initiated, the exact mechanism of substrate recognition and early events involved in NMD are not yet fully understood.

1.4.2 Recruitment of the SURF complex to an EJC triggers NMD

The ability of this surveillance system to distinguish a PTC from a normal termination codon is predicated on the notion that all EJCs should be upstream of the correct termination codon. Translation termination promotes the assembly of the SURF complex (SMG1, unphosphorylated Upf1, an RNA helicase also known as RENT1

(Perlick et al., 1996), and the translation termination factors eRF1-eRF3) on the termination codon (Figure 1.1c) (Kashima et al., 2006). Present also are SMG8 and SMG9, two recently identified SMG proteins which suppress SMG1 kinase activity (Arias-Palomo et al., 2011; Fernandez et al., 2011; Yamashita et al., 2009). If a SURF complex is >~55nt *upstream* of an EJC, CBP80 promotes SURF recruitment to the downstream EJC via binding of Upf1 to Upf2 (Figure 1.3a), forming the decay-inducing complex (DECID) (Cheng et al., 1990; Hosoda et al., 2005; Hwang et al., 2010; Ivanov et al., 2008; Kadlec et al., 2006; Kashima et al., 2006; Nagy and Maquat, 1998), which initiates the process of RNA destruction.

1.4.3 The RNA/DNA helicase Up-frameshift 1 (Upf1) is a central NMD component

The RNA/DNA helicase Upf1 is one of the most highly conserved NMD proteins (Figure 1.2a), with homologues in *Homo sapiens, Mus musculus* (Rent1), *Danio rerio, Drosophila melanogaster, Caenorhabditis elegans* (SMG2) and *Saccharomyces cerevisiae* (Upf1p), reflecting the evolutionary importance of Upf1 for NMD (Applequist et al., 1997; Culbertson et al., 1980). An ATP-dependent RNA binding protein (Figure 1.2b), Upf1 displays RNA-dependent ATPase and 5'-3' RNA/DNA helicase activity *in vitro,* capable of unwinding duplex DNA (Bhattacharya et al., 2000; Czaplinski et al., 1995) and believed to remodel messenger ribonucleoprotein (mRNP) complexes during NMD (Chamieh et al., 2008; Cheng et al., 2007; Franks et al., 2010; Sun et al., 1998). When Upf1 is not associated with the EJC, intra-molecular interactions of the conserved N-terminal CH and C-terminal SQ domains with the highly conserved helicase core cause allosteric inhibition of ATPase and helicase activities (Figure 1.2c) (Cheng et al., 2007; Clerici et al., 2009; Fiorini et al., 2012).

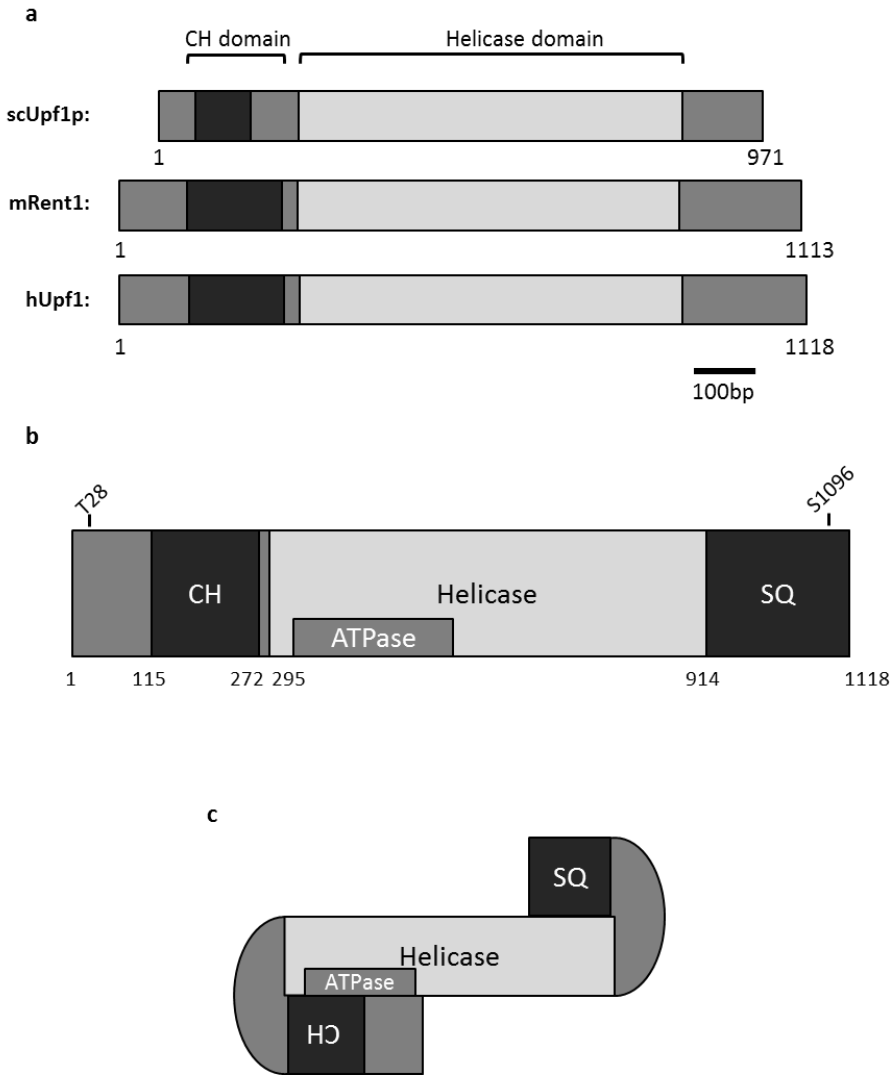

Figure 1.2 Structure of the DNA/RNA helicase Upf1

a) Schematic illustration of Upf1 in *S.cerevisiae* (sc), *M.musculus* (m) and *H.sapiens* (h), indicating the general domain structure and protein sizes. b) Structural regions within human Upf1: CH = highly conserved Upf2 interaction domain, Helicase = highly conserved central super family (SF1) helicase domain, ATPase = region associated with Upf1 ATPase activity, SQ = C-terminal SQ motif rich region. Known *in vivo* Upf1 phosphorylation sites at T28 and S1096 are indicated. c) Allosteric binding of the CH and SQ domains in unbound Upf1 inhibits ATPase and helicase activity.

1.4.4 The PIKK SMG1 induces mRNA decay through phosphorylation of Upf1

Upon Upf2 binding, displacement of the CH domain from the helicase core partially stimulates these activities and decreases the affinity of Upf1 for RNA (Figure 1.3a). This is thought to switch Upf1 from an RNA clamping mode to an RNA unwinding mode, aiding helicase translocation along the mRNA and facilitating mRNA decay (Chakrabarti et al., 2011; Chamieh et al., 2008; Clerici et al., 2009).

Human Upf1 contains 28 S/T-Q motifs, the consensus sequence for phosphorylation by PIKK kinases, located predominantly in the N-terminal 100 amino acids and in the clustering of 14 S/T-Q motifs at the extreme C-terminus. Dissociation of SMG8 and SMG9 upon DECID formation alleviates SMG1 suppression and stimulates Upf1 phosphorylation on T28, S1096 as well as additional C-terminal sites, causing three key events, i) the dissociation of the ribosome and release factors from the DECID (Figure 1.3b), ii) the displacement of the C-terminal SQ domain to fully stimulate ATPase and helicase activity and iii) the recruitment of SMG5-7 (Figure 1.3c) (Arias-Palomo et al., 2011; Brumbaugh et al., 2004; Clerici et al., 2009; Fiorini et al., 2012; Hosoda et al., 2005; Isken et al., 2008; Kashima et al., 2006; Ohnishi et al., 2003; Okada-Katsuhata et al., 2012; Pal et al., 2001; Yamashita et al., 2009; Yamashita et al., 2001).

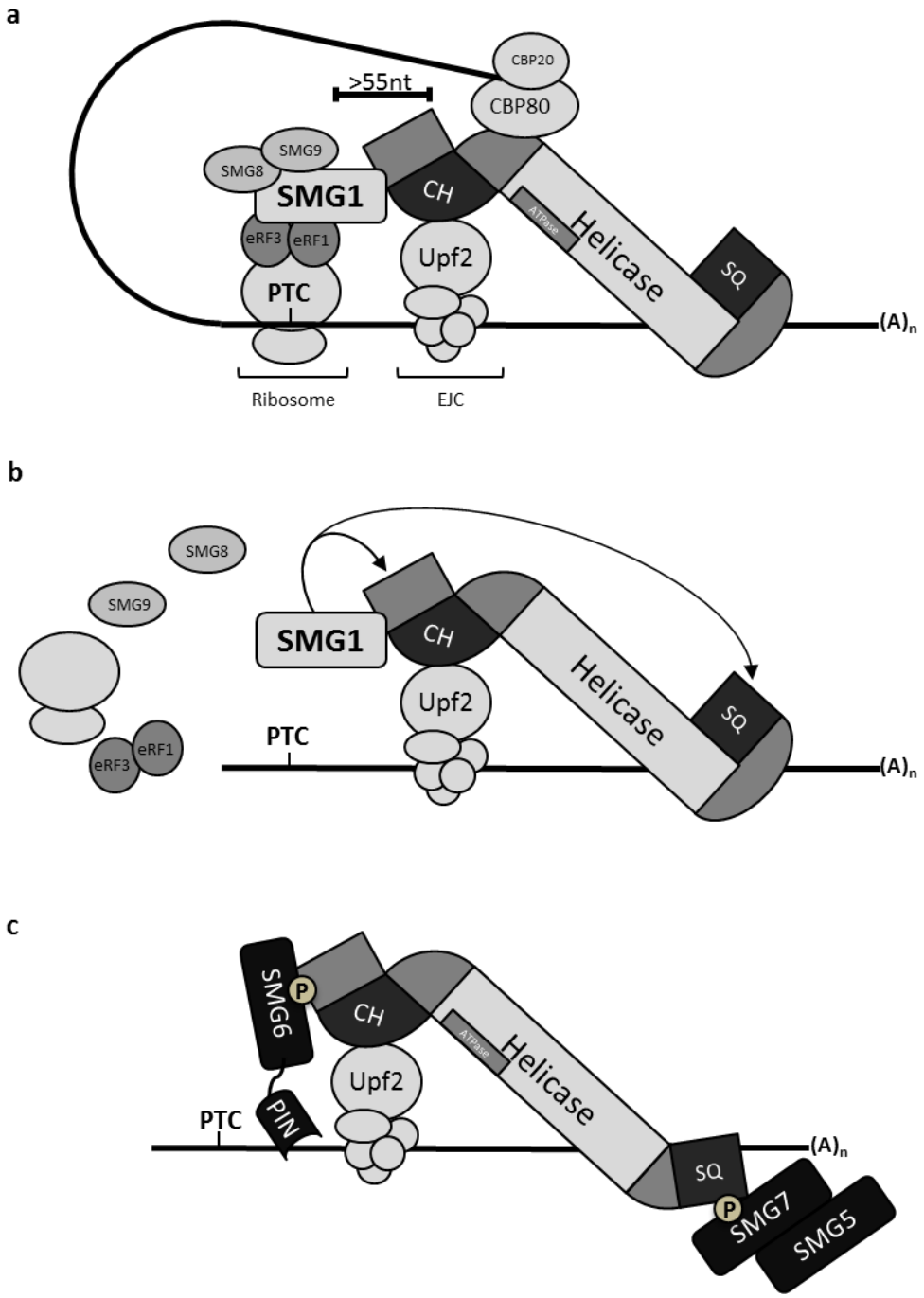

Figure 1.3 Upf1 biochemical activation and protein-protein interactions during NMD

a) SURF complex formation >55 nucleotides upstream of an EJC, mediated by CBP80, promotes binding of Upf1 (SURF) to Upf2 (EJC). CH domain displacement upon Upf2 binding partially stimulates ATPase and helicase activity. b) Decay-inducing complex (DECID) formation displaces SMG8 and SMG9, stimulating SMG1 mediated Upf1 phosphorylation and dissociation of the ribosome and eRF1/3. c) Upf1 phosphorylation at T28 and S1096 elicits mRNA decay through displacement of the SQ domain to fully stimulate unwinding activity, and recruits SMG5-7 and other mRNA decay factors (not shown).

1.4.5 Decay mechanisms of nonsense mRNAs

Cycles of Upf1 phosphorylation and dephosphorylation are essential for mRNP remodelling and decay of PTC-containing transcripts, where phospho-Upf1 serves as a scaffold for recruitment of mRNA decapping, deadenylation and exonucleolytic decay factors (Lejeune et al., 2003; Ohnishi et al., 2003; Okada-Katsuhata et al., 2012). Binding of the SMG5:SMG7 heterodimer to phospho-S1096 (Figure 1.3c) recruits proline-rich nuclear receptor coregulatory protein 2 (PNRC2), the decapping enzyme Dcp1, the Xrn1 nuclease, protein phosphatase 2A (PP2A) and other factors required for 3' mRNA decay (Cho et al., 2012a; Cho et al., 2009; Gatfield et al., 2003; Lehner and Sanderson, 2004; Lejeune et al., 2003; Loh et al., 2013; Lykke-Andersen, 2002; Ohnishi et al., 2003; Okada-Katsuhata et al., 2012; Unterholzner and Izaurralde, 2004). Association of SMG6 with phospho-T28 induces simultaneous endonucleolytic cleavage of the 5' mRNA, through the SMG6 C-terminal PilT N-terminal (PIN) domain, shown to possess single-stranded (ss) RNA endonuclease activity (Eberle et al., 2009; Glavan et al., 2006; Huntzinger et al., 2008; Mascarenhas et al., 2013; Okada-Katsuhata et al., 2012). Thus, the N- and C-termini are key Upf1 regulatory domains, acting not only to suppress helicase and ATPase activity, but also to modulate Upf1-protein interactions depending on the specific phospho-status of Upf1.

1.4.6 NMD regulates normal cellular mRNAs and is critical for embryogenesis

NMD also regulates selenium-dependent proteins, the processing of the HIV and Rous sarcoma viruses and a broad range of mRNA transcripts in the absence of PTCs, demonstrating a global role for NMD in the regulation of the transcriptome. (Ajamian et al., 2008; Banerjee et al., 2012; LeBlanc and Beemon, 2004; Moriarty et al., 1998; Serquina et al., 2013). The presence of an upstream open reading frame (uORF), a 3' long untranslated region (3' UTR) or a 3' UTR intron within an mRNA are all known NMD-inducing features (Reviewed in Schweingruber et al., 2013). This global surveillance by NMD regulates ~10% of normal mRNA transcripts and is critical for the establishment of early developmental cell lineages in *M.musculus*, *D.rerio* and *D.melanogaster* and influences mammalian neuronal development and function (Anastasaki et al., 2011; Avery et al., 2011; Bruno et al., 2011; Correa-Cerro et al., 2005; Frischmeyer-Guerrerio et al., 2011; Li et al., 2013; Long et al., 2010; McGlincy et al., 2010; McIlwain et al., 2010; Medghalchi et al., 2001; Mendell et al., 2004; Metzstein and Krasnow, 2006; Tarpey et al., 2007; Weischenfeldt et al., 2008; Wittkopp et al., 2009; Wittmann et al., 2006). *S.cerevisiae* and *C.elegans* mutants lacking functional Upf1 or other NMD proteins however present only mild phenotypes and proliferate normally (He et al., 1993; Hodgkin et al., 1989). The increased complexity of the higher eukaryote transcriptome and the multicellular coordination of gene expression during embryogenesis therefore appear to place greater dependency upon mRNA surveillance and transcriptional regulation.

1.4.7 NMD down-regulation is tolerated by differentiated cells

However, this dependence upon NMD is restricted to embryogenesis, as long term suppression of NMD in differentiated human cells in culture has no effect on cellular survival. NMD inhibition also occurs in response to cellular stress and is a feature of some solid tumours (Mendell et al., 2004; Wang et al., 2011; Wengrod et al., 2013; Wittmann et al., 2006; Yang et al., 2013). Intriguingly, the mRNA transcripts of Upf1, SMG5 and SMG7 contain NMD-inducing features, indicating an intrinsic self-regulation of NMD activity (Huang et al., 2011; Yepiskoposyan et al., 2011) and during adipogenesis and myogenesis NMD is down-regulated in favour of a related mRNA surveillance pathway, Staufen-mediated decay (SMD) (Cho et al., 2012b; Gong et al., 2009). SMD targets mRNAs lacking PTCs but which contain binding sites for the Staufen proteins Stau1 and Stau2 in their respective 3' UTR, responsible for the recruitment of Upf1 and promotion of Upf1 helicase activity. Whether the cell performs SMD or NMD depends on the relative levels of proteins involved in either pathway. Increased Stau1 and PNRC2 protein expression during development results in competition with NMD factors for interaction with Upf1, thus favouring SMD-mediated regulation of mRNA targets and inhibition of NMD (Cho et al., 2012b; Jolly et al., 2013; Kim et al., 2005; Kim et al., 2007; Park et al., 2012), presumably via sequestration of Upf1 in SMD related macromolecular complexes.

1.5 The nuclear functions of hUpf1 are essential for the maintenance of genomic stability

Upf1 has been demonstrated to undergo bidirectional nuclear-cytoplasmic shuttling in mammalian cells (Mendell et al., 2002). While evidence exists for both nuclear and cytoplasmic NMD, S phase-specific Upf1-dependent pathways exist,

integrating both nuclear and cytoplasmic events that act to preserve genomic integrity through the regulation of histone mRNAs and telomere replication (de Turris et al., 2011; Iborra et al., 2001; Maquat, 2005; Stalder and Muhlemann, 2009; Trcek et al., 2013).

1.5.1 Regulation of replication dependent histone mRNAs requires Upf1 during S-phase

As cells replicate their genome, the cellular demand for factors required for DNA metabolism increases dramatically. Newly synthesised DNA is extremely fragile and interacts with complexes of histone proteins, forming nucleosomes to stabilise chromatin. Histone mRNA and protein levels are therefore tightly co-ordinated with DNA synthesis and perturbing this balance has serious consequences for genomic stability (Han et al., 1987; Meeks-Wagner and Hartwell, 1986; Pettitt et al., 2002; Zhao et al., 2004)

Cell cycle regulated histone mRNAs are unique in the cell as they lack a poly A tail, containing instead a 3' stem loop structure bound by Hairpin/Stem-Loop Binding Protein (HBP/SLBP) essential for the regulation of histone mRNA stability and nuclear export (Battle and Doudna, 2001; Martin et al., 1997; Michel et al., 2000; Sullivan et al., 2009; Wang et al., 1996). To supply the demand for histone proteins during DNA replication, histone mRNA levels are increased dramatically during S-phase (DeLisle et al., 1983) and remain elevated until S-phase completion, where levels rapidly fall (Harris et al., 1991). Histone mRNAs have a half-life of 50-60 min during S-phase, but upon DNA replication completion this decreases to 10-15 min (Marzluff and Duronio, 2002). Increased levels of cyclinA/cdk1 and CK2 at the end of S-phase phosphorylate

HBP/SBLP (Koseoglu et al., 2010; Zheng et al., 2003) and cause the regulated decay of histone mRNAs through translation dependent, HBP/SLBP-mediated recruitment of factors that cause oligouridylation of the histone mRNA 3' end (Kaygun and Marzluff, 2005b; Mullen and Marzluff, 2008). Recruitment of Lsm1-7, decapping factors and the exosome to this poly(U) tail initiates 5'-3' and 3'-5' mRNA decay (Hoefig et al., 2013; Mullen and Marzluff, 2008; Su et al., 2013).

Interestingly, inhibition of DNA replication by exposure to cytosine arabinoside or hydroxyurea (HU), an inhibitor of the enzyme ribonucleotide reductase, which causes replication fork stall due to insufficient free nucleotides (Krakoff et al., 1968), was demonstrated to cause a rapid decline in the levels of histone mRNA during S-phase (DeLisle et al., 1983; Sittman et al., 1983). Later studies into this replication dependent histone mRNA decay (HD) pathway demonstrated histone mRNA level fall to around 20% within 60 min after exposure to HU (Kaygun and Marzluff, 2005a; Muller et al., 2007b). Upf1 has been implicated in this pathway, as Upf1 co-immunoprecipitated with HBP/SLBP and siRNA induced knockdown of Upf1, or expression of Upf1 mutants lacking ATPase and helicase activity, reduced the efficiency of HD in cells treated with hydroxyurea (Kaygun and Marzluff, 2005a). Upon replication stress this stem loop-HBP/SLBP structure may be considered analogous to the EJC in NMD, in that interaction of Upf1 with RNA-bound HBP/SLBP stimulates HD. Unlike NMD however, which acts constitutively during the cell cycle to remove PTC containing mRNAs, HD occurs exclusively during S-phase, does not require Upf2 (Kaygun and Marzluff, 2005a) and as histone genes lack introns, are not degraded through an EJC dependent mechanism.

During HD, replication stress activates a DNA damage checkpoint in the nucleus, and how this nuclear event causes the decay of cytoplasmic histone mRNAs is unknown. While the requirement for SMG5-7 or the exact mechanism of Upf1 recruitment to HBP/SLBP are not yet understood, signalling components of the replication checkpoint have been implicated in mediating HD, as cells lacking ATR and/or DNA-PK activity show reduced capacity to perform HD (Kaygun and Marzluff, 2005a; Muller et al., 2007b).

Two recent studies have begun to suggest that HD may indeed occur in the nucleus and target newly synthesised histone mRNAs, rather than the cytoplasmic population. In the current model of global protein synthesis, newly synthesised mRNAs bound by CBC (CBP80-20) are exported to the cytoplasm, upon which exchange of CBC for EIF4E facilitates steady state translation (Maquat et al., 2010). Choe et al., 2013, demonstrated HBP/SLBP interacts with CTIF (CBP80/20-dependent translation initiation factor), which recruits translation factors to CBC bound mRNAs during pioneer round translation (Kim et al., 2009). The majority of histone mRNAs analysed in this study were found to be CBC-bound, and replication stress induced decay of predominantly CBC, but not EIF4E, bound histone mRNAs (Choe et al., 2013).

Rattray et al., 2013 demonstrated replication stress during S-phase induced the alternative splicing of the HBP/SLBP transcript, generating multiple HBP/SLBP isoforms. The levels of these HBP/SLBP isoforms decreased after recovery from the replication stress, identifying HBP/SLBP itself as a target of the intra-S phase checkpoint (Rattray et al., 2013). One isoform, in which exon three is lost, caused the nuclear accumulation of HBP/SLBP, and taken with data presented by Choe and colleagues, possibly reflects

a new model of HD. Replication stress and activation of DNA-PK/ATR may generate an HBP/SLBP isoform lacking exon three, which binds the hairpin structure of immature, newly synthesised, CBC bound histone mRNAs and causes their nuclear retention. DNA-PK/ATR may also phosphorylate nuclear Upf1, recruiting it to SLBP and cause histone mRNA decay within the nucleus. Although unproven, this model is consistent with data demonstrating histone mRNA levels gradually decline over a period of 60 min after exposure to HU (Kaygun and Marzluff, 2005a; Muller et al., 2007b), suggesting natural turnover of cytoplasmic histone mRNAs, coupled with the decay of newly synthesised histone mRNAs in the nucleus, could be the mechanism by which the cell responds to replication stress.

1.5.2 hUpf1 is loaded onto chromatin during S-phase in a PIKK-dependent manner

A fraction of Upf1 localises to chromatin as cells enter late G_1, with levels increasing during S-phase (Azzalin and Lingner, 2006b). Chromatin-bound Upf1 is hyperphosphorylated on S/T-Q motifs compared to its soluble counterpart, suggesting a PIKK-dependent mechanism of chromatin loading. SMG1, the kinase responsible for Upf1 phosphorylation during NMD is implicated in chromatin recruitment, as exposure to γ-radiation (a known SMG1 stimulus) increases total cellular phospho-Upf1 and the fraction of Upf1 associated with chromatin (Azzalin and Lingner, 2006b; Brumbaugh et al., 2004). Unfortunately, knockdown of SMG1 induces DNA damage, evidenced in SMG1-deficient cells displaying constitutive phosphorylation of Chk2 and p53, and nuclear foci containing phosphorylated histone 2AX (γH2AX), in the absence of extrinsic genotoxic agents. (Brumbaugh et al., 2004). Phosphorylation of these proteins occurs in response to DNA damage to initiate cell cycle arrest and DNA repair

(Reviewed in Sancar et al., 2004). The induction of this DNA damage response in SMG1 knockdown cells resulted in Upf1 chromatin recruitment in the absence of γ-radiation, therefore the absolute contribution of SMG1 to Upf1 chromatin recruitment has not been determined (Azzalin and Lingner, 2006b). ATR has also been shown to be a Upf1 kinase *in vitro*, and knockdown of ATR, but not ATM, decreases total cellular phospho-Upf1 levels and prevents replication stress-induced Upf1 chromatin recruitment (Azzalin and Lingner, 2006b).

1.5.3 The helicase activity of hUpf1 may facilitate replication fork progression through interactions with DNA polymerase δ

Whether Upf1 interacts directly with DNA or through protein-protein interactions is unknown, however bovine Upf1, purified close to homogeneity, preferentially binds to fork-like DNA structures *in vitro* (Carastro et al., 2002; Li et al., 1992). Interactions with the DNA replication machinery may also mediate this interaction, as Upf1 co-purifies and co-immunoprecipitates with distinct subunits of DNA polymerase δ from bovine thymus extracts and HeLa cells respectively (Azzalin and Lingner, 2006b; Carastro et al., 2002). Functioning in both lagging strand DNA synthesis and DNA repair, the multi-subunit (p125, p66, p50, p12) DNA polymerase δ is one of a group of replicative DNA polymerases utilised by the cell during DNA replication (Hubscher et al., 2002). DNA replication is initiated from replication origins; specific genomic loci licensed in G_1 by the assembly of the origin recognition complex (ORC), Cdc6 and Mcm2–7 (MCM/P1 proteins) on DNA. Increased activity of cyclin-dependent kinases and Cdc7/ASK brings about origin firing as cells enter S-phase and at specific times during S-phase to facilitate global DNA replication (Reviewed in

Aparicio, 2013; Hochegger et al., 2008; and Jares et al., 2000). After replication origin firing, progressive synthesis on both leading and lagging strands requires the DNA duplex ahead of the replication fork to be unwound by helicase proteins, allowing the replication machinery access to single stranded DNA (Figure 1.4). The MCM2-7 helicase is believed to be the predominant replicative helicase, however a number of additional helicases have been identified, some of which play a role in resolving aberrant structures which arise during DNA replication. Blooms disease, Werners disease and Xeroderma pigmentosa are a few of a broad spectrum of diseases associated with a loss of specific helicases giving rise to increased genomic instability and an inability to repair particular aberrant DNA structures or regions of DNA damage (Ellis, 1997; Monnat and Saintigny, 2004). Similarly, chromatin associated Upf1, either directly or via interactions with DNA polymerase δ, may unwind duplex DNA ahead of the progressing replication fork or resolve aberrant DNA structures, possible by utilising the helicase activity of Upf1.

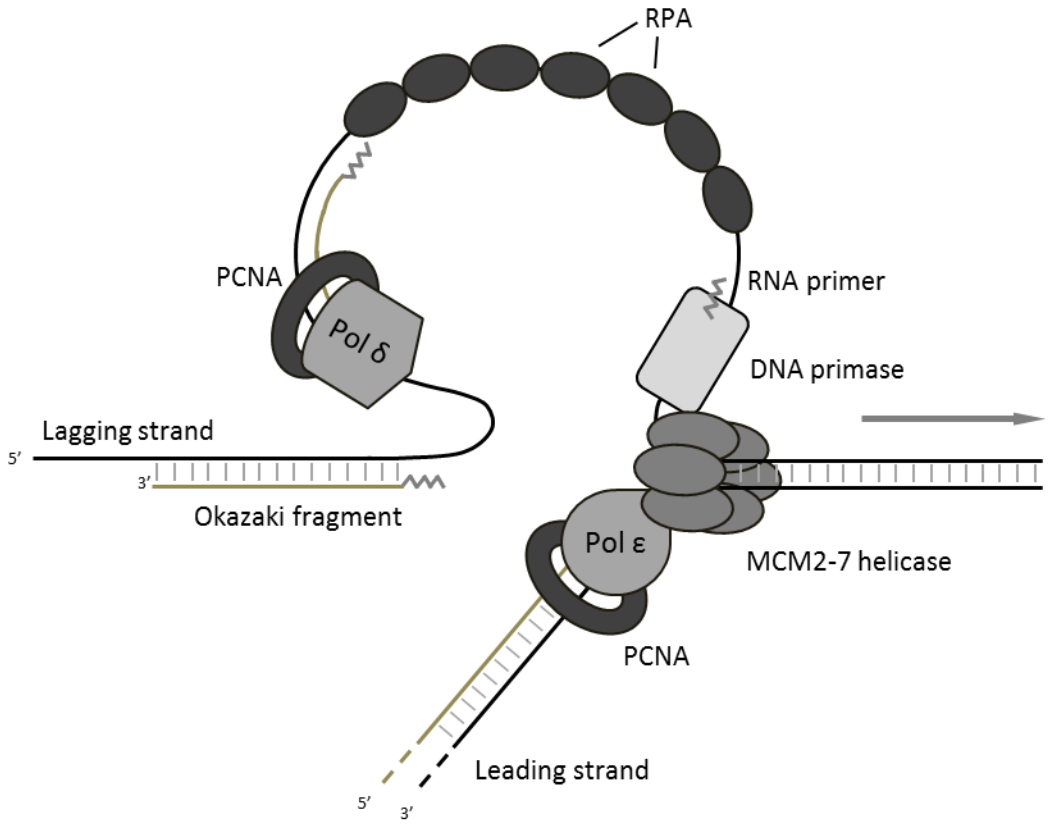

Figure 1.4 Leading and lagging strand DNA synthesis at the replication fork

Duplex DNA is unwound ahead of the progressing replication fork by the MCM2-7 DNA helicase and differential replication machinery is then recruited to each single DNA strand. Leading strand DNA synthesis is performed by DNA polymerase ε, whereas lagging strand synthesis requires the generation of short RNA primers by DNA primase, which are then extended by DNA polymerase δ. These Okazakhi fragments are then joined together by DNA ligase (not shown). RPA (replication protein A) binds to, and stabilises single stranded DNA generated by lagging strand synthesis and PCNA (proliferating cell nuclear antigen) is a DNA clamp that increases the processivity of DNA polymerases.

1.5.4 Cells depleted of hUpf1 shown signs of replication stress and genomic instability

Intriguingly, HeLa cells depleted of Upf1 fail to proliferate and were reported to undergo an early S-phase replication arrest in the absence of extrinsic DNA damaging agents (Azzalin and Lingner, 2006b). These cells also accumulated chromosomal breaks and nuclear foci containing single stranded DNA binding protein RPA and phosphorylated histone 2AX (γH2AX), two markers of DNA damage indicative of replication difficulty (Azzalin and Lingner, 2006b). As described previously, ATR is required for maximal loading of Upf1 to chromatin and knockdown of ATR in Upf1-depleted cells prevents the accumulation of these DNA damage foci, providing further evidence that ATR is a key mediator of chromatin associated functions of Upf1 (Azzalin and Lingner, 2006b).

The chromatin associated functions of Upf1 appear to be distinct from global mRNA surveillance as i) cells can tolerate long term suppression of NMD without affecting genomic stability, ii) Upf2 knockdown does not generate γH2AX foci or cause S-phase arrest and iii) NMD is unaffected in ATR-depleted cells (Azzalin and Lingner, 2006b; Azzalin et al., 2007; Wittmann et al., 2006). One possible mechanism by which Upf1 might be differentially regulated to undertake NMD as well as genome stability functions might involve alternative phosphorylation sites. Upf1 contains multiple S/T-Q motifs and the differential phosphorylation of nuclear Upf1 by ATR, potentially in combination with SMG1 could allow simultaneous Upf1 function in multiple pathways.

1.6 The identification of the ever-shorter telomere (EST) family proteins and their homology to NMD factors

Studies in *S.cerevisiae* identified a family of proteins (ever-shorter telomere, (EST)) which, when depleted, induced telomere shortening and the up-regulation of telomere associated genes. Interestingly EST1A/B/C were found to be homologous to the SMG5-7 proteins involved in NMD, suggesting global mRNA surveillance regulates telomeric DNA replication at least in this organism and may function in mammalian telomere homeostasis (Dahlseid et al., 2003; Enomoto et al., 2004; Lew et al., 1998).

1.6.1 Telomeric structures insulate and protect chromosomal ends

Telomeres are specialised DNA structures located at the end of chromosomes preventing genetic information loss arising from replication dependent telomere shortening (De Lange, 2005b; Olovnikov, 1973). These structures present a unique challenge for the cell as semi-conservative DNA replication of telomeric TTAGGG-3'/CCCTAA-3' repeats generate a naked DNA "end" resembling a double strand break (Bertuch and Lundblad, 1998; Moyzis et al., 1988; Shay and Wright, 2004). If not processed correctly, this "end-protection problem" activates a DNA damage response and prevents mitotic entry (Reviewed in de Lange, 2009). To circumvent this, a telomeric 'cap' is formed late S/G_2 by the invasion of the chromosomal terminus into the upstream DNA duplex (Figure 1.5a), to form a T-loop (Griffith et al., 1999). Formation of this structure is dependent upon stabilisation by the shelterin complex (Telomeric Repeat Binding Factor 1 and 2 (*TRF1 and TRF2*), Protection Of Telomeres 1 (*POT1*), TRF1-Interacting Nuclear protein 2 (*TIN2*), *Rap1* and Tripeptidyl Peptidase 1 (*TPP1*)) (Figure 1.5b) and exclusion of these regions from the DNA damage response. Normal telomeric cap processing generates intermediary DNA structures that

resemble regions of genomic DNA damage, such as the 3' single stranded DNA overhang essential for T-loop formation (Chow et al., 2012; de Lange, 2005a). These regions become 'protected' from recognition by ATR at the end of S-phase, through hnRNPA1 (heterogeneous nuclear ribonuclear protein 1A) mediated displacement of ssDNA-bound RPA from telomeric DNA, and replacement with POT1 (Denchi and de Lange, 2007).

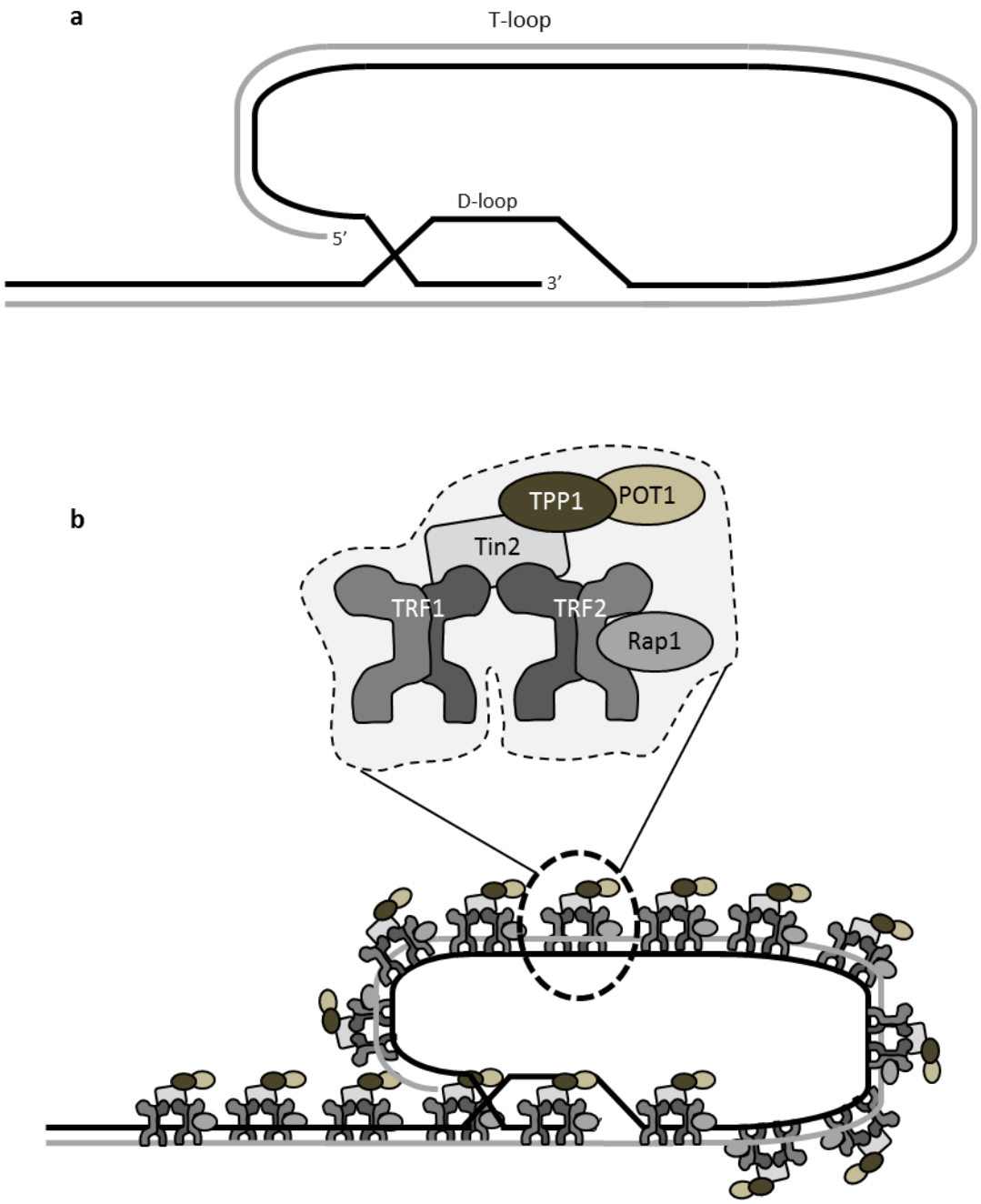

Figure 1.5 Telomeric DNA ends are protected from the DNA damage response by the shelterin complex

a) Telomeric DNA replication generates a 3' overhang, which through coordinated activation of ATM, ATR and DNA-pk loops back to invade the upstream DNA duplex, forming the minor D-loop and major T-loop structures. b) The shelterin complex (TRF1, TRF2, Rap1, Tin2, TPP1 and POT1) assembles on telomeric DNA and protects telomere caps from recognition by DNA damage response pathways.

1.6.2 PIKKs regulate the genomic integrity of telomeres

PIKKs are, however, recruited to telomeres at specific stages of the cell cycle, with ATR, ATM and DNA-PK performing distinct functions essential for normal telomere replication. DNA-PK and ATM are recruited to telomeres during G_2 and mediate the strand invasion-like events essential for telomere cap processing (Bailey et al., 2001; Verdun et al., 2005). SMG1 is the critical kinase required for Upf1 phosphorylation during NMD but no role for it in global telomere replication has yet been described. The G4 quadruplex DNA structures found at telomeres have been proposed to form secondary structures similar to those found at genomic fragile sites (Rizzo et al., 2009). Indeed, depletion of hnRNPA1, the shelterin component TRF1 or exposure to aphidicolin-induced replication stress causes strand-breakage phenotypes at telomeres characteristic of fragile site breakage (Le et al., 2013; Martinez et al., 2009; Sfeir et al., 2009). ATR has been shown to suppress the emergence of genomic fragile sites (Casper et al., 2002) and, as it is recruited to telomeres in late S-phase and required for the completion of telomeric replication and overhang generation (Casper et al., 2002; Sfeir et al., 2009; Verdun and Karlseder, 2006), may also be involved in suppression of telomere-specific fragile sites.

1.6.3 Nonsense mediated mRNA decay factors regulate a subset of telomeres in human cells

Azzalin et al., 2006, demonstrated Upf1 is recruited to chromatin during S-phase and later showed that the NMD factors SMG1, Upf1, Upf2, EST1A/SMG6, EST1B/SMG5 and EST1C/SMG7 specifically interact with telomeric DNA in chromatin immunoprecipitation (ChIP) assays (Azzalin et al., 2007; Chawla et al., 2011). The low

frequency loss of whole telomeric tracts upon knockdown of SMG1, SMG6 and Upf1 and telomeric γH2AX foci in Upf1 depleted cells indicate a failure of DNA replication at a subset of telomeres (Azzalin et al., 2007).

The *S.cerevisiae* Upf1 homologue (Upf1p) is found exclusively in the cytoplasm and does not appear to regulate genomic stability, reflecting evolutionary divergence in the regulation of telomeres between yeast and humans (Atkin et al., 1995; He et al., 1993). Indeed, when the core NMD component Upf2 is depleted, only mild telomeric phenotypes are observed in HeLa cells, suggesting mammalian telomeric regulation is not dependent on the canonical NMD pathway (Azzalin et al., 2007). One possibility is that Upf1 performs helicase functions at telomeres to facilitate lagging strand DNA synthesis through interaction with DNA polymerase δ, the lagging strand polymerase at telomeres (Gilson and Geli, 2007; Lormand et al., 2013; Moser et al., 2009). However, in Upf1-depleted cells, *leading* strand telomeres are predominantly affected, with only mild effects seen at lagging DNA strands (Chawla et al., 2011). Further classification of this effect and whether Upf1 interacts with the leading strand machinery, including DNA polymerase ε would shed further light on the role of Upf1 in telomeric DNA replication.

1.6.4 Long non-coding RNAs and the regulation of telomeres

Telomeric DNA was long considered transcriptionally silent but is now known to be transcribed in early G_1 by RNA polymerase II into Telomeric Repeat Containing RNA (TERRA). These long non-coding RNA (lncRNA) $UUAGGG_n$ repeat sequences range from 100bp-9kb and exist exclusively in the nucleus in two distinct populations, a polyadenylated pool in the nucleoplasm and a non-polyadenylated fraction shown to

associate with a subset of telomeres *in vivo* (Azzalin et al., 2007; Luke and Lingner, 2009; Luke et al., 2008; Porro et al., 2010; Schoeftner and Blasco, 2008; Xu et al., 2010). The exact function of TERRA at telomeres is unknown, however it has been shown to bind to telomerase *in vivo*, inhibiting its activity *in vitro* (Redon et al., 2010; Schoeftner and Blasco, 2008) and to inhibit hnRNPA1, preventing the RPA-POT1 switch required for telomere protection during normal DNA replication (Flynn et al., 2011; Redon et al., 2013).

1.6.5 TERRA regulation by the NMD factors Upf1 and SMG6 but not Upf2

The S-phase specific shuttling of Upf1 to chromatin correlates with a regulated degradation of TERRA during S-phase (Porro et al., 2010), indicating Upf1 may regulate these lncRNAs during specific stages of the cell cycle. TERRA forms telomeric DNA-RNA hybrids *in vitro* and *in vivo*, existing as G-quadruplex structures that protect TERRA from enzymatic degradation (Balk et al., 2013; Luke et al., 2008; Martadinata and Phan, 2009; Randall and Griffith, 2009; Redon et al., 2010; Xu et al., 2008a; Xu et al., 2008b). The 5'-3' RNA helicase activity of Upf1 has been proposed to remodel the TERRA molecule, displacing it from DNA and promoting endonucleolytic degradation through interactions with the PIN domain of SMG6 (Eberle et al., 2009; Glavan et al., 2006; Huntzinger et al., 2008). Indirect evidence for Upf1-mediated TERRA remodelling and destruction *in vivo* may be observed in cells expressing Upf1 ATPase mutants lacking helicase activity (Bhattacharya et al., 2000). These accumulate telomere-free ends (TFEs) and knockdown of Upf1 or SMG6 increases the number of telomeric TERRA foci (Azzalin et al., 2007; Chawla et al., 2011). Although found at telomeric DNA, Upf2 depletion does not increase TERRA foci (Azzalin et al., 2007) suggesting allosteric

inhibition of Upf1 ATPase and helicase functions by the CH/SQ domains may be modulated through interactions with other, currently unknown proteins at telomeres.

Association of Upf1 with telomeric DNA and the telomerase/shelterin complex is decreased upon ATR knockdown (Chawla et al., 2011) and accumulation of TERRA foci in SMG1-depleted cells suggest complex coordination of PIKKs at telomeres is required in the regulation of TERRA-dependent telomere replication (Azzalin et al., 2007).

1.6.6 The regulated degradation of TERRA has been proposed to modulate telomerase activity

One hypothesis proposed to explain the regulated degradation of TERRA is that NMD components are ultimately involved in telomere cap formation, through the regulation of telomerase enzymatic activity and telomere protection. Telomerase is an enzyme that uses an internal RNA template (hTR) to synthesise the 100-200bp lost during telomeric DNA replication to maintain telomere length (Reviewed in Gomez, 2012). Telomerase activity is required in late S-phase for telomere extension, mediated by interactions with the shelterin complex, prior to end processing and cap formation (Nandakumar and Cech, 2013; Verdun et al., 2005). Upf1, SMG6 and TERRA interact with telomerase *in vivo* and Upf1 also competitively associates with the shelterin component TPP1, known to modulate telomerase activity (Chawla et al., 2011; Redon et al., 2007; Reichenbach et al., 2003; Snow et al., 2003). TERRA inhibits hnRNPA1 mediated end-protection and telomerase *in vitro* (Flynn et al., 2011; Redon et al., 2010) and was recently shown to cluster telomerase molecules in early S-phase, proposed to inhibit telomerase activity until late S-phase, when these clusters

associate with specific telomeres (Cusanelli et al., 2013). Removal of TERRA at the end of S-phase may be necessary to alleviate inhibition of telomerase and hnRNPA1, allowing telomere extension and end protection before T-loop formation (Figure 1.6a).

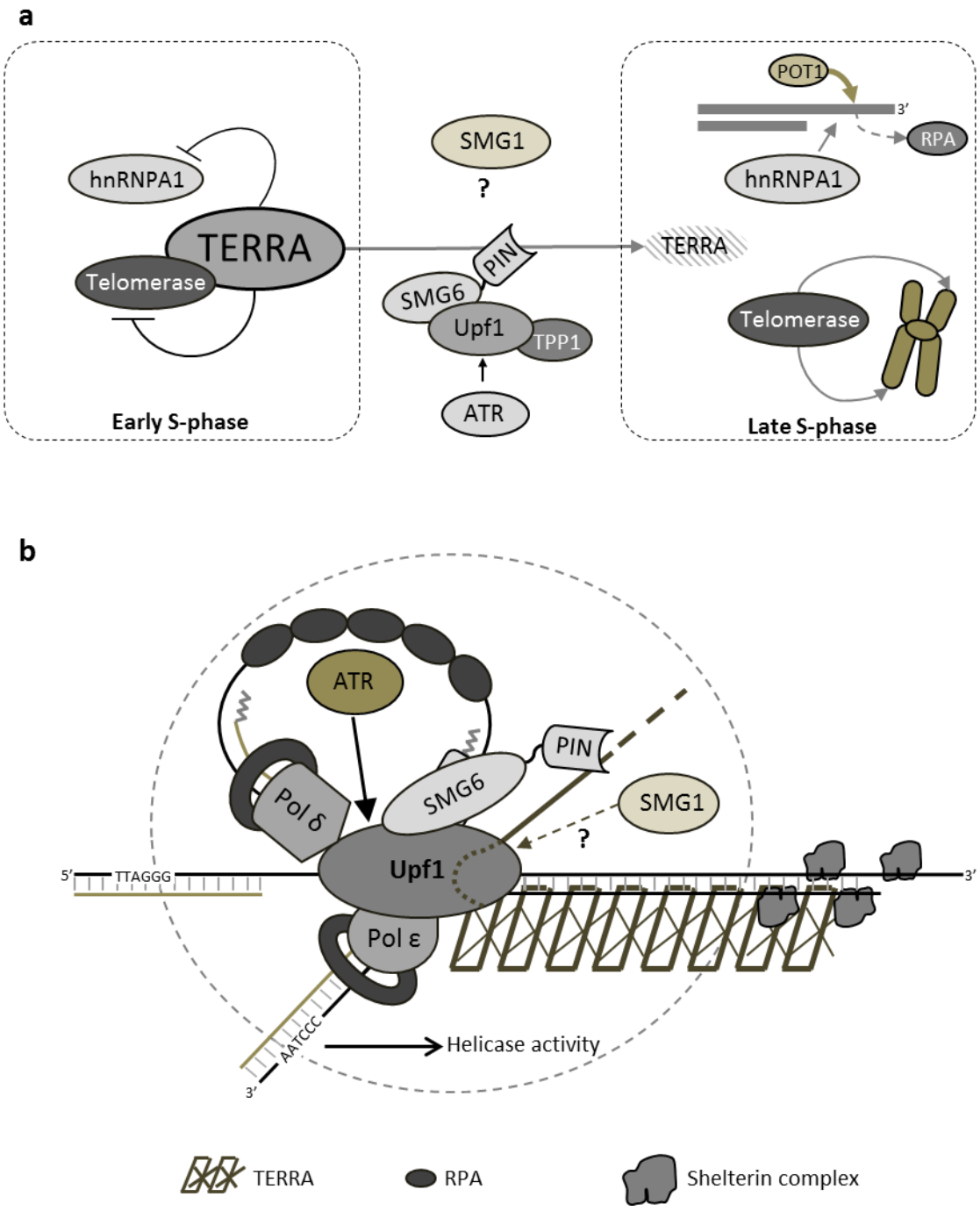

Figure 1.6 Two models of Upf1-dependent TERRA regulation at telomeres

a) *End processing model*: Upf1 and SMG6 degrade TERRA at the end of S-phase, removing TERRA-induced inhibition telomerase and hnRNPA1. b) *Replication fork progression model:* TERRA forms secondary structures resembling R-loops at a subset of telomeres, generating replication fork stall. Through activation of ATR, Upf1 is recruited to these chromatin regions and Upf1 helicase activity remodels TERRA, facilitating SMG6-mediated RNA decay. SMG1 functions in TERRA regulation but direct target has not been identified. See text for further details.

1.6.7 TERRA resolution may alternatively aid replication fork progression at a subset of telomeres

However, in disagreement with the hypothesis presented above, recent studies have shown increased levels of both naturally occurring and artificially induced TERRA did not affect the ability of telomerase to extend telomeres in human cell lines (Farnung et al., 2012), and short-term TERRA transcription does generate telomere shortening (Arora et al., 2012). An alternative hypothesis therefore is that TERRA bound to telomeres forms a physical barrier to the progressing replication fork (Figure 1.6b) (Maicher et al., 2012). Telomeric DNA replication is unique as it is initiated in sub-telomeric regions and progresses unidirectionally into the telomere, where no downstream replication origins have been identified (Reviewed in Gilson and Geli, 2007). Therefore replication fork failure cannot be recovered by the firing of adjacent origins, and replication fork stall at telomeric regions, if not resolved, is more likely to generate double strand breaks than at other genomic loci. Hybridisation of a TERRA molecule to a stretch of telomeric DNA may generate secondary structures similar to those found at genomic fragile sites. R-loops, DNA-RNA hybrids, form where RNA polymerase II transcribed RNA hybridizes with its original template DNA strand (McIvor et al., 2010), and are known to block progressing replication forks. The activation of ATR and recruitment of specific helicases is required to facilitate progression over such regions (Aguilera and Gomez-Gonzalez, 2008; Casper et al., 2002). TERRA fits the criteria to induce an R-loop and interestingly, a recent study in *S.cerevisiae* showed TERRA molecules interacting with their specific telomere of origin (Cusanelli et al., 2013). One such helicase involved in the resolution of these structures at genomic loci, Senataxin, shares large C-terminal homology with Upf1 (Alzu et al., 2012; Suraweera et

al., 2009). Upf1 may therefore function at a subset of telomeres presenting TERRA-DNA hybrids, through associations with DNA polymerase δ/ε, providing RNA helicase activity to displace the TERRA molecule and allow replication fork progression.

1.6.8 Upf1 may maintain genomic stability through the regulation of telomeric DNA replication

Telomere dysregulation and subsequent telomere shortening is a hallmark of cellular ageing, chromosomal instability and tumorigenesis (Reviewed in Artandi and DePinho, 2010; Gilson and Geli, 2007; Harley et al., 1990; Karlseder et al., 1999; Kim Sh et al., 2002; Nakamura et al., 2008). Increased incidence of telomeric defects observed in Immunodeficiency, Centromeric region instability, Facial anomalies (ICF) syndrome cases corresponds to high levels of TERRA in these patients (Yehezkel et al., 2008). It has been noted that TERRA down regulation correlates with tumour progression (Schoeftner and Blasco, 2008) which may allow enhanced telomerase activity and telomere extension, providing tumour cells a proliferative advantage over non-cancerous cells. The loss of complete telomeric tracts in the absence of Upf1 suggests replication forks are failing during early stages of telomeric replication, or chromosomes with extremely short existing telomeres, therefore highly dependent upon telomerase, are most severely affected in these cells. Both proposed mechanisms involve the S-phase specific degradation of TERRA and therefore may not be mutually exclusive. Determining the contribution of Upf1 in TERRA-mediated telomere replication is vital to increase our understanding of how telomere homeostasis impacts upon the genomic integrity of the cell.

1.7 Therapeutic targeting of the NMD pathway is dependent upon understanding the S-phase specific role of the RNA helicase Upf1

The surveillance of cellular mRNAs encompasses a broad spectrum of targets, from PTC-containing nonsense transcripts, to the global regulation of subsets of normal genes during embryogenesis. A core component of these pathways is the RNA helicase Upf1, and while NMD is dispensable for organismal survival, Upf1 has been shown to have nuclear functions critical for the maintenance of genomic stability in human cells.

Transcripts containing a PTC downstream of critical domains, although targeted by NMD, could generate proteins with either full or partial function if translated. The ability of the adult cell to tolerate down regulation of global NMD is of great interest, as therapeutic modulation of the NMD pathway, potentially through Upf1 suppression, has been proposed as an alternative to current read-through therapies for conditions exacerbated by NMD such as Duchenne Muscular Dystrophy and Cystic Fibrosis (Johnson et al., 2012; Linde and Kerem, 2011; Malik et al., 2010; Peltz et al., 2013). The chronic conditions amenable to this approach require lifelong suppression of NMD, so understanding how Upf1 coordinates mRNA surveillance and genomic stability is vital to ensure sustained genomic instability and cancer predisposition is not generated in these patients.

1.8 Aims and objectives of this work

The objective of this body of work was to investigate roles of Upf1 in S-phase progression and genome stability, as there is increasing evidence that Upf1 has functions within the nucleus, distinct from mRNA surveillance, that are coupled to DNA replication and are essential for the maintenance of genomic stability.

In this chapter I have highlighted the role of checkpoint signalling in maintaining the fidelity of DNA replication and described the current understanding of how Upf1 functions in mRNA surveillance. I have introduced key studies in which Upf1 was shown to interact with chromatin and be essential for S-phase specific pathways involved in the regulation of histone mRNAs and telomere integrity.

The first two stages of my research focused on the mechanisms of how Upf1 interacts with chromatin during S-phase. Initially, I attempted to set up a yeast two-hybrid assay to perform molecular analysis of the interaction between Upf1 and the p66 subunit of DNA polymerase δ. In a second line of study, I set out to identify the Upf1 structural motifs essential for interaction with chromatin during S-phase.

The third stage of the research was the investigation of how Upf1 chromatin recruitment during S-phase may function to sustain DNA replication at genomic and telomeric sites, and the significance for the genomic integrity of the cell when these functions are lost. Using these approaches I hoped to gain insight into the mechanism by which Upf1 specifically contributes to the genomic stability of the cell during S-phase.

Chapter 2 Materials and Methods

2.1 Reagents

General laboratory chemicals were obtained from Sigma-Aldrich Limited (The Old Brickyard, New Road, Gillingham, England, SP8 4XT) or VWR international Limited (Merck House, Poole, England, BH15 1TD), unless otherwise stated. Chemicals were AnalaR grade. Deionised water was obtained using a Millipore Ultra-pure protogel 30% (w/v) acrylamide: 0.8% (w/v) bis-acrylamide stock, solution (37.5:1) mix was from Geneflow limited (Fradley Business Centre, Wood End Lane, Fradley, England WS13 8NF). Enhanced Chemiluminescence (ECL), Enhanced Chemiluminescence Plus (ECL+), ECL Chemiluminescence Advance (ECL A) were from Amersham Biosciences UK Limited (Pollards Wood, Nightingales Lane, Chalfront Street, Giles, England HP8 4SP).

Tissue culture plastic ware was obtained from Greiner Bio-one (Brunei Way, Stroudwater Business Park, Stonehouse, Glos, GL103SX). Bio-Rad protein (Bradford) Assay reagent, Mini-Protean II protein gel electrophoresis equipment were from Bio-Rad Laboratories Ltx (Bio-Rad House, Marylands Avenue, Hemel Hemstead, England, HP2 3TD). Schleicher &Schuell Protran Nitrocellulose transfer membrane was from Inverclyde Biologicals (2 Teal Court, Strathclyde Business Park, Bellshill, Scotland, ML4 3NN). Whatmann 3mm paper was from Fisher Scientific UK Limited (Bishop Meadow Road, Loughborourgh, England, LEU 5RG). Complete inhibitor cocktail tablets were from Roche Diagnostics Limited (Bell Lane, Lewes, England, BN7 1LG). Dulbecco's Modified Eagle Medium (DMEM), Dulbecco's phosphate buffered saline (DPBS, trypsin-EDTA, glutamine, Zeocin©, Blasticidin, Hygromycin, Doxycycline were obtained from Invitrogen Limited (3 Fountain Drive, Inchinnan Business Park, Paisley, Scotland, OA49RF). Plasmid DNA purification kits and QIAquick gel extraction kits, Polyfect and

Oligofectamine were from Qiagen (Qiagen house, Fleming Way, Crawley, England, RH10 2AX). Molecular biology reagents, such as restriction endonucleases and associated buffers were from New England Biolabs Limited (73 Knowl Piece, Wilbury Way, Hithcin, England, SG4 OTY), Promega UK Limited (Delta House, Chilworth Science Park, Southampton, England, SO16 7NS) or Fermentas (Helena Biosciences Europe, Colima Avenue, Sunderland Enterprise Park, Sunderland, England, SR5 3XB). PNA telomeric FISH probe and reagents were obtained from Cambridge Research Biochemicals, 10 Belasis Court, Belasis Hall Technology Park, Billingham, Cleveland, TS23 4AZ UK). Quickchange mutagenesis kits, XL-10 Gold ultra-competent cells and Pfu Ultra DNA polymerase were from Agilent Technologies UK Limited (Lakeside, Cheadle Royal Business Park, Stockport, Cheshire, England, SK8 3G). The Scottish National Blood Transfusion Service (Castlelaw Building, Pentlands Science Park, Penicuik, idlothian, Scotland, EH26 0PZ) supplied anti-serum raised against human Upf1. Jackson Immunoresearch HRP- conjugated secondary antibodies were obtained from Stratech Scientific Limited (Unit 4 Northfield Business Park, Northfield Road, Soham, England, CB7 SUE). Konica AX bue x-ray film was obtained from Hospital Engineering Limited (Unit 6, Mercury Way, Mercury Park, Manchester, England, M41 7HS).

2.2 Antibodies

2.2.1 Primary antibodies

Antibody	Species	Raised against	Supplier	Dilution
Anti-Upf1	Sheep serum	Human Upf1	Scottish National Blood Transfusion Service Ref: C5B9	WB: 1:5000
Anti-Upf1	Goat affinity purified	Human Upf1	Bethyl Prod code: (A301-038a)	WB: 1:1000 IP: 1µg/mg protein
Anti-Upf2	Rabbit affinity purified	Human Upf2	Cell signalling (Prod code: D4A7)	WB: 1:1000 IP: 1:50
Anti-Flag	Mouse affinity purified	Flag Tag	Sigma (Prod code: F1804)	WB: 1:5000 IP: 1µg/mg protein
Anti-p66	Rabbit affinity purified	Human p66	Bethyl (Prod code: A301-243a)	IP: 1µg/mg protein
Anti-p66	Rabbit affinity purified	Human p66	Bethyl (Prod code: A301-244a)	WB: 1:1000
Anti-PCNA	Mouse affinity purified	Rat PCNA	Abcam (Prod code: ab29)	WB: 1:1000
Anti-Actin	Mouse affinity purified	Modified β-actin peptide	Sigma (Prod code: A1978)	WB 1:10000
Anti-alpha Tubulin	Mouse affinity purified	Rat brain tubulin	Sigma (Prod code: T8203)	WB 1:10000
Anti-phospho histone 2AX	Mouse affinity purified	Human H2AX (phospho ser139)	Millipore (Prod code: 05-636)	WB 1:1000
Anti-ORC2	Rabbit affinity purified	Human ORC2	BD Pharmingen (Prod code: 559266)	WB 1:1000
Anti-nucleolin	Mouse affinity purified	Human nucleolin	Santa Cruz (Prod code: sc-17826)	WB 1:10000
Anti-GFP	Rabbit affinity purified	Recombinant GFP	Abcam (Prod code: ab6556	WB 1:1000
Anti-Gal-AD	Rabbit affinity purified	Anti-GalAD	Sigma G9293	WB 1:1000

Table 1 Primary antibodies used in this project

Table detailing the species, source, suppliers and working concentrations of the primary antibodies used in this project.

2.2.2 Secondary antibodies

Antibody	Species	Raised against	Supplier	Dilution
Anti-sheep HRP	Sheep affinity purified	Sheep IgG	Santa Cruz (Prod code: sc-2473)	WB: 1:5000
Anti-goat HRP	Goat affinity purified	Goat IgG	Santa Cruz (Prod code: sc-2020)	WB: 1:5000
Ant-mouse HRP	Mouse affinity purified	Mouse IgG	Santa Cruz (Prod code: sc-2060)	WB: 1:5000
Anti-rabbit HRP	Rabbit affinity purified	Rabbit IgG	Santa Cruz (Prod code: sc-2004)	WB: 1:5000

Table 2 Secondary antibodies used in this project

Table detailing the species, source, suppliers and working concentrations of the secondary antibodies used in this project.

2.3 Primers

2.3.1 Primers used in Chapter 3

Subcloning of human Upf1 into pGBDU-C2 and pGAD-C2

F 5' –GATCGGATCCCCATGAGCGTGGAGGCGTACGGGCCCAGCTGC- 3'

R 5' –GATCATCGATGGTTATTAATACTGGGACAGCCCCGTCACCCC- 3'

Subcloning of human p66 into pGBDU-C2 and pGAD-C2

F 5' –GATCGGATCCCCATGGCGGACCAGCTTTATCTGGAAAAT- 3'

R 5' –GATCATCGATGGTTATTATTTCCTCTGGAAGAAGCCAGTAAT- 3'

Subcloning of *S.pombe* PCNA (Pcn1) into pGBDU-C2 and pGAD-C2

F 5' –GATCGGATCCCCATGCTTGAAGCTAGATTTCAGCAGGCT- 3'

R 5' –GATCATCGATGGCTACTACTCCTCATCCTCCTCACCATT-3'

2.3.2 Primers used in Chapter 4

Upf1^{res} siRNA resistance site directed mutagenesis

F 5' –GGTGTCACTGCAGCCGATCGTGTCAAGAAGGGATTTGA- 3'

R 5' –TCAAATCCCTTCTTGACACGATCGGCTGCAGTGACACC- 3'

Flag-tag addition and subcloning of Flag-Upf1^{res}

F 5' –CCGGATCCATGGACTACAAAGACGATGACGACAAGCTTAGCGTGGAGGCGTACGGGCCCA- 3'

R 5' –GATCGCGGCCGCGGTTATTAATACTGGGACAGCCCCGTCACCCCGCCA– 3'

Subcloning of Flag-Upf1^{res}Δ1-91aa into pCDNA5/FRT/TO/CAT

F 5’ –CCGGATCCATGGACTACAAAGACGATGACGACAAGAGTGTAGCCAAGACCAGCCA- 3’

R 5’ –GATCGCGGCCGCGGTTATTAATACTGGGACAGCCCCGTCACCCCGCCA– 3’

Site directed mutagenesis of Flag-Upf1^{resS10A}

F 5’ –GTGAGAGTCTGCGCGCTGGGCCCGTAC- 3’

F 5’ –GTACGGGCCCAGCGCGCAGACTCTCAC- 3’

Site directed mutagenesis of Flag-Upf1^{resT28A}

F 5’ –GTACGGGCCCAGCGCGCAGACTCTCAC- 3’

R 5’ –CGGAGCCCTGTGCGTCGGCGCCAAG- 3’

Site directed mutagenesis of Flag-Upf1^{resS42A}

F 5’ –GACTTTACTCTTCCTGCCCAGACGCAGACGC- 3’

R 5’ –GCGTCTGCGTCTGGGCAGGAAGAGTAAAGTCGG- 3’

Site directed mutagenesis of Flag-Upf1^{resS42E}

F 5’ –CCGACTTTACTCTTCCTGAGCAGACGCAGACGCCCCC- 3’

F 5’ –GGGGGCGTCTGCGTCTGCTCAGGAAGAGTAAAGTCGG- 3’

Site directed mutagenesis of Flag-Upf1^{resS1096A}

F 5’ –CGACGTGGCGCTCGCACAGGACTCCAC- 3’

R 5’ –GTGGAGTCCTGTGCGAGCGCCACGTCG- 3’

Site directed mutagenesis of Flag-Upf1^{resS1116A}

F 5’ –GGGGTGACGGGGCTGGCCCAGTATTAATAACC-3’

R 5’ –GGTTATTAATACTGGGCCAGCCCCGTCACCCC- 3’

β-globin qPCR primers

F 5’ -CACCTGGACAACCTCAAGGGCA- 3’

R 5’ -TGCAGCGGGGGTGAAATCCTTG- 3’

MUP qPCR primers

F 5’ -CCAATGCCAATCGCTGCCTCCA-3’

R 5’ -AGGGATGATGGTGGAGTCCTGGTG- 3’

2.4 siRNA used in Chapters 4 and 5

ON-Target plus siRNAs were obtained from Thermo Scientific

Upf1 siRNA sense sequence

CAGCGGAUCGUGUGAAGAAUU

Upf1 siRNA antisense sequence

5’ P.UUCUUCACACGAUCCGCUGUU

A non-targeting siRNA (Thermo Scientific D-001810-01) was used as a negative control.

2.5 Plasmids used in this study

Plasmid	Origin	Antibiotic^{R}
pCI-Neo-Flag-Upf1	Prof J. Lingner	Ampicillin
pEGFP-P66	Dr Emma Warbrick	Kanamycin
pACT-Pcn1	Dr Emma Warbrick	Ampicillin
Yeast two hybrid plasmids		
pGBDU-C2	Prof K.Ayscough	Ampicillin
pGBDU-C2-Upf1	This study	Ampicillin
pGBDU-C2-p66	This study	Ampicillin
pGBDU-C2-Pcn1	This study	Ampicillin
pGAD-C2	Prof K.Ayscough	Ampicillin
pGAD-C2-Upf1	This study	Ampicillin
pGAD-C2-p66	This study	Ampicillin
pGAD-C2-Pcn1	This study	Ampicillin
FLP-IN plasmids		
pOG44	Invitrogen	Ampicillin
pCDN5/FRT/TO/CAT	Invitrogen	Ampicillin
pCDN5/FRT/TO/CAT-Upf1^{res}	This study	Ampicillin
pCDN5/FRT/TO/CAT-Flag-Upf1^{res}	This study	Ampicillin
pCDN5/FRT/TO/CAT-Flag-Upf1$^{resΔ1-91aa}$	This study	Ampicillin
pCDN5/FRT/TO/CAT-Flag-Upf1^{resS10A}	This study	Ampicillin
pCDN5/FRT/TO/CAT-Flag-Upf1^{resT28A}	This study	Ampicillin
pCDN5/FRT/TO/CAT-Flag-Upf1^{resS42A}	This study	Ampicillin
pCDN5/FRT/TO/CAT-Flag-Upf1^{resS42E}	This study	Ampicillin
pCDN5/FRT/TO/CAT-Flag-Upf1$^{resT28A/S1096A/S1116A}$	This study	Ampicillin
NMD reporter assay		
pmCMV-G1 Norm	Dr L. Maquat	Ampicillin
pmCMV-G1 Ter	Dr L. Maquat	Ampicillin
phCMV-MUP	Dr L. Maquat	Ampicillin

Table 3 Plasmids used in this study

Table showing the plasmids used and generated in this study.

2.6 Molecular biology techniques

2.6.1 Plasmid construction

A human Upf1 cDNA was amplified from pCI-Neo-Flag-Upf1 ((Sun et al., 1998), a kind gift from Professor Joachim Lingner) using the AccuprimeGC DNA polymerase (Invitrogen) using manufacturer guidelines and the following amplification conditions (95^{O}C 3 min/30x(95^{o}C 30 s/60-70^{o}C 30s/72^{o}C 4.5 min)/72^{o}C 10 min). Human p66 cDNA was amplified from pEGFP-p66 and *S.pombe* Pcn1 cDNA amplified from pACT-Pcn1 (both kindly obtained from Emma Warbrick) using Phusion DNA polymerase (NEB) using the manufacturer guidelines. BamHI/ClaI digested cDNAs of each sequence were then inserted into both the pGBDU-C2 and pGAD-C2 plasmids (a kind gift from Prof Kathryn Ayscough) using standard cloning procedures (J. Sambrook, 1989) and verified by DNA sequencing (see below).

2.6.1.1 Introduction of siRNA resistance mutations into Upf1

Due to the presence of a high GC nucleotide region and a lack of compatible restriction sites within Upf1, a standard cloning approach using the complete Upf1 DNA sequence was not possible. The detailed cloning strategy used in this study is described below.

A Kpn1/BclI Upf1 fragment (1785-2903) was digested out of pGBDU-Upf1 and ligated into the appropriately digested psl1180 plasmid to generate psl1180-Upf1(1785-2903). Two silent mutations (G2184C and G2193C) conferring resistance to a specific Upf1 siRNA were generated using the Quickchange XL mutagenesis kit (Stratagene) to generate psl1180-Upf1(1785-2903)^{res} (see mutagenesis section for conditions).

2.6.1.2 pcDNA5/FRT/TO/CAT-Upf1^{res} construction

A (1785-2903) KpnI/Bcli Upf1^{res} fragment was digested out of psl1180-Upf1(1785-2903)^{res} and ligated into the appropriately digested pGBDU-C2-Upf1 plasmid to generate pGBDU-C2-Upf1^{res}. A BamHI/BglII complete Upf1^{res} fragment was then digested out of pGBDU-C2-Upf1^{res} and ligated into an appropriately digested psl1180 plasmid to generate psl1180-Upf1^{res}. A BamHI/Not1 fragment was then digested out of psl1180-Upf1^{res} and ligated into the appropriately digested pcDNA5/FRT/TO/CAT plasmid to generate pcDNA5/FRT/TO/CAT-Upf1^{res}.

2.6.1.3 pcDNA5/FRT/TO/CAT-Flag-Upf1^{res} construction

A single N-terminal flag tag was added by PCR to pcDNA5/FRT/TO/CAT-Upf1^{res} using Accuprime GC PCR, but mutations were present >230 bp into the resultant cDNA. To address this, a BamHI/Sfil Flag-Upf1(1-155) fragment was digested out of this pcDNA5/FRT/TO/CAT-Flag-Upf1^{res} (incorrect 3' sequence) and ligated into an appropriately digested pcDNA5/FRT/TO/CAT-Upf1^{res} plasmid to generate pcDNA5/FRT/TO/CAT-Flag-Upf1^{res}. The absence of mutations in this construct was confirmed by DNA sequencing.

2.6.1.4 Alanine substitution of Upf1 S10, T28, S42 and S42E generation

A BamHI/Sfil Flag-Upf1 fragment was digested out of pcDNA5/FRT/TO/CAT-Flag-Upf1^{res} and ligated into an appropriately digested psl1180 plasmid to generate psl1180-Flag-Upf1(1-155). Alanine substitution mutagenesis was performed using the Quickchange XL mutagenesis kit (Stratagene) and repeated for S10, T28 and S42 to generate pls1180-Upf1(1-155)^{S10A}, pls1180-Upf1(1-155)^{T28A} and pls1180-Upf1(1-155)^{S42A}. Glutamic acid substitution of S42 was also performed to generate pls1180-

Upf1(1-155)^{S42E}. A BamHI/SfiI fragment containing each individual mutation was ligated into an appropriately digested pcDNA5/FRT/TO/CAT-Flag-Upf1^{res} to generate pcDNA5/FRT/TO/CAT-Flag-Upf1^{resS10A}, pcDNA5/FRT/TO/CAT-Flag-Upf1^{resT28A}, pcDNA5/FRT/TO/CAT-Flag-Upf1^{resS42A} and pcDNA5/FRT/TO/CAT-Flag-Upf1^{resS42E}.

2.6.1.5 pcDNA5/FRT/TO/CAT-Upf1$^{resΔ1-91}$ construction

An N-terminal deletion of amino acids 1-91 was performed by PCR using Phusion high fidelity DNA polymerase and this BamHI/NotI fragment was digested and ligated into the appropriately digested pcDNA5/FRT/TO/CAT plasmid to generate pcDNA5/FRT/TO/CAT-Upf1$^{resΔ1-91}$.

2.6.1.6 pcDNA5/FRT/TO/CAT-Upf1$^{resT28A/S1096A/S1116A}$ construction

Alanine substitution mutagenesis of Upf1 serine 1116 was performed on pcDNA5/FRT/TO/CAT-Upf1$^{resΔ1-91}$ to generate pcDNA5/FRT/TO/CAT-Upf1$^{resΔ1-91-S1116A}$. Additional mutagenesis of serine 1096 was performed on pcDNA5/FRT/TO/CAT-Upf1$^{resΔ1-91-S1116A}$ to generate pcDNA5/FRT/TO/CAT-Upf1$^{resΔ1-91-S1096A/S1116A}$. A SbfI/NotI fragment was digested from pcDNA5/FRT/TO/CAT-Upf1$^{resΔ1-91-S1096A/S1116A}$ and ligated into the appropriately digested pcDNA5/FRT/TO/CAT-Flag-Upf1^{resT28A} to generate pcDNA5/FRT/TO/CAT-Upf1$^{resT28A/S1096A/S1116A}$.

2.7 DNA digestion with restriction enzymes

Digests were performed on miniprep DNA, maxiprep DNA and PCR products. Analytic digests were performed in a maximum volume of 60µl using 5U of enzyme per microgram of DNA, appropriate enzyme buffer and MilliQ H_2O. 10% of total digest volume was used for analytical agarose gel electrophoresis.

In order to obtain larger quantities of digested DNA for sub-cloning, increased amounts of DNA and corresponding amounts of restriction enzyme were used scaled to the appropriate volume. Reactions were mixed thoroughly by pipetting and incubated at the recommended temperature for 1 h or overnight. All enzymes specified were obtained from NEB. To reduce levels of background re-ligation of plasmids containing only a single cut after digestion, 1U of calf intestinal phosphatase (Promega) was added for 1 h at 37°C.

2.8 DNA ligation

The parental plasmid and the DNA fragment to be inserted were digested with the appropriate restriction enzymes. Digested fragments were separated by gel electrophoresis and gel extracted (see below). 0.1µg of digested vector was transferred to a clean 1.5ml Eppendorf tube with differing amounts of insert DNA in 1:1 to 1:6 ratios. 2µl of 10x T4 ligase buffer, 1µl of T4 DNA ligase were added to a final volume of 20µl, made up with MilliQ H_2O, and incubated overnight at room temperature. Control reactions including plasmid-only ligation reactions and T4 DNA ligase-free reactions were also performed. Prior to transformation, ligated DNA was re-isolated using a QIAquick PCR purification kit (see below)

2.9 Electrophoretic analysis of DNA

The electrophoresis apparatus was prepared and the electrophoresis tank filled with sufficient 1x TAE (40 mM Tris (20 mM acetic acid, 1 mM EDTA pH8.0) buffer to cover the agarose gel. The appropriate amount of agarose was transferred to a heat proof flask with 100ml 1x TAE. The slurry was heated until the agarose dissolved and allowed to cool to 60°C before adding ethidium bromide to a final concentration of

1µg/ml. The agarose solution was poured into the gel mould and the comb positioned. After the gel was completely set, the comb was removed and the gel mounted in the tank. The DNA samples were mixed with 1x sample buffer type IV (40% sucrose, .025% bromophenol blue) and loaded into the wells using a micropipette. The molecular weight marker set DNA hyperladder I (NEB) (5µl) was also loaded for reference. The tank lid was attached and electric current applied across the gel (typically 100 V, 400mA for 30-60 min) to facilitate migration of DNA towards the anode. After electrophoresis, the gel was examined under UV light at 312nm and images taken Uvitech UviProchemi camera system.

2.10 Purification of DNA (QIAquick PCR purification kit) from reaction mixtures

DNA was purified using a kit from Qiagen according the manufacturer's instructions. The kit was used to purify DNA fragments generated by PCR or following other enzymatic reactions. Briefly, 5x volumes of Qiagen buffer PB were added to 1 volume of the solution to be purified and mixed. The sample was added to a spin column placed in a collection tube and centrifuged for 1 min at 13000 rpm to bind DNA. The flow-through was discarded and the column washed with 0.75ml Qiagen buffer PE by centrifugation for 1 min at 13000 rpm and the flow-through discarded. The column was placed back in the same collection tube and re-centrifuged to remove traces of the washing buffer. The column was then placed in a clean 1.5ml Eppendorf tube and 50µl of Qiagen buffer EB added and allowed to stand for 1 min. DNA was eluted by centrifugation at 13000 rpm for 1 min. DNA was stored at -20°C.

2.11 DNA extraction and purification from agarose gels (QIAquick gel extraction kit)

DNA was extracted from agarose gel and purified using a kit from Qiagen according to the manufacturer's instructions. For gel extractions, ethidium bromide was replaced by the SYBR Safe (Invitrogen) DNA gel stain as this can be visualised without the need for UV light. A gel slice containing the DNA of interest was excised with a clean, sharp scalpel and weighed. 3 volumes of Qiagen buffer QG were added to 1 volume of weighed agarose gel and incubated for 10 min at 50°C. After the gel slice had dissolved, 1 volume of isopropanol was added and the solution mixed. The solution was transferred to a QIAquick column and centrifuged for 1 min at 13000 rpm. The flow-through was discarded and 0.75ml Qiagen PE buffer added and the column centrifuged for 1 min and re-centrifuged to remove residual wash buffer. DNA was eluted in either 50µl (plasmids) or 30µl (PCR products) Qiagen buffer EB into a clean 1.5ml Eppendorf tube by centrifugation for 1 min at 13000 rpm.

2.12 Transformation of competent bacteria with plasmid DNA

2.12.1 Antibiotic solutions

The following antibiotics were routinely used. Stock solutions were created as described and used at the following concentrations in liquid and solid media. Kanamycin stock solution was (10mg/ml) and used at 50µg/ml and Ampicillin stock solution was (100mg/ml) and used at 100µg/ml. Antibiotic agar plates were generated by adding the appropriate amount of stock antibiotic after partial cooling of the media, and once set, plates were stored at 4°C.

2.12.2 Routine cloning

20µl of chemically competent E.coli (DH5α, produced by D.Sutton using the described method (Sambrook et al, 1989) were thawed on ice and 10% of each ligation reaction added to the cells, gently swirled to mix and incubated on ice for 30 min. Bacteria and DNA mixtures were heat shocked at 42°C for exactly 30 s and then placed on ice for 5 min. 200µl of pre-warmed SOC media (2% w/v tryptone, 0.5% w/v Yeast extract, 10mM NaCl, 2.5mM KCl, 10mM $MgCl_2$, 20mM glucose) was added and cells incubated at 37°C in an orbital shaker at 225rpm for 1 h. Bacteria were plated on agar medium containing the appropriate antibiotic and incubated overnight at 37°C. Control transformations lacking added DNA or insert were also performed in parallel where appropriate.

2.12.3 Cloning following site-directed mutagenesis

XL10 Gold Ultracompetent cells (obtained from Agilent Technologies) were thawed slowly on ice. 45µl of competent cells were placed in pre-chilled 14ml BD Falcon polypropylene round bottom tubes. 2µl of β-mercaptoethanol was added and the cells incubated on ice and swirled gently every 2 min for 10 min. 2µl of Dpn1-treated DNA (see below) was added and incubated on ice for a further 30 min. The cells were heat shocked at 42°C for 30 s and returned to ice for 2 min. 500µl of pre-warmed NZY+ broth (Fisher BP2465 dissolved in water and autoclaved, supplemented with 5mM $MgSO_4$ and 20mM glucose) was added and incubated at 37°C at 225rpm for 1 h. 200µl of the transformation was plated on the appropriate antibiotic agar medium and incubated overnight at 37°C.

2.13 Isolation of plasmid DNA from bacteria using the QIAquick spin Miniprep kit

DNA was purified using a kit from Qiagen according to the manufacturer's instructions. A single bacterial colony was transferred into 4ml of Luria-Bertani (LB) (1% Bacto tryptone, 0.5% Bacto yeast extract, 1% NaCl) media containing 100µg/ml ampicillin and incubated overnight at 37°C with shaking at 225rpm. 1.5ml of this culture was transferred to an Eppendorf tube and centrifuged at 13000 rpm for 1 min. The media was removed by aspiration and the process repeated to give a bacterial pellet representative of 3ml of culture. The pellet was then resuspended in 250µl of Qiagen buffer P1, 250µl of Qiagen buffer P2 was added and mixed by inversion until the solution became viscous and slightly clear. Afterwards, 350µl of Qiagen buffer N3 was added and the sample inverted until the solution became cloudy. The sample was centrifuged at 13000 rpm for 10 min and the resulting supernatant was applied to a QIAprep spin column placed in a collection tube. After centrifugation for 1 min at 13000 rpm, the flow-through was discarded and the column washed by adding 0.75ml of Qiagen buffer PE and centrifuging at 13000 rpm for 1 min. The flow-through was discarded and QIAprep column was returned to the collection tube and re-centrifuged at 13000 rpm for 1 min to remove residual wash buffer. Finally, the column was transferred to a clean 1.5ml Eppendorf tube and 50ul of Qiagen buffer EB added and left to stand for 1 min prior to elution of the DNA by centrifugation at 13000 rpm for 1 min. DNA obtained by this method was used for transfection, molecular biology and DNA sequencing. DNA was stored at -20°C.

2.14 Isolation of plasmid DNA from bacteria using the Invitrogen HiPure Maxiprep kit

DNA was purified using a kit from Invitrogen according to the manufacturer's instructions. A starter culture was established by inoculating a single bacterial colony into 3ml of LB media containing 100µg/ml ampicillin at 37°C in an orbital shaker rotating at 225rpm for 6 h. This starter culture was then transferred to 500ml LB media containing 100µg/ml ampicillin and incubated at 37°C overnight in an orbital shaker rotating at 225rpm. The culture was centrifuged at 4000 g for 10 min at 4°C using a Beckman Avanti J-26XP (JLA 8.1 rotor) centrifuge and media discarded. A Maxicolumn was equilibrated by adding 30ml Invitrogen buffer EQ1 and allowed to flow through. The bacterial pellet was resuspended in 10ml of Invitrogen buffer R3 (containing RNase A (20µg/ml) and further diluted with 10ml of Invitrogen lysis buffer L7, mixed and left at room temperature for 5 min. DNA was precipitated by adding 10ml of Invitrogen buffer N3 and sample transferred to the equilibrated Maxi column. Lysate filtered through the column by gravity flow and was washed with 50ml Invitrogen buffer W8, discarding the flow-through. A sterile 50ml centrifuge tube was used to collect eluted DNA after adding 15ml elution buffer E4. 10.5ml isopropanol was added to the eluted DNA and centrifuged at >12,000 g for 30 min at 4°C, discarding the supernatant. DNA pellet was washed with 5ml 70% ethanol and centrifuged at 12,000 g for 5 min at 4°C. Pellet was allowed to air dry before re-suspending in 500ul TE buffer. DNA was stored at -20°C.

2.15 Glycerol stocks of transformed bacterial cells

Single colonies were picked from an agar plate and grown overnight at 37°C in an orbital shaker at 225rpm in 4ml LB medium with the required selective antibiotic.

700µl of cell culture was mixed with 300µl of sterile 50% glycerol. Cells were then stored at -80°C.

2.16 Site-directed mutagenesis

Site-directed mutagenesis was performed using the Stratagene QuickChange kit (Stratagene) according to the manufacturer's instructions. Each reaction contained 10x Pfu ultra buffer (5µl), double-stranded DNA template (10ng), 5' primer (125ng), 3' primer (125ng), dNTP (1µl of 100mM mix((25mM each of dATP, dGTP, dCTP, dTTP)), QuickSolution (3µl) in a final volume of 49µl. 1µl of Pfu ultra HF DNA polymerase (Stratagene) was added to the reaction and mixed gently.

The cycling parameters were as follows.

Segment	Cycles	Temperature	Time
1	1	95°C	1 min
2	18	95°C 60°C 68°C	50 s 50 s 1min/kb
3	1	68°C	7 min

Subsequently, the template plasmid was digested by adding 1µl of Dpn1 restriction enzyme and incubating at 37°C for 1 h. The remaining DNA (mutated) was then transformed into XL-10 Gold ultra-competent *E. coli* cells, as described in 2.12.3 above.

2.17 DNA sequencing

All DNA sequencing reactions were performed by the Genetics Core Facility at the University of Sheffield.

2.18 Yeast methods

2.18.1 Yeast strains

The following *Saccharomyces cerevisiae* strains were used in this study (courtesy of Professor Kathryn Ayscough), PJ69-4α (MATalpha trp1-901 leu2-3,112 ura3-52 his3-200 gal4(deleted) gal80(deleted) LYS2::GAL1-HIS3 GAL2-ADE2 met2::GAL7-lacZ) and PJ69-4a (MATa trp1-901 leu2-3,112 ura3-52 his3-200 gal4(deleted) gal80(deleted) LYS2::GAL1-HIS3 GAL2-ADE2 met2::GAL7-lacZ). Cells were maintained on YPD (1% yeast extract (BD 212750), 2% peptone (BD 211677), 2% glucose) agar plates at room temperature. PJ69-4α cells were transformed with pGBDU-C2 bait constructs and PJ69-4A cells with pGAD-C2 prey constructs.

2.18.2 Transformation with plasmid DNA

Yeast cultures were grown overnight in YPD to mid to late log phase (OD_{600} 0.5-0.6) and 10ml of culture used per transformation. Cells were harvested by centrifugation at 1000 rpm Beckman Alegra centrifuge (6H 3.8 rotor) for 5 min at 4°C and washed 1x in 5ml TE (10 mM Tris-Cl, pH 7.4, 1 mM EDTA), re-centrifuged, and then washed in 5ml 0.1M LiOAc in TE before re-isolation by centrifugation once more. The cell pellet was resuspended in 0.1ml (0.1M) LiAOc to which was added 15µl of 10µg/µl herring sperm DNA (Promega) and 1µg of plasmid DNA before gentle mixing. Cells were then treated with 700µl 40% PEG4000 in 0.1M LiAOc in TE prior to incubation for 1 h with rotation at 225RPM at 25°C. Heat shock was performed at 42°C for 15 min. Cells were centrifuged and resuspended in selective dropout (SD) media (0.675% w/v yeast N_2 base w/o amino acids (BD 291940), 0.14% w/v quadruple dropout mix (Formedium DSCK282), 2% glucose, tryptophan and histidine supplemented with

either uracil or Leucine to select for plasmid uptake (Formedium)). SDΔ^{URA} media was used for pGBDU-C2 constructs or SDΔ^{LEU} media for pGAD-C2 constructs. Transformants were plated out on SDΔ^{URA} or SDΔ^{LEU} agar plates for 48 h at 30°C. Single colonies were picked and streaked out on the appropriate SD agar plates. Empty pGBDU-C2 and pGAD-C2 vectors were transformed as negative controls.

2.18.3 Glycerol stocks of yeast cells

A single yeast colony was picked and grown overnight in SD media until stationary phase. 500µl of culture was added to 500µl sterile 30% glycerol in a sterile cryovial, mixed and stored at -80°C.

2.18.4 Yeast mating

Haploid 4α and 4a strains containing pGDBU-C2 or pGAD-C2 Upf1/p66/Pcn1 fusions were mixed together with 5µl of sterile H_2O and left to mate for 5 h at 30°C on YPD agar plates. Crosses were then streaked out on SDΔ^{URA}Δ^{LEU} agar plates and incubated at 30° until colonies were observed. Double transformants were selected by streaking of a single colony on fresh SDΔ^{URA}Δ^{LEU} agar plates. All combinations of bait and prey strains were crossed.

2.18.5 Plasmid extraction from diploid yeast strains

To extract plasmids from diploid *S.cerevisiae* strains, a 5ml culture was grown overnight and a 1ml sample centrifuged for 5min at 13000 rpm in an Eppendorf 5417R (5417 C/R rotor) centrifuge. Supernatant was removed and cell pellet washed in 1ml TE (10 mM Tris-Cl, pH 7.4, 1 mM EDTA), before cells spun as before and supernatant discarded. Cell pellet was resuspended in 500µl Buffer S (10mM K_2PO_4 pH 7.2, 10mM

EDTA pH 7.5, 50mM, 50mM β-mercaptoethanol, supplemented with 50µg/ml Zymolase before use) and incubated for 30 min at 37°C. Then 100µl of lysis buffer (25mM Tris-Cl pH 7.5, 25mM EDTA, 2.5% (w/v) SDS) added to sample, vortexed briefly and then incubated for 30 min at 65°C. 166µl of 3M potassium acetate was added and samples incubated on ice for 10 min, centrifuged at 13000 rpm for 10 min at 4°C, and supernatant transferred to a new Eppendorf tube. 800µl of ice cold ethanol was added and sample incubated on ice for 10 min, then DNA pelleted by centrifugation for 10 min at 13000 rpm, and DNA washed in 70% ethanol. Samples were then spun down at 8000 rpm for 5 min, ethanol removed and pellet air dried and resuspended in ddH_2O. Plasmids were either stored at -20°C until use.

2.18.6 Preparing protein extracts from *S.cerevisiae*

To prepare protein extracts from diploid *S.cerevisiae*, a 10ml cell culture was grown overnight and the following morning NaAzide added to a final concentration of 10mM and sample centrifuged at 4°C for 5 min at 4000 g in a Beckman Alegra centrifuge (6H 3.8 rotor). Cell pellet was resuspended in 1ml 10mM NaAzide and PMSF added to a final concentration of 10mM, incubated on ice for 5 min and pelleted at 3000 rpm for 5 min. Supernatant was removed and the wet weight of the pellet calculated. Cell pellet was then resuspended in 400µl Yeast Lysis Buffer (50mM Tris-Cl pH 8.0, 150mM NaCl, 10% Glycerol, 20mM Na-pyrophosphate, 50mM Na-flouride, 60mM Na-β-glycerophosphate, 2mM Na-orthovanadate, 1x protease inhibitor (Roche), 10mM PMSF). 2mg of acid washed glass beads/mg pellet wet weight were added to each sample and subjected 1 min vortexing at full power, followed by 1 min on ice, repeated 5 times. Supernatant was then removed into a fresh eppendorf, centrifuged

at 13000 rpm for 5min in an Eppendorf 5417R (5417 C/R rotor) centrifuge, and supernatant retained as the soluble nuclear fraction. Lysates were used immediately or stored at -20°C.

2.18.7 Miller assays

Miller assays were performed as described previously to determine β-galactosidase activity (Miller, 1972). Briefly, 5ml cultures were grown overnight in SD$\Delta^{URA}\Delta^{LEU}$ media at 30°C with rotation, before a sample of this culture was inoculated in fresh media the following morning until an OD_{600} of 0.6-1 achieved and this value recorded. 1ml of culture was centrifuged at 13000 rpm for 5 min and supernatant discarded. Cells were resuspended in 1ml of Z-buffer (60mM $Na_2HPO_4.7H_2O$, 40mM $NaH_2PO_4.H_2O$, 10mM KCL, 1mM $MgSO_4.7H_2O$, 50mM β-mercaptoethanol, pH7). 100µl chloroform and 60ul 0.1% SDS were added and cells vortexed at top speed for 10 s. Samples were pre-incubated at 28°C for 5 min, then the reaction was started by addition of 200µl of 4mg/ml ONPG (ortho-Nitrophenyl-β-galactoside) (Sigma N1127) in Z-buffer. Reactions were stopped by addition of 500µl of 1M Na_2CO_3 when samples had developed a pale yellow colour and the assay time was recorded. Cell debris was removed by centrifugation at 13000 rpm for 10 min and the $0D_{420}$ values (optical density of the o-nitrophenol product) of each reaction measured. Enzymatic activity (β-galactosidase units) was calculated as shown below.

$$\frac{1000 \times 0D_{420}}{OD_{600} \text{ of assayed culture x volume assayed (ml) x time (min)}}$$

Where required, 200mM hydroxyurea or 0.1% Methyl methanesulfonate (MMS) was added to liquid cultures for 3 h and Miller assay performed as described above.

2.18.8 Long term growth on Histidine-deficient plates

Diploid yeast strains were grown overnight at 30°C with rotation in SD$\Delta^{URA}\Delta^{LEU}$ - media. The following day cultures were diluted to 1x10^7cells/ml and serially diluted 1/10 in PBS. 5µl of each dilution was spotted onto both SD$\Delta^{URA}\Delta^{LEU}\Delta^{HIS}$ agar plates lacking Histidine (for low stringency detection of positive interactions) and YPD agar (loading control). 3-amino-1,2,4-triazole (3-AT) (Formedium) was added to additional SD$\Delta^{URA}\Delta^{LEU}\Delta^{HIS}$ plates for intermediate (2mM 3-AT) and high stringency (6mM 3-AT) assessment of positive interactions. Plates were incubated at 30°C for seven days before imaging and analysis in Photoshop.

2.19 Tissue culture techniques

2.19.1 HeLa cell culture

HeLa cells were maintained in Dulbecco's minimum essential media (DMEM) (Sigma D5796) supplemented with 10% FBS (Sigma F7524) and 1X glutamine (Gibco 25030) at 37°C with 5% $C0_2$ unless stated otherwise.

2.19.2 FLP-IN cell lines

Stable cell lines were created using the FLP-IN T-REX core kit as per manufacturer guidelines (Invitrogen) to integrate Flag-Upf1 structural and phosphosite mutants into the T-Rex host HeLa cell line. T-Rex stage HeLa cells containing integrated genomic FRT sites (a generous gift from Dr P. Eyers) were maintained in DMEM

supplemented with 10% FBS, 1x glutamine, 4µg/ml Blasticidin and 50µg/ml Zeocin (Invitrogen).

To generate FLP-IN stable cell lines, 100mm dishes were seeded with $1.6x10^6$ T-Rex HeLa cells the day before transfection in media containing 4µg/ml blasticidin and 50µg/ml Zeocin. The following day, the plasmids PCDNA5/FRT/TO/CAT-Flag-Upf1^{res} and pOG44 were co-transfected in a 1:9 ratio using Polyfect reagent (see 2.19.4.1 Polyfect transfection). Transfected cells were maintained in DMEM supplemented with 10% FBS, glutamine and 4µg/ml blasticidin without Zeocin for 24 h and media then replaced with fresh media containing 4µg/ml blasticidin without Zeocin for an additional 24 h. 48 h after transfection, cells were trypsinised (2ml of 0.005% Trypsin/EDTA) and transferred into T25 flasks at a range of densities (10-40% confluent in media containing 4µg/ml blasticidin), incubated for 4 h to facilitate adherence to the substrate. The medium was then replaced with DMEM supplemented with 10% FBS, glutamine, 4µg/ml Blasticidin and 20µg/ml Hygromycin (Invitrogen). This media was changed every 2-3days until isolated colonies of proliferating cells were observed, and then these colonies expanded to produce stable cell lines. This process was repeated for all Flag-Upf1 mutants used in this study.

2.19.3 Doxycycline treatment of FLP-IN cells

Expression of Flag-Upf1^{res} in cell lines was induced through the addition of a 100µg/ml Doxycycline/PBS stock to a final concentration of 0.1-1ug/ml in media for the required length of time.

2.19.4 Mammalian cell transfection techniques

2.19.4.1 Polyfect transfection of plasmid DNA

The quantities below were used for transfections in 6-well plates or 3.5cm dishes. The day before transfection, $2x10^5$ cells were seeded in 2ml of DMEM containing 10% FBS and 1% glutamine (complete DMEM). On the day of transfection 1.5µg of DNA was diluted into 100µl of serum-free DMEM (without FBS or glutamine). 12µl of Polyfect reagent was added to the DNA solution and mixed by pipetting. Cells were washed in 2ml of PBS and 1.5ml of complete DMEM added to the cells. The Polyfect/DNA mixture was incubated at room temperature for 10 min. 600µl of complete DMEM was added to the Polyfect/DNA mix and the whole sample added to the cells.

For 100mm dishes, $1.6x10^6$ cells were seeded the day before transfection in 8ml of complete DMEM. 6µg of DNA was dissolved in 300µl of serum-free DMEM and 50µl of Polyfect was added and processed as described above. 7ml of complete DMEM was then added to cells and 1ml complete DMEM added to the Polyfect/DNA mix before adding to cells. Transfected cells were left to express for 24-96 h.

2.19.4.2 Oligofectamine transfection of siRNA

The quantities below were used for transfections in 6-well plates or 3.5cm dishes. The day before transfection, $2x10^5$ cells were seeded in 2ml of DMEM containing 10% FBS and 1% glutamine (complete DMEM) free of antibiotics. 5µl of Oligofectamine reagent (Invitrogen) was diluted with 25µl of serum-free DMEM and incubated at room temperature for 10 min. 5µl of 20µM siRNA stock was diluted with 175µl serum-free DMEM to give a final concentration of 100nM siRNA. 30µl of diluted

Oligofectamine was mixed with the diluted siRNA and incubated at room temperature for 20 min. Cells were washed 1x with serum-free DMEM and 800µl fresh serum-free DMEM added to cells. The siRNA/Oligofectamine was added to cells and incubated at 37°C for 4 h. After 4 h 500µl of 30% FBS/DMEM was added to cells and knockdowns left for 24-96 h. A non-targeting siRNA (Thermo Scientific D-001810-01) was used as a negative control.

2.19.5 Cryo-preservation of cells

Cell lines were pelleted at 1000 g for 5 min in a Biofuge Primo Heraeus bench top centrifuge (Heraeus #7591 rotor) and resuspended in 10% DMSO and 90% FBS. Cells were slowly frozen using a Mr Frosty cell freezing chamber (Invitrogen) at -80°C for one week before being transferred to liquid nitrogen for long-term storage.

2.20 Flow cytometry

Briefly, $2x10^5$ FLP-IN cells were seeded into 6-well plates and transfected with 100nM siRNA and 1µg/ml doxycycline for 72 h. Cells were washed twice in PBS before trypsin added and cells incubated at 37°C and monitored by light microscopy until cells had detached. They were resuspended in 10ml IFA buffer (10mM HEPES pH7.4, 150mM NaCl, 4% serum, 0.1% sodium azide) and were centrifuged at 1000 rpm for 5 min at room temperature, supernatant removed and cells resuspended in residual 0.5ml of IFA buffer. 4.5ml of ice-cold 70% ethanol was added drop-wise while shaking and cells incubated on ice for 30 min then centrifuged at 1000 rpm for 5 min at 4°C. Supernatant was removed and cells resuspended in residual 70% ethanol, before 70% ethanol was step was repeated and cells stored at -20°C in ethanol until required or

immediately stained with propidium iodide (PI) as described below. Fixed cells were centrifuged at 1000 rpm for 5 min at 4°C before removing supernatant and washing in 10ml of ice-cold PBS. 1ml of PI stain (20µg/ml propidium iodide, 200µg/ml RNase A in PBS) was added to cells and incubated at room temperature for 30 min. Samples were analysed using a BDLSRII flow cytometer at the University Of Sheffield Medical School and data analysis performed using FlowJo software.

2.21 Telomeric Fluorescent *In situ* Hybridisation (FISH)

Telomeric regions of HeLa metaphase spreads were identified with a Cy3-$(C_3TAA)_3$ PNA (protein-nucleic acid) telomeric C-probe (Panagene F1002-5) as described previously (Azzalin et al., 2007). Briefly, $2x10^5$ FLP-IN cells were seeded into 6-well plates and transfected with 100nM siRNA and 1µg/ml doxycycline for 72 h. 0.05µg/ml Colcemid (Sigma D1925) was then added for 4 h at 37°C. Media was removed and cells washed gently in PBS before adding 1ml of trypsin and incubating at 37 °C until cells had detached. 6ml of 56mM KCl (pre-warmed to 37°C) was added, and the cell suspension transferred to a Falcon tube prior to centrifugation at 1200 rpm for 3 min Beckman Alegra centrifuge (6H 3.8 rotor) and supernatant removed. The cell pellet was resuspended carefully (to not disrupt cell membranes) in 10ml of 37°C 56mM KCl and incubated at 37°C for 5 min before centrifugation for 5 min at 1200rpm. Supernatant was removed and cells resuspended in 1ml residual KCl to remove cell clumps. Cells were fixed by slowly adding 1ml of methanol/acetic acid (3:1) while gently agitating the tube followed by an additional 4ml of fixative. Fixed cells were centrifuged at 1200 rpm, before the supernatant almost completely discarded, leaving a small volume in the tube. Cells resuspended in this residual liquid before spreading

onto ethanol-cleaned glass slides (Thermo Scientific BS7011/2) and then air dried for 1 h at room temperature. Slides were treated in 4% formaldehyde/PBS for 4 min at room temperature followed by 2 x 5 min washes in PBS. Slides were treated with 100µg/ml RNase in 2xSSC buffer (0.3M NaCl, 0.03M NaCitrate) for 1 h at 37°C before dehydration though a 70%/85%/100% ethanol series and air-drying at room temperature. 15µl of PNA telomeric probe solution (70% formamide, 0.5% blocking reagent (Roche), 10mM TrisHCl pH7.2, 0.5µg/ml Cy3-$(C_3TAA)_3$ PNA probe) was added to a coverslip, placed on the slides and sealed with rubber cement. Slides were then incubated at 80°C for 5 min in a thermal cycler and incubated at room temperature overnight. The following day, coverslips were removed and the slides washed 2x 15 min in 70% Formamide, 10mM Tris-HCl pH7.2 and then 3x 5 min in 0.1 M Tris-HCl, 0.15 M NaCl, 0.08% Tween-20 (pH7.5) at room temperature. DNA was stained with 100ng/ml DAPI in 2xSSC for 20 min and slides washed once in 0.1M Tris-HCl, 0.15 M NaCl, and 0.08% Tween-20 (pH7.5) for 5 min. 15µl of 2xSSC was added to slides and sealed with a coverslip.

Images stacks were acquired a Deltavision RT widefield system fitted with an Olympus UPLSAPO 60x/1.35 objective. Image stacks were deconvolved and processed using SoftWorX (Applied Precision, Issaquah, Washington). Telomere-free ends were classified by eye using the Image J software and defined as a terminal DAPI signal (blue) lacking a telomeric FISH signal (red).

2.22 Protein techniques

2.22.1 Whole cell extract preparation

For preparation of whole cell extracts for analysis by Western blot, dishes or flasks containing HeLa cells were placed on ice, media was aspirated and cells washed once with ice cold PBS. Cells were lysed by addition of IPLB (20mM Tris acetate pH7.5, 0.27M sucrose, 1mM EGTA, 1mM EDTA, 1mM sodium orthovanadate, 10mM sodium β-glycerophosphate, 5mM sodium pyrophosphate, 1% Triton X-100, 50mM sodium fluoride, 0.1% β-mercaptoethanol, 0.2mM PMSF, 1X protease inhibitor cocktail(Roche), 1µM microcystin) and transferred to an Eppendorf tube. Lysates were then clarified through 3x freeze-thaw cycles and centrifuged at 13000 rpm for 5min in an Eppendorf 5417R bench top centrifuge to pellet insoluble material. For large-scale lysate preparations, cells resuspended in IPLB were passed 7x through a 25 gauge needle instead of freeze-thaw cycles. The supernatant (soluble protein fraction) was transferred to a new tube. Protein concentration was determined by Bradford assay and lysates stored at -20°C.

2.22.2 Bradford assay

Protein concentration was determined using Bio-Rad Protein Assay reagent based on the protein dye binding method of Bradford, (1976). The protein sample being measured was mixed with 800µl MiliQ H_2O and 200µl Bradford reagent. The absorbance was measured at OD_{595} and compared to known BSA standards.

2.22.3 SDS-polyacrylamide gel electrophoresis

Polyacrylamide gel electrophoresis was carried out under denaturing conditions using mini-gels (82mm x 102mm) according to the method of Laemlli

(Laemmli, 1970). Prior to electrophoresis, protein samples were boiled for 5 min in 1x SDS loading gel buffer (50mM Tris-Cl (pH6.8), 100mM DTT, 2% SDS, 10% glycerol, 0.01% (w/v) bromophenol blue). Polymerised gels were assembled into the Bio-Rad Mini-PROTEAN II apparatus, before the inner and outer reservoirs were filled with SDS electrophoresis running buffer and current applied to run samples through the gel under typical electrophoresis conditions (150V, 400mA, for 30-60min)

2.22.4 Immunoblotting

Immunoblotting was performed essentially as described (Burnette, 1981). Immediately after electrophoresis, polyacrylamide gels were removed from their retaining plates, and overlaid with nitrocellulose paper (Whatmann Protran). Protein was transferred to nitrocellulose sandwiched between 4 sheets of Whatman paper at 100V, 400mA for 75 min using the Bio-Rad Mini-PROTEAN II apparatus. After transfer onto nitrocellulose, protein bands were visualised using Ponceau S stain (0.1% Ponceau S in 5% acetic acid) by staining for 1 min before being washed away with ddH_2O. The nitrocellulose membrane was blocked for 1 h at room temperature using TBS (Tris-CL pH7.5, 150mM NaCl) containing 5% Marvel milk powder. The nitrocellulose was incubated with primary antibody diluted in either TBS containing 5% Marvel milk powder or BSA depending on antibody requirement for 1 h at room temperature or 4°C overnight. Membranes were then washed in TBS for 6 x 5 min. The blots were then incubated with the secondary antibody again diluted in TBS/5% milk for 1 h at room temperature. Nitrocellulose was washed 1 x 10 min and 5 x 5 min using TBS before blots were incubated with ECL reagents according to manufacturer's instructions and chemiluminescence detected using x-ray film.

2.22.5 Cellular fractionation

Actively growing HeLa cells were untreated or S-phase enriched by exposure to 2mM hydroxyurea for 24 h before being washed, fresh media added and incubated for a further 3 h at 37°C. Sub-cellular fractionation was performed as described previously (Mendez and Stillman, 2000). Briefly, cells were trypsinised, resuspended in PBS and counted to establish total cell number. After centrifugation at 1000 rpm for 5 min in a Biofuge Primo Heraeus bench top centrifuge (Heraeus #7591 rotor), the cell pellet was resuspended in an appropriate volume of Buffer A (10mM HEPES, 10mM KCl, 1.5mM $MgCl_2$, 0.34M sucrose, 10% glycerol, 1mM DTT, 1x protease inhibitor cocktail (Roche), 0.1mM PMSF) to give a final cell concentration of $4x10^4$/ml. 0.1% TritonX-100 was added and cells incubated on ice for 5 min. Samples were centrifuged at 13000 g for 4min and the supernatant (cytoplasmic components) removed and centrifuged at 20000 g to remove insoluble material and stored as the S2 fraction. The nuclear pellet was washed in 2x the original volume of buffer A used by incubating on ice for 5min, centrifuging as before then discarding the supernatant. The washed nuclear pellet was resuspended in the same volume of Buffer B (3mM EDTA, 0.2mM EGTA, 1mM DTT, 1x protease inhibitor cocktail (Roche) as in the initial Buffer A resuspension. Nuclei were incubated on ice for 30min and centrifuged at 1700 g for 4min. The supernatant was removed and retained as the soluble nuclear (S3) fraction. The pellet was washed in 2x the original volume of buffer B by incubating on ice for 5min and centrifuging at 1700 g for 5 min then discarding the supernatant. The insoluble material was retained as the chromatin-associated fraction (P3). The P3 fraction volume was measured and mixed with an equal volume of 5x SDS loading buffer (250mM Tris-HCl (pH6.8), 500mM DTT, 10% SDS, 50% glycerol, bromophenol blue). Samples were normalised to cell number

prior to analysis by SDS-PAGE and a sample representative of an equal number of cells loaded into each lane. The amount of chromatin bound Flag-Upf1 in each experiment was quantified using ImageJ and normalised to the amount of Flag-Upf1 found in the nuclear soluble fraction, assuming equal loading in each lane.

2.22.6 Nuclear extract preparation

100mm dishes of confluent HeLa cells were trypsinised, resuspended in PBS and counted to establish total cell number. Cell pellet was resuspended in an appropriate volume of Buffer A (10mM HEPES, 10mM KCL, 1.5mM $MgCl_2$, 0.34M sucrose, 10% glycerol, 1mM DTT, 1x protease inhibitor cocktail (Roche), 0.1mM PMSF) to give a final cell concentration of $4x10^4$/ml. 0.1% Triton-X-100 was added and cells incubated on ice for 5 min. Samples were centrifuged at 1300 g for 4min and the supernatant (cytoplasmic components) discarded. Pellet containing intact nuclei was washed in 2x the original volume of buffer A used by incubating on ice for 5min before centrifugation as before and supernatant discarded. The structural integrity of prepared nuclei was determined by light microscopy and the nuclei pellet was subjected to lysis in IPLB and processed as described for whole cell extracts.

2.22.7 Co-immunoprecipitation

For whole cell extract immunoprecipitations, cells were lysed in 150mM NaCl, 10mM Tris-HCL pH7.4, 2.5mM $MgCl_2$, 0.5% NP-40, 0.2mM Na_3VO_4, 1x complete protease inhibitor (Roche). 2mg of whole cell extract was incubated with 3.3µg of specific antibody or IgG of the same species for 16 h at 4°C with rotation. 50µl of 50% (w/v) Protein G bead slurry in PBS was added and incubated for an additional 1 h at 4°C with rotation. Immunoprecipitated complexes were collect by centrifugation in a

micro-centrifuge at 1000 rpm for 3 min and washed 5x 5 min in 1ml lysis buffer. Beads were collected and 50µl of sample buffer added before boiling for 5 min, re-centrifugation as before to remove the beads, and the supernatant used for SDS-PAGE.

For nuclear extract immunoprecipitations, intact nuclei were lysed in IPLB plus Triton (20mM Tris acetate pH7.5, 0.27M sucrose, 1mM EGTA, 1mM EDTA, 1mM sodium orthovanadate, 10mM sodium β-glycerophosphate, 5mM sodium pyrophosphate, 0.1% Triton X-100, 50mM sodium fluoride, 0.1% β-mercaptoethanol, 0.2mM PMSF, 1X protease inhibitor cocktail (Roche), 1µM microcystin). 0.25mg of nuclear extract was incubated with 1µg of specific antibody or IgG of the same species for 1 h at 4°C with rotation. A 20µl aliquot of a 50% protein G bead slurry pre-washed into IPLB was added to each sample and incubated for a further 1 h at 4°C. Complexes were left unwashed or washed 3x 5 min in 1ml IPLB. Beads were collected and 20µl of sample buffer added before boiling for 5 min re-centrifugation as before to remove the beads, and the supernatant used for SDS-PAGE.

2.23 RNA techniques

2.23.1 Phenol/chloroform RNA extraction

Cells were washed twice in ice-cold PBS before addition of 1ml of TRI reagent (Sigma 93289). A cell scraper was used to collect cellular material then passed several times through a 1ml pipette and vortexed thoroughly. Samples were incubated for 5 min at room temperature before centrifugation in a micro-centrifuge at 13000 rpm for 5 min. The supernatant was transferred to a fresh Eppendorf tube to which was added 0.2ml chloroform and samples vortexed for 20 s then centrifuged 12000 g Eppendorf 5417R (5417 C/R rotor) for 15 min at 4°C. The colourless upper aqueous phase was taken to a clean Eppendorf tube and 0.5ml isopropanol added. The mixture was incubated for 10 min at room temperature before centrifuging at 12000 g in an Eppendorf 5417R (5417 C/R rotor) for 10 min at 4°C. The supernatant was removed and the RNA pellet washed twice with 70% ethanol and centrifuged at 7400 g Eppendorf 5417R (5417 C/R rotor) for 5 min at 4°C. The RNA pellet was air-dried and dissolved in 15µl MilliQ H_2O. RNA concentration was determined by absorbance measurement at 260nm using a Nanodrop 1000 spectrophotometer and samples stored at -20°C.

2.23.2 Nonsense mediated decay assay qPCR

The plasmids pmCMV-G1 Norm, pmCMV-G1 Ter and phCMV-MUP (a kind gift from Dr Lynne E Maquat) were transiently transfected into cells using Polyfect 24 h before RNA was harvested by phenol/chloroform extraction. 2µg of RNA extract was converted to cDNA using the high capacity RNA-cDNA kit (Applied Biosciences) and cDNA concentration measured using at 260nm using a Nanodrop spectrophotometer.

cDNA samples were diluted to 100ng/µl and 1µl cDNA added to the qPCR mix (5µl SYBR Green, 0.0125µl forward primer (100µM stock concentration), 0.0125µl reverse primer (100µM stock concentration) and 3.98µl H_2O) in a 96-well plate well, in triplicate. Relative mRNA levels were determined by the standard curve method (Larionov et al., 2005) and normalised to MUP mRNA levels in each sample. Protein lysates were also prepared in parallel to assess knockdown and expression levels.

The qPCR cycling parameters are shown below.

Segment	**Cycles**	**Temperature**	**Time**
1	1	95°C	3 min
2	39	95°C	30 s
		62°C	30 s

2.24 Statistical analysis

Graphs were produced in Microsoft Excel and statistical analysis undertaken using a two tailed T-test assuming unequal variance to compare the means between different conditions in the NMD assays.

Chapter 3 Yeast two-hybrid analysis of the interaction between human Upf1 and the p66 subunit of DNA polymerase δ

3.1 Introduction

Studies investigating frameshift suppression in *S.cerevisiae* identified Up-frameshift 1 (Upf1p), a superfamily 1 RNA helicase required for NMD and transcriptional regulation (Cui et al., 1995; Culbertson et al., 1980; He et al., 1993; Leeds et al., 1992). Whilst Upf1p null *S.cerevisiae* display no significant phenotype (Leeds et al., 1991), knockdown of Upf1 in human cells causes genomic instability and Upf1 null mouse embryos die at early developmental stages (Azzalin and Lingner, 2006b; Medghalchi et al., 2001). The underlying cause of this dependency in mammalian cells is not yet known, however Upf1 was demonstrated to co-purify with the p66 subunit of DNA polymerase δ (polδ) in bovine thymus extracts and co-immunoprecipitate both the p125 and p66 polδ subunits in HeLa cells (Azzalin and Lingner, 2006b; Carastro et al., 2002; Li et al., 1992). The S-phase recruitment of Upf1 to chromatin and interaction with polδ in human cells suggest Upf1 may have functions as a replicative helicase for lagging strand DNA synthesis (Azzalin and Lingner, 2006b; Carastro et al., 2002). Characterisation of the structural domains through which Upf1 associates with pol δ should provide further insight into how this interaction contributes to DNA replication, the maintenance of genomic stability and ultimately, the contribution of Upf1-mediated mechanisms of genomic stability to both organismal development and survival.

My aim in this section was the structural dissection of the interaction between human Upf1 and the p66 polδ subunit using a yeast two-hybrid assay, and in particular structural motifs in Upf1 that might *uniquely* be required for this molecular interaction,

an approach used previously to show human Upf1 interactions with mRNA decay proteins (Cho et al., 2009) and in dissection of the human p66-PCNA interaction (Pohler et al., 2005). The objective was to use this information to generate cell lines containing mutant Upf1, lacking this unique function, to establish its contribution to checkpoint function and genomic stability, independently of its role in mRNA surveillance.

3.2 Assessment of Upf1-p66 interaction through biochemical analysis of β-galactosidase activity

Before I could investigate the Upf1 domains required for interaction with p66, I had to demonstrate this interaction could be recapitulated in the yeast two-hybrid system.

I generated plasmid constructs expressing full-length human Upf1 and p66 fusions either with the DNA binding (BD) or transcriptional activating (AD) domains of the Gal4 transcription factor, as described in Materials and methods. An additional construct expressing the *S.pombe* PCNA homologue Pcn1 fused to the Gal4-AD was also generated, as a positive control for detecting interaction with p66 (Pohler et al., 2005). These constructs were transformed into *S.cerevisiae* strains and when established, mated to generate diploid strains expressing both BD- (bait) and AD- (prey) proteins fusions, as described in Materials and methods. The presence of both constructs in diploid strains was demonstrated by extraction of plasmids from cells and restriction digests used to confirm the presence of the relevant cDNA in each construct (Figure 3.1). Expression of fusion proteins was confirmed by Western blot (Figure 3.2). In the case of the AD-Upf1 fusion construct, the resultant protein was not recognised

by Upf1 antibodies, however a Gal4-AD specific antibody reacted with a species of the correct molecular mass (Figure 3.2).

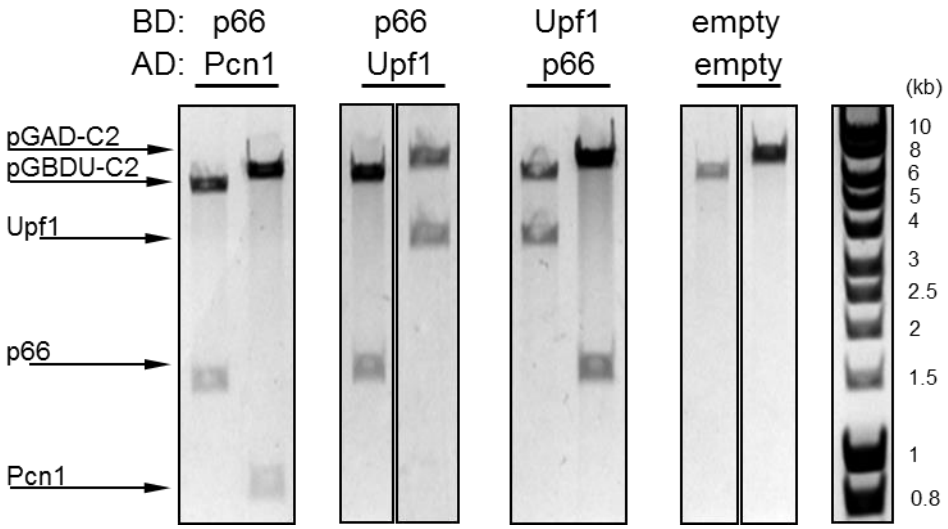

Figure 3.1 Conformation of plasmids in diploid strains

Plasmids were extracted from diploid *S.cerevisiae* as described in Materials and methods. They were then transformed into competent *E.coli*, before single colonies isolated and grown into liquid cultures. Plasmids were then isolated from these, digested with BamHI/ClaI and separated by agarose gel electrophoresis to identify the relevant original cDNA in each strain. Strains are indicated above and the relative positions of expected fragments highlighted. Expected fragment sizes: AD = pGAD-C2 (6.7kb), BD = pGBDU-C2 (6kb), Upf1 (3.4kb), p66 (1.4kb) and Pcn1 (0.8kb).

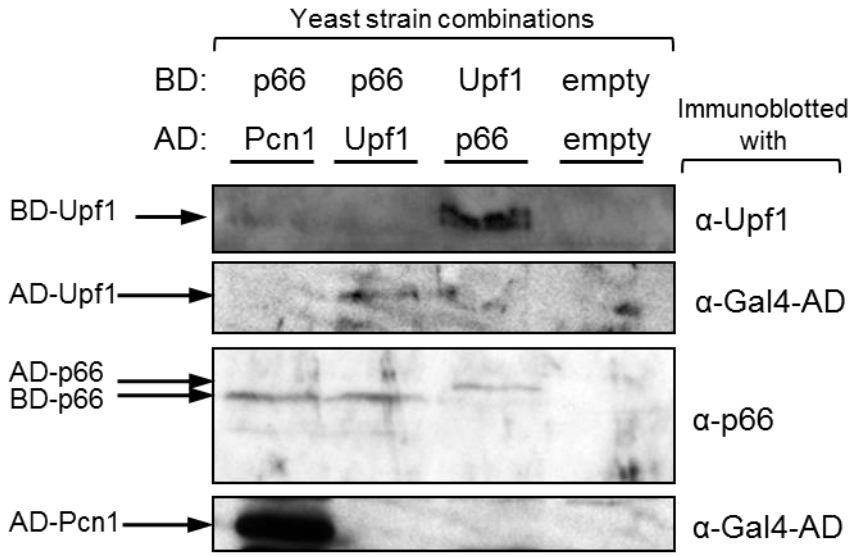

Figure 3.2 Fusion protein expression in diploid strains

Protein extracts were prepared from yeast cells as described in Materials and methods. Samples were separated by SDS-page and analysed by Western blot using specific antibodies against human Upf1, human p66 or yeast Gal4-AD. Above each lane is indicated the combination of Gal4-DNA binding (BD) or Gal4-Activation (AD) fusions with Upf1, p66 or Pcn1 contained within each diploid strain. BD=13kDa AD=20kDa.

Interaction between Upf1 and p66, in either bait and prey configuration, should bring the two halves of the transcription factor into sufficiently close proximity to induce transcription of the LacZ reporter gene. The product of this gene, the enzyme β-galactosidase, was used to assess the extent of Upf1-p66 interaction, through biochemical measurement of β-galactosidase enzymatic activity using a Miller assay (Miller, 1972). Briefly, diploid *S.cerevisiae* strains containing AD- and BD- fusions were grown overnight until an OD_{600} 0.6-1 was reached, then a sample of cells permeabilised, prior to incubation with the β-galactosidase substrate ONPG (ortho-nitrophenyl-β-galactoside). Reactions were stopped when a pale yellow colour developed and the OD_{420} of the reaction product in alkali (o-nitrophenolate) measured and β-galactosidase activity units calculated, as described in Materials and methods.

Positive control cells expressing p66 bait and Pcn1 prey fusions generated high levels of β-galactosidase activity indicative of a successful interaction (Figure 3.3, lane 1). Only background levels of enzymatic activity were produced in cells expressing both Upf1 and p66 fusions in either orientation, ie as either bait or prey (Figure 3.3, lanes 3 and 4), demonstrating Upf1 and p66 did not interact in this assay.

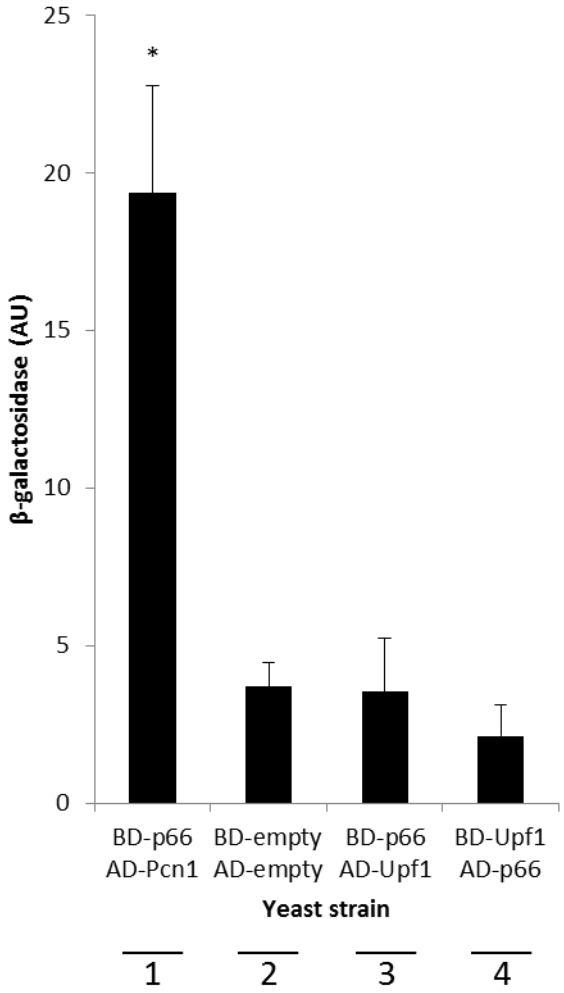

Figure 3.3 Assessment of protein interaction in Miller assays

Bait proteins were expressed as Gal4 DNA binding (BD) fusions in the pGBDU-C2 plasmid and transformed to the PJ69-4α yeast strain. Prey proteins were expressed as Gal4 activation (AD) fusions and transformed into the PJ69-4a yeast strain. Mating of bait and prey strains generated diploid cells which were maintained on SD-Ura/Leu medium, to select for this presence of both plasmids. Liquid cell cultures of double transformants were grown overnight then β-galactosidase enzymatic activity was assessed using Miller assays (see Materials and methods). The binding of a PCNA homologue (*S.pombe* Pcn1) to human p66 provided a positive control and negative controls contained empty pGBDU-C2 and pGAD-C2 plasmids only. n=3 *$p<0.05$.

3.3 Exposure to DNA damage does not induce the interaction between Upf1 and p66 in *S.cerevisiae*

PIKK-dependent Upf1 hyperphosphorylation and chromatin recruitment in response to genomic stress suggested phosphorylation may regulate Upf1 nuclear interactions in mammalian cells (Azzalin and Lingner, 2006b; Denning et al., 2001; Muller et al., 2007b; Yamashita et al., 2001). If Upf1 is recruited to sites of DNA damage through interaction with polδ, then I hypothesised this may also occur in response to replication stress. I therefore decided to expose cells to genomic stress in an attempt to stimulate this interaction.

Diploid *S.cerevisiae* strains containing AD- and BD- fusions were grown overnight, and the following morning cultures were incubated for an additional three h in the presence of 200 mM hydroxyurea (HU) (Bachant et al., 2005), to induce replication fork stall and 0.1% methyl-methane-sulfonate (MMS) (Harvey et al., 2005), to cause double-strand DNA breaks. Miller assays were then repeated as described previously. Exposure to HU or MMS did not generate an increase in β-galactosidase activity in cells expressing Upf1 and p66 fusions in either orientation (Figure 3.4), suggesting this interaction was not stimulated by replication stress in this assay.

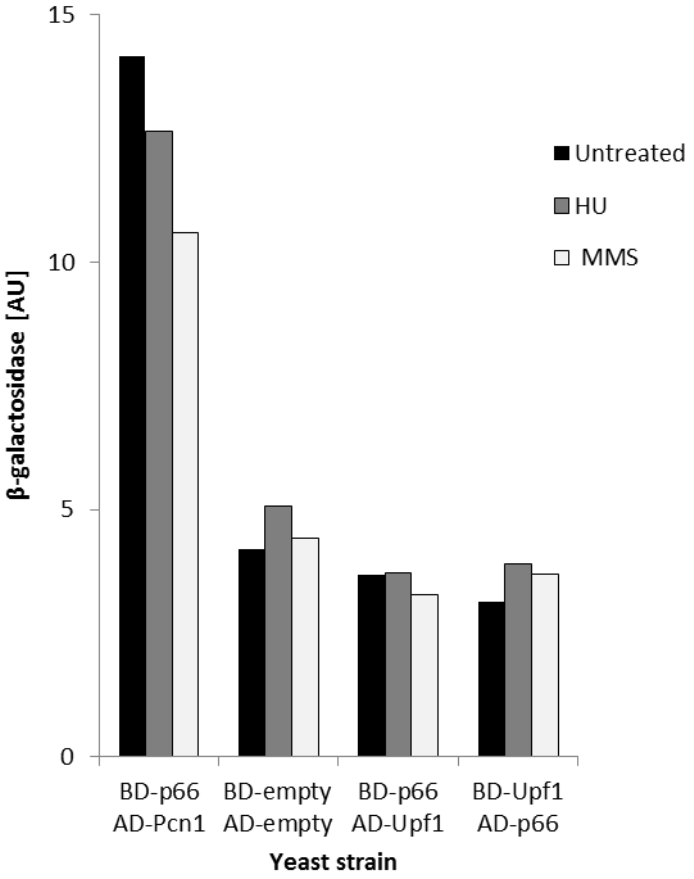

Figure 3.4 Replication stress does not stimulate an interaction between Upf1 and p66

Liquid cell cultures of double transformants were grown overnight, and the following morning incubated for three h with 200mM hydroxyurea or 0.1% MMS before Miller assays were performed as described previously. n=1

3.4 Analysis of the Upf1-p66 interaction using histidine dependency

Miller assays proved unsuccessful in demonstrating an interaction between Upf1 and p66, so I decided to investigate this interaction using an alternative yeast two-hybrid method. A successful yeast two-hybrid interaction also brings about the transcription of the GAL4-driven HIS3 gene. This results in the synthesis of Imidazole glycerol-phosphate dehydratase, an enzyme essential for the synthesis of the amino acid histidine, allowing for identification of cells facilitating histidine synthesis on selective agar plates lacking this amino acid. This approach differs from the β-galactosidase assay as it involves cell growth over several days and therefore weak or transient interactions, that occur under relatively low stringency conditions, may be detected by allowing cellular proliferation under these conditions.

Diploid *S.cerevisiae* strains containing AD- and BD- fusions were grown overnight and serial dilutions of cells spotted out onto selective, histidine-lacking (-HIS), “dropout” plates or YPD plates to ensure equal loading of cells, and incubated for seven days. Duplicate samples were spotted onto plates containing 3-AT (3-Amino-1,2,4-triazole), a competitor of histidine synthesis, to generate medium and high stringency growth conditions to assess the strength of any interactions.

The positive control proliferated in low (Figure 3.5a) and high-stringency conditions (Figure 3.5b) demonstrating a strong interaction between p66 and Pcn1. Cells expressing Upf1 and p66 fusions did not proliferate above background growth at any level of stringency (Figure 3.5a-b) demonstrating no significant interaction between Upf1 and p66. I attempted to repeat this experiment while transiently

exposing cells to DNA damage, in a manner analogous to that described in section 3.3, but all cell growth was prevented under these conditions (data not shown).

Cumulatively, these data demonstrated the interaction between human Upf1 and p66 could not be recapitulated in the yeast two-hybrid assay under any of the experimental conditions tested.

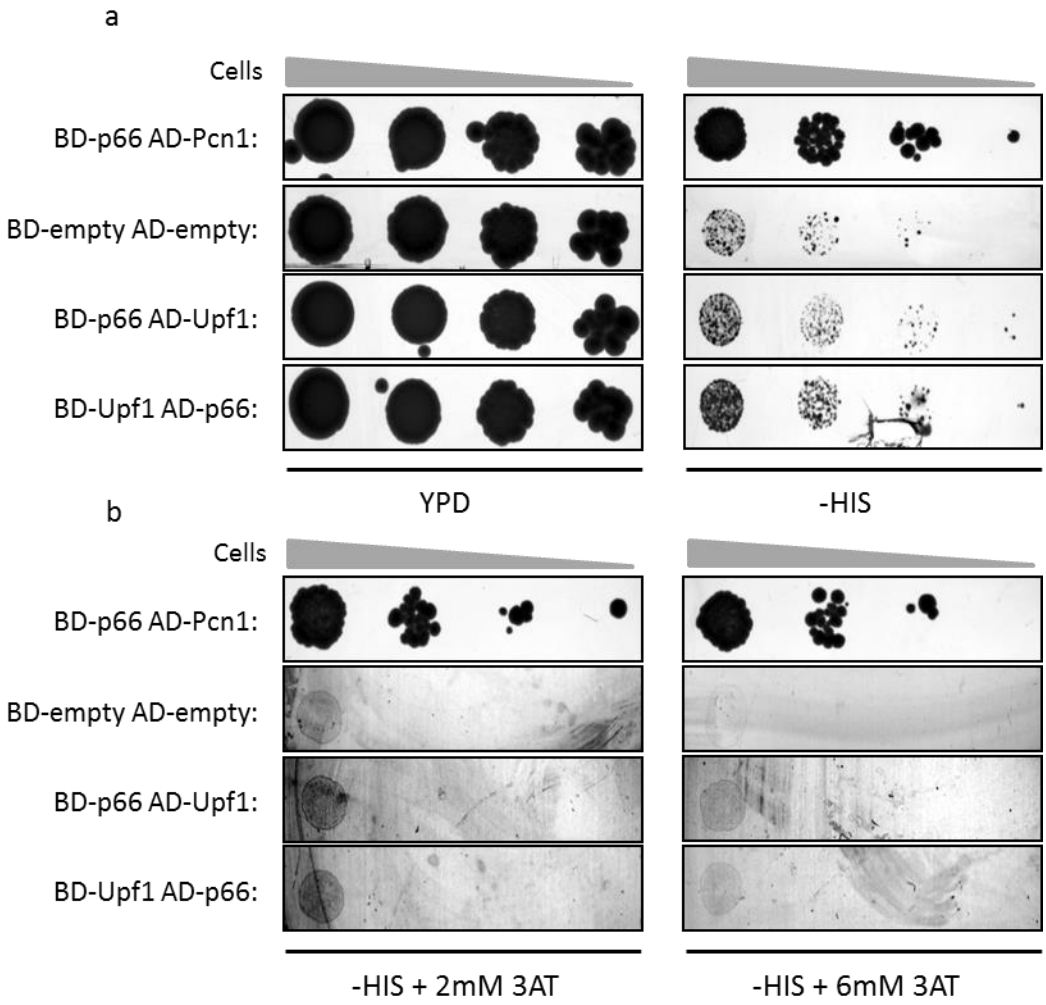

Figure 3.5 Assessment of Upf1 and p66 interaction using histidine dependency

Liquid cell cultures of double transformants were grown overnight before serial dilutions of double transformants were plated onto agar plates and grown for seven days at 30°C. a) YPD plates show loading of cells and -His plates highlight low stringency positive interactions. b) -His plates containing 3AT (3-amino-1,2,4-triazole), a competitive inhibitor of histidine synthesis, allow for medium (2mM) and high (6mM) stringency assessment of positive interactions. Results presented are representative of two independent experiments.

3.5 Discussion

The mRNA surveillance roles of Upf1 are well documented but emerging data in mammalian cells has identified nuclear Upf1 functions involved in the maintenance of genomic stability (Azzalin and Lingner, 2006b). The interaction of Upf1 with chromatin has been proposed to occur through interaction with polδ and utilise the helicase activity of Upf1 during DNA replication or repair (Azzalin and Lingner, 2006b; Carastro et al., 2002). My initial aim in this section of work was to recapitulate the interaction between Upf1 and the p66 polδ subunit in the yeast two-hybrid assay, but I was unable to demonstrate an interaction between Upf1 and p66 under any experimental conditions. In contrast, positive control cells generated strong signals in all assays (Figure 3.3, lane 1 and figure 3.5), demonstrating the absence of signal seen in Upf1 and p66 Gal4 fusion protein expressing cells was a genuine consequence of the absence of interaction in this system. The absence of cross-reactivity of a Upf1 antibody, raised against a C-terminal Upf1 epitope, with Gal4 AD-Upf1 was surprising. I cannot exclude the possibility that the Gal4 AD-Upf1 fusion protein expressed in yeast lacked some elements of the C-terminus of full-length Upf1. An alternative explanation is that, for unknown reasons, the relative expression levels of Gal4 BD- and AD-Upf1 fusions were vastly different, and the sensitivity offered by the Gal4-AD antibody allowed the detection of low levels of this protein fusion.

The yeast two-hybrid system relies on the fusion of domains originating from the GAL4 transcription factor to the N-terminus of proteins of interest. It is possible with these kinds of binding studies that the addition of specific functional domains to particular proteins of interest may prevent normal function of the latter. N-terminal

domains of both Upf1 and p66 have been now demonstrated to contain motifs required for protein-protein interactions (Gong et al., 2009; Okada-Katsuhata et al., 2012; Pohler et al., 2005) and the addition of these 10-20kDa GAL4 sequences to create the relevant fusion proteins *in vivo* may have blocked protein-protein interactions or disrupted essential structure in these regions. N-terminal MYC-tagged hUpf1 co-immunoprecipitated endogenous p66 in HeLa cells (Carastro et al., 2002), suggesting the addition of a small N-terminal tag to Upf1 does not prevent this interaction. However, it is conceivable that the addition of a significantly larger tag to the N-terminus of Upf1, and/ or the addition of a tag to p66 prevented the interaction.

An alternative explanation for the two-hybrid results is that Upf1 and p66 do not physically interact directly *in vivo*. When polδ was purified from bovine thymus extracts, an unknown protein co-purifying with polδ was initially referred to as 'δ-helicase', before being identified as the bovine homologue of Upf1 (Li et al., 1992). Upf1 was then subsequently shown to specifically co-purify with the p66 polδ subunit in thymus extracts (Carastro et al., 2002) to almost complete homogeneity. Polδ is a multi-subunit enzyme (p125, p66, p50, p12) (Hubscher et al., 2002) and although Upf1 has been demonstrated to co-immunoprecipitate the p66 polδ subunit in HeLa cells (Carastro et al., 2002), it also co-immunoprecipitated the p125 polδ subunit (Azzalin and Lingner, 2006b). These data demonstrated Upf1 interaction with multiple polδ subunits, but did not demonstrate Upf1 directly interacts with the p66 subunit. Upf1 may indirectly associate with p66 through interaction with alternate polδ subunits, or via an interaction domain generated by the interaction of multiple subunits, but this is

yet to be tested. However, this could explain why I could not reproduce the interaction between Upf1 and p66 in a yeast two-hybrid assay.

Alternatively, as this interaction is predicted to occur exclusively during S-phase, the stability between Upf1 and p66 observed in bovine thymus (Carastro et al., 2002) may be due to the function of this tissue in immunity. To appropriately ensure telomere homeostasis during clonal expansion, immune cells, found in the thymus, are highly regulated by TERRA. Upf1 has been shown, presumably through interaction with polδ, to regulate TERRA-dependent telomeric DNA replication in S-phase (discussed in Chapter 5). As a result, this interaction may be dependent upon S phase-specific stimuli that target Upf1 *in vivo*. Phosphorylation of Upf1 has been demonstrated to regulate the interactions and biochemical function of Upf1 in NMD (Denning et al., 2001; Kashima et al., 2006; Yamashita et al., 2001) and chromatin-bound Upf1 was demonstrated to be hyperphosphorylated on S/T-Q motifs (Azzalin and Lingner, 2006b). Upf1 is also recruited to chromatin in response to genotoxic stress, and it is a substrate for the PIKKs ATR and SMG1 *in vitro* (Azzalin and Lingner, 2006b; Yamashita et al., 2001) and ATR and SMG1 regulate the phospho-status of Upf1 *in vivo* (Azzalin and Lingner, 2006b; Denning et al., 2001). These data suggest PIKK activity may regulate Upf1 functions when it is located on chromatin (Azzalin and Lingner, 2006b) or associated with proteins involved with DNA metabolism, such as p66.

Exposure to compounds that generate genotoxic stress, with the aim of causing hyperphosphorylation, or other uncharacterised post-translational modification of Upf1 or p66, failed to stimulate an interaction between Upf1 and p66, suggesting either that this interaction may not be dependent on genotoxic stress signalling, or

that the heterologous nature of the system precluded the reconstitution in yeast of the relevant molecular signalling pathways to generate interaction-competent components.

It is not clear whether the signalling pathways specifically phosphorylating Upf1 in response to replication stress in human cells occur in *S.cerevisiae.* Although an ATR homologue (Mec1) is present in this organism (Cha and Kleckner, 2002), no evidence for Mec1-dependent phosphorylation of Upf1p has yet been presented. SMG1 regulates the phosphorylation of Upf1 during NMD (Yamashita et al., 2001) in metazoan systems and it cannot be excluded that SMG1 is involved in the replication stress-dependent recruitment of Upf1 to chromatin in HeLa cells (Azzalin and Lingner, 2006b). The absence of an SMG1 homologue (Yamashita et al., 2001) or nuclear Upf1p in *S.cerevisiae* (Atkin et al., 1995) suggests the specific signalling events required to specifically target human Upf1 to chromatin in the nucleus may be evolutionary acquired mechanisms restricted to higher eukaryotes.

However, at the time this approach was utilised, I did not have access to resources to carry out a full analysis of the post-translational state of either Upf1 or p66 after genotoxic stress treatment in yeast cells. Reduced cellular growth on HU/MMS containing agar plates (data not shown) provided indirect, weak, evidence suggesting replication checkpoint activation, but the identification of phospho-H2A1 and -H2A2, the *S.cerevisiae* H2AX homologues (Harvey et al., 2005; Wyatt et al., 2003) and phospho-hUpf1 using anti-phospho-S/T-Q antibodies, after HU/MMS exposure would be required to confirm whether the DNA damage response had been induced

under the experimental conditions used, and whether Upf1 phosphorylation had been induced.

In conclusion therefore, this experimental approach did not provide any evidence for a direct interaction between Upf1 and the p66 subunit of DNA polymerase δ. In the absence of any evidence that modifications of this approach might bring about a positive signal in either of the versions of yeast two-hybrid experimental approaches tested, it was decided that the yeast two-hybrid system was unlikely to be suitable for further investigation of the role of Upf1 in S-phase.

Chapter 4 Generation of a stable Upf1 expression system to identify Upf1 motifs required for the S-phase specific association with chromatin

4.1 Introduction

A key question is how Upf1, a protein involved in mRNA surveillance, is also involved in the maintenance of genomic stability, a process fundamentally dependent upon the structural integrity of DNA. The involvement of Upf1 in TERRA-mediated telomeric DNA replication, and histone mRNA decay, has been proposed to occur through S-phase specific interactions of Upf1 with both chromatin and components of the DNA replication machinery (Azzalin et al., 2007; Chawla et al., 2011; Kaygun and Marzluff, 2005a; Muller et al., 2007a, b). Incorporation into the multi-component machinery operating at the replication fork, through interactions with DNA polymerase δ, and specifically the p66 polδ subunit (Carastro et al., 2002) was proposed as a mechanism of Upf1 recruitment to chromatin (Azzalin and Lingner, 2006b).

In the previous chapter however, I was unable to find evidence for direct interaction between Upf1 and p66 using a yeast two-hybrid system, suggesting that the association of Upf1 with replication components, and chromatin in general, during S-phase, may involve interactions between multiple components or involve inter-dependent post-translational modifications. Purified Upf1 binds DNA oligonucleotide sequences directly *in vitro* ((Li et al., 1992), Dehghani and Sanders, unpublished) and interacts with both chromatin and telomeric DNA sequences during S-phase *in vivo* (Azzalin and Lingner, 2006b; Azzalin et al., 2007), but, despite the existence of crystal structures of core helicase and CH domains of Upf1 (Cheng et al., 2007; Kadlec et al., 2006), the mechanism by which Upf1 physically associates with chromatin in S-phase is currently unknown (Azzalin and Lingner, 2006b; Azzalin et al., 2007). Blocking NMD

function via siRNA-mediated knockdown of essential NMD components has no effect on genome integrity (Azzalin and Lingner, 2006b), indicating that the role of Upf1 in the maintenance of genome stability must be independent of its NMD function. It is not clear whether the association of Upf1 with chromatin or replication fork machinery plays any role in the co-ordination of DNA replication with histone mRNA stability. Therefore it was important to establish whether domains required for mRNA surveillance are functionally distinct from those involved in the chromatin-associated roles of Upf1. The aim of this section of work therefore was to explore the interaction of Upf1 with chromatin in human cell lines and identify structural motifs within Upf1 required for S-phase recruitment to chromatin.

4.2 Transient transfection of Flag-Upf1 in HeLa cells fails to reproduce known cellular functions

Initially, I transiently transfected a Flag-Upf1 construct into HeLa cells and attempted to demonstrate known Upf1 interactions, prior to analysis of chromatin recruitment. I was unable to immunoprecipitate endogenous p66 with Flag-Upf1 (data not shown) and interaction with NMD proteins could not be demonstrated in mass spectrometric analysis of immunoprecipitated Flag-Upf1 (R.Beniston, data not shown). Western blot analysis of cellular extracts after transient transfection demonstrated Flag-Upf1 expression was significantly in excess of the endogenous protein (Figure 4.1) and generated high background in co-immunoprecipitation experiments (data not shown). Increasing the stringency of immunoprecipitation wash steps, to an extent where this background was reduced, failed to demonstrate co-immunoprecipitation of p66 (data not shown, see Chapter 5). These data suggested that the large excess of Flag-Upf1 generated by over-expression, while not increasing the frequency of

relevant Upf1 interactions *in vivo*, increased the sampling of non-relevant Upf1 molecules, and may therefore potentially have masked any weak or transient Upf1 interactions that may occur during normal cell metabolism.

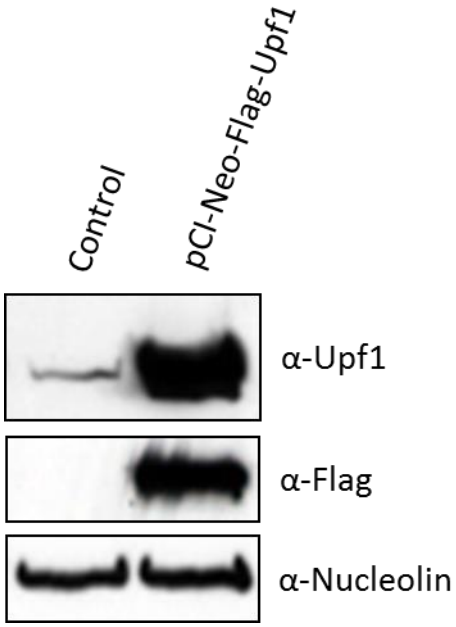

Figure 4.1 Flag-Upf1 expression after transient transfection in HeLa cells

HeLa cells were transfected with pCI-Neo-Flag-Upf1 or pCI-Neo control plasmid. 24 h later lysates were prepared and analysed by western blot analysis using α-Upf1 or α-Flag antibodies. α-nucleolin is used as a loading control.

4.3 Developing a FLP-IN stable cell line expression system to analyse Upf1 cellular function

Upf1 has been shown to be predominately cytoplasmic (Fukuhara et al., 2005; Jin et al., 2009), consistent with the cytoplasm being the site of decay for the majority of NMD targets (Trcek et al., 2013). The chromatin recruitment of Upf1 during S-phase involves only a fraction of the total cellular protein however, and previous studies have shown the amount of Upf1 interacting with chromatin components reflects a very small fraction of the Upf1 available in the cell (Azzalin and Lingner, 2006b; Azzalin et al., 2007), and therefore overexpression, observed using transient transfection (Figure 4.1), is likely to make analysis of this sub-population difficult.

Consequently, I proceeded to develop an expression system in HeLa cells which, through low-level, controlled, protein expression, would facilitate a molecular analysis of how Upf1 is recruited to chromatin. The FLP-IN cell system is capable of generating stable HeLa cell lines expressing a gene of interest under the control of an inducible doxycycline dependent promoter (Figure 4.2). Benefits of this system compared to transient transfection include: the ability to control, more accurately, levels of gene expression via the titrated addition of doxycycline; avoidance of liposomal transfection and associated cell death; the opportunity to integrate allelic and mutant forms of the gene of interest into a single chromosomal site, combined with rapid antibiotic selection for cells expressing the gene of interest, generating true isogenic cell lines which ensures a homogenous population of expression competent cells, thus removing transfection efficiency and variable genomic integration sites, as experimental variables.

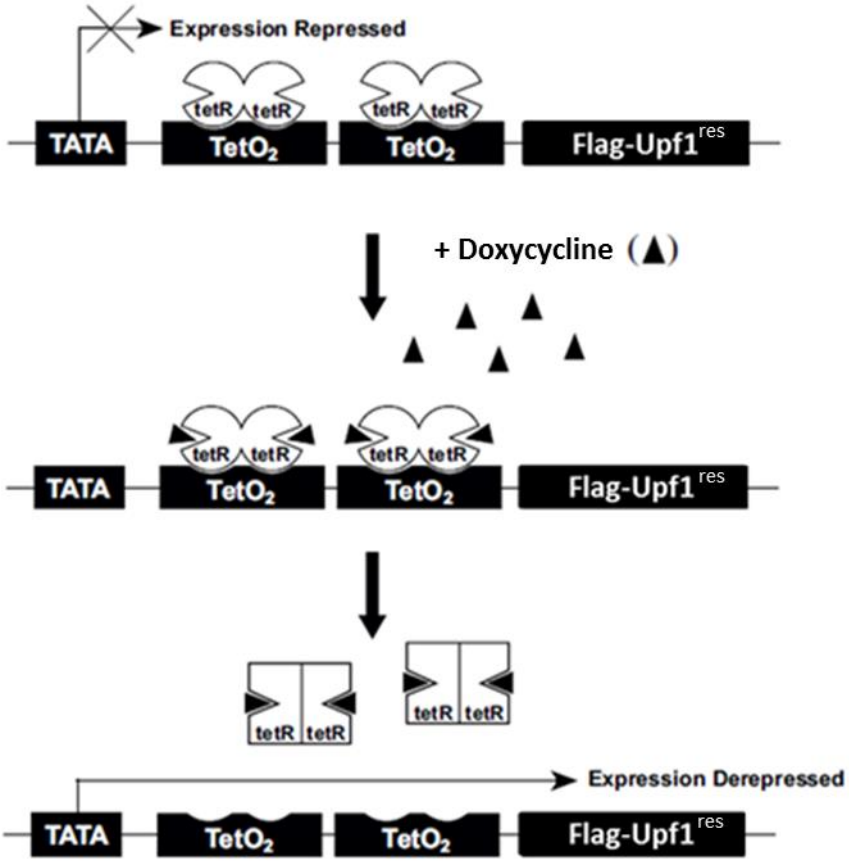

Figure 4.2 The FLP-IN expression system

A single Flag-Upf1^{res} gene copy is recombined into a single genomic site in HeLa cells to generate FLP-IN stable cell lines as described in Materials and methods. The tet repressor (tetR) binds to the promoter sequence and blocks transcription. Addition of doxycycline to cells causes a conformational change in tetR structure, causing it to be released from the promoter. This alleviates repression of the promoter and allows transcription of Flag-Upf1^{res}. Figure adapted from;

http://tools.lifetechnologies.com/content/sfs/manuals/flpintrex_man.pdf

4.4 Upf1 expression levels and siRNA resistance in the FLP-IN system

To determine doxycycline-induced expression levels in the FLP-IN system and to optimise expression conditions, I initially generated a cell line capable of stably expressing untagged Upf1. Because a longer term aim was to investigate the ability of the ectopically expressed Upf1, and derived mutants, to rescue cells lacking endogenous Upf1 following siRNA-mediated knockdown, a cell line was constructed using a form of the Upf1 gene (referred to hereafter as Upf1^{res}) containing two silent mutations, designed to confer resistance to a specific Upf1 siRNA.

Exposure to a range of doxycycline concentrations for 24-48 h revealed Upf1^{res} expression to be broadly similar to endogenous levels (Fig 4.3), as evidenced by a consistent small increase in total Upf1 protein detected by anti-Upf1 antibody. Significantly, high levels of expression were not usually observed in this system, as increasing the doxycycline levels above the recommended range did not dramatically increase protein expression levels (data not shown).

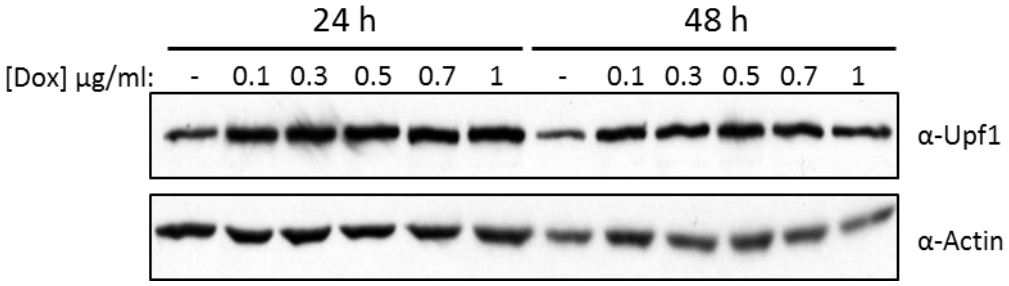

Figure 4.3 Doxycycline optimisation in the FLP-IN system

Upf1^{res} FLP-IN HeLa cells were mock treated with PBS or 0.1-1µg/ml doxycycline for 24 or 48 h. Lysates were prepared and total cellular Upf1 levels determined by western blot analysis with α-Upf1 antibodies. α-actin was used as the loading control.

4.5 Ectopic expression of Upf1 containing silent mutations is resistant to knockdown of endogenous protein using siRNAs directed against wild-type sequence

In parallel, a FLP-IN cell line containing a doxycycline-inducible, Flag-tagged derivative of Upf1^{res} (Flag-Upf1^{res}) was also constructed. This line was used to prove that doxycycline treatment did indeed induce expression of ectopic Upf1^{res}, and to establish whether expression of Upf1^{res} was stable following exposure of cells to siRNA directed against wild-type Upf1. Flag-Upf1^{res} HeLa cells were transfected with non-targeting control or Upf1 siRNA with or without doxycycline for 48 h and expression levels determined by Western blot (Figure 4.4). Using this protocol, Upf1-specific siRNA, but not non-targeting control siRNA, resulted in significant knockdown of endogenous protein in this protocol (Figure 4.4, lane 3). The addition of doxycycline resulted in the induction of modest levels of Flag-Upf1^{res} (Figure 4.4, lane 2). Importantly, levels of Upf1 protein were maintained at levels very close to those observed in control cells, when siRNA-mediated knockdown was undertaken in the presence of doxycycline, but not in its absence, demonstrating that the tagged version of Upf1^{res} was indeed resistant to siRNA-induced knockdown of endogenous protein (Figure 4.4, compare lanes 1 and 4).

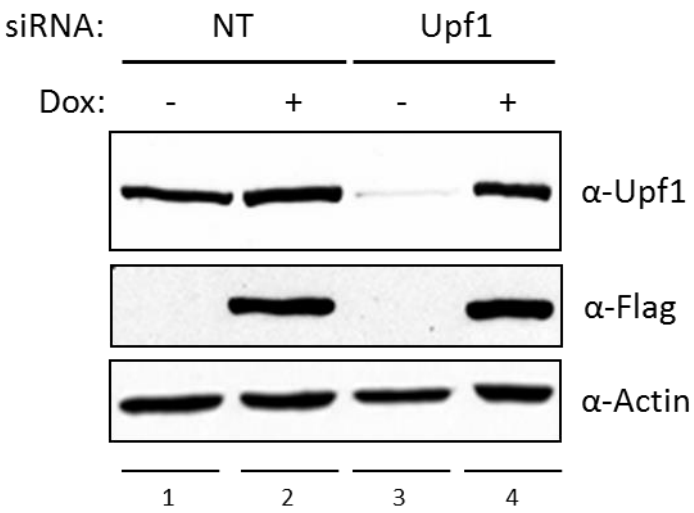

Figure 4.4 Flag-Upf1^{res} can restore Upf1 at physiological levels

Flag-Upf1^{res} HeLa cells were transfected with non-targeting control or Upf1 siRNA, with or without 1μg/ml doxycycline for 48 h, before expression levels determined by western blotting with α-Upf1 or α-Flag antibodies. α-actin was used as a loading control.

4.6 Identification of a region in Upf1 required for chromatin association

4.6.1 Introduction

The role of Upf1 in DNA replication is predicated on the notion that Upf1 is specifically targeted to bind chromatin as cells replicate their genome. Specific motifs must therefore exist, to target a fraction of Upf1 to appropriate chromatin sites. Having established an *in vivo* expression system in HeLa cells, my aim was to use this to identify motifs within Upf1 essential for the S-phase specific recruitment to chromatin and investigate the consequences when those motifs were absent.

4.6.2 Analysis of the subcellular distribution of FlagUpf1^{res} in HeLa cells

Previously, it has been shown that a small fraction of total cellular Upf1 may be found on chromatin during S-phase (Azzalin and Lingner, 2006). To establish whether Flag-tagged-Upf1 recapitulated the observed behaviour of endogenous Upf1, extracts from asynchronous or S-phase enriched Flag-Upf1^{res} expressing cells were prepared and fractionated into cytoplasmic, nuclear-soluble, and chromatin-enriched fractions as described in Materials and methods and based on the protocol described in Mendez and Stillman, 2000. Flag-Upf1^{res} was found to be distributed between the cytoplasm, the nuclear soluble fraction and a very small chromatin-bound fraction in asynchronous cells (Fig 4.5). A 2.6-fold increase in levels of chromatin-associated Flag-Upf1^{res} in S-phase enriched cells (Figure 4.5 compare lanes 3 and 6, higher exposure), confirms that Flag-Upf1^{res} is behaving in a manner akin to the endogenous protein (Azzalin and Lingner, 2006b), and indicates that the addition of an N-terminal Flag tag does not disrupt the association of Upf1 with chromatin.

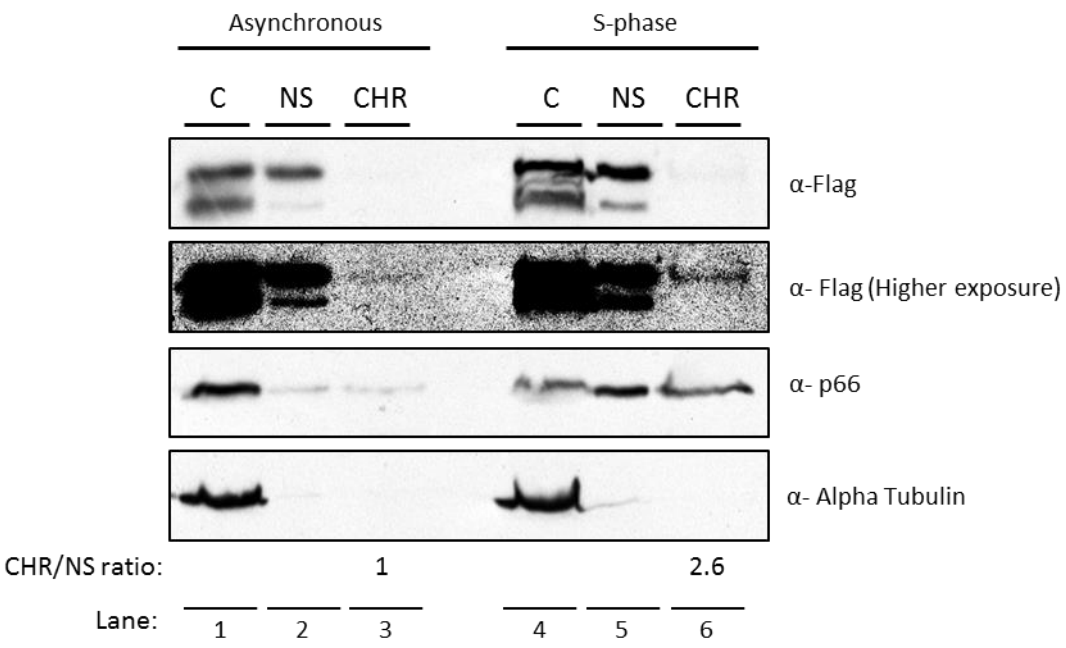

Figure 4.5 Chromatin association of Flag-Upf1^{res} increases during S-phase

Flag-Upf1^{res} FLP-IN HeLa cells were exposed to 0.5µg/ml doxycycline for 48 h (asynchronous) or S-phase enriched. S-phase enrichment was performed by 24 h exposure to 0.5µg/ml doxycycline, then 2mM hydroxyurea (HU) added for an additional 24 h, to arrest cells in S-phase or at the G1/S transition. HU was washed out and cells released into S-phase for 3 h. Cells were then biochemically fractionated into cytoplasmic (C), nuclear soluble (NS) or chromatin enriched (CHR) fractions as described in Materials and methods. Samples representative of equal numbers of cells were separated by SDS-page and analysed by Western blotting with α-Flag antibodies. The purity of each fraction was determined with antibodies against alpha tubulin (cytoplasmic protein) or p66 (chromatin associated during S-phase). Movement of the polδ p66 subunit from cytoplasmic to nuclear fractions was used to indicate S-phase. Representative of 3 independent experiments. The multiple bands detected in Flag blots most likely represent a degree of proteolysis occurring during the fractionation protocol.

4.6.3 Upf1 amino acids 1-91 are essential for the recruitment to chromatin

Having demonstrated that Flag-Up1^{res} is recruited to chromatin in an S-phase dependent manner, I wanted to identify Upf1 structural domains essential for this interaction and the regulation of genome stability. The N-terminal 270 amino acids of Upf1 have been shown to bind SMG6, Upf2 and Staufen 1 proteins (Clerici et al., 2009; Gong et al., 2009; Okada-Katsuhata et al., 2012) for their respective RNA surveillance functions. Upf2, which has been shown to be dispensable for genomic stability (Azzalin and Lingner, 2006) associates with the CH domain of Upf1, corresponding approximately to amino acid residues (115-272). While by no means conclusive, this suggested that the CH domain might not be directly involved in chromatin association and genomic stability, but does not provide insight into any putative role of the extreme N-terminus.

In a first step, to investigate whether the association with chromatin occurs through N-terminal interactions independently of the CH domain, and thus Upf2, I generated a mutant lacking amino acids 1-91 (Flag-Upf1$^{resΔ1-91}$). This deletion removes the N-terminus, but retains the CH domain, and indeed both Flag-Upf1^{res} and Flag-Upf1$^{resΔ1-91}$ could be co-immunoprecipitated by Upf2 (Figure 4.6).

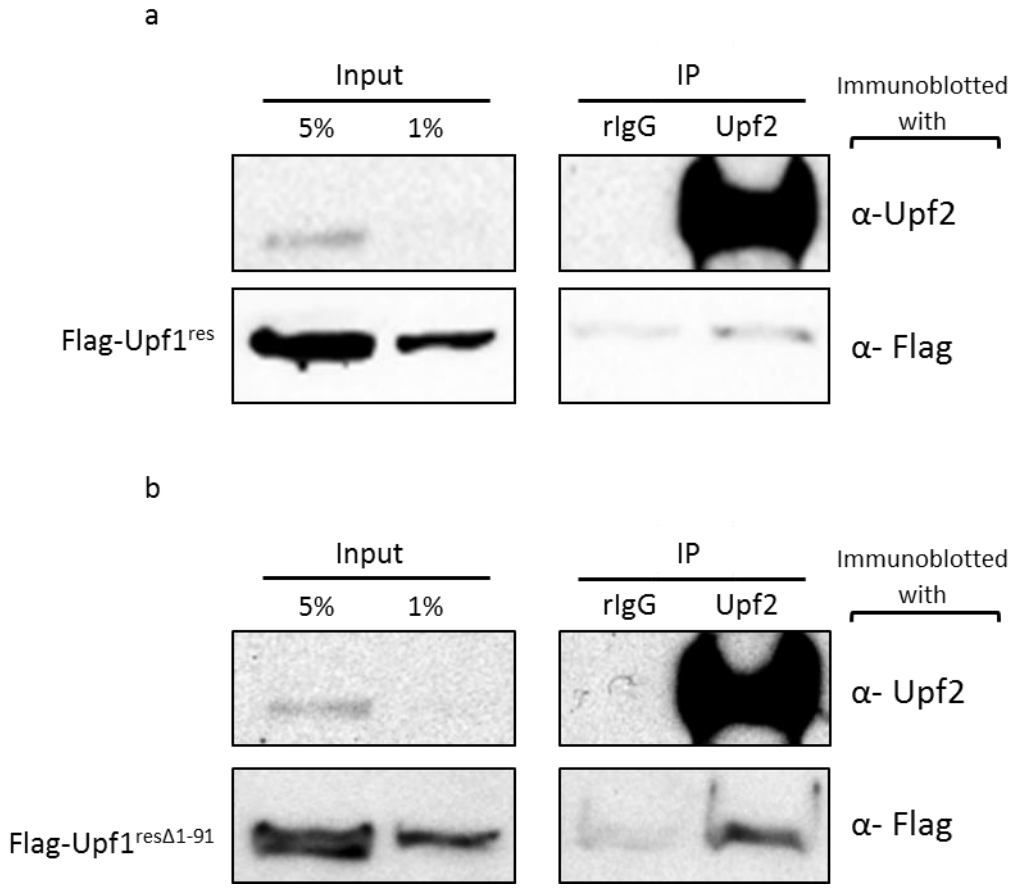

Figure 4.6 Flag-Upf1^{res} and Flag-Upf1$^{resΔ1-91}$ co-immunoprecipitate with Upf2

a) Flag-Upf1^{res} FLP-IN cells were exposed to 0.1µg/ml doxycycline for 48 h and whole cell extracts prepared as described in Materials and methods. Samples were immunoprecipitated overnight with Upf2 antibodies or a rabbit immunoglobulin control. The following day protein G sepharose beads were added, samples washed three times and eluted complexes analysed by SDS-page and western blotted with α-Upf2 or α-Flag antibodies. Inputs are representative of 5% and 1% total protein in each immunoprecipitation. b) Flag-Upf1$^{resΔ1-91}$ FLP-IN HeLa cells under the same conditions as in (a). Flag signal observed in IgG lanes represents low level cross reactivity of Flag-Upf1 to the IgG/Protein G sepharose used in immunoprecipitations.

The subcellular distribution of this mutant was analysed by biochemical fractionation as before. Flag-Upf1$^{resΔ1-91}$ was found to localise both in the cytoplasmic and soluble nuclear fractions. Unlike the full-length protein, the ratio of cytoplasmic to nuclear protein was altered, with proportionately more protein present in the soluble nuclear fraction (Figure 4.7). Importantly, however, no Flag-Upf1$^{resΔ1-91}$ could be detected in the chromatin-enriched fraction, either in asynchronous or S-phase cells (Figure 4.7). These results, together with those shown in Figure 4.6, demonstrate that the association of Upf1 with chromatin is dependent on the presence of the N-terminal 91 amino acids of Upf1, and that this is not mediated through interactions with Upf2.

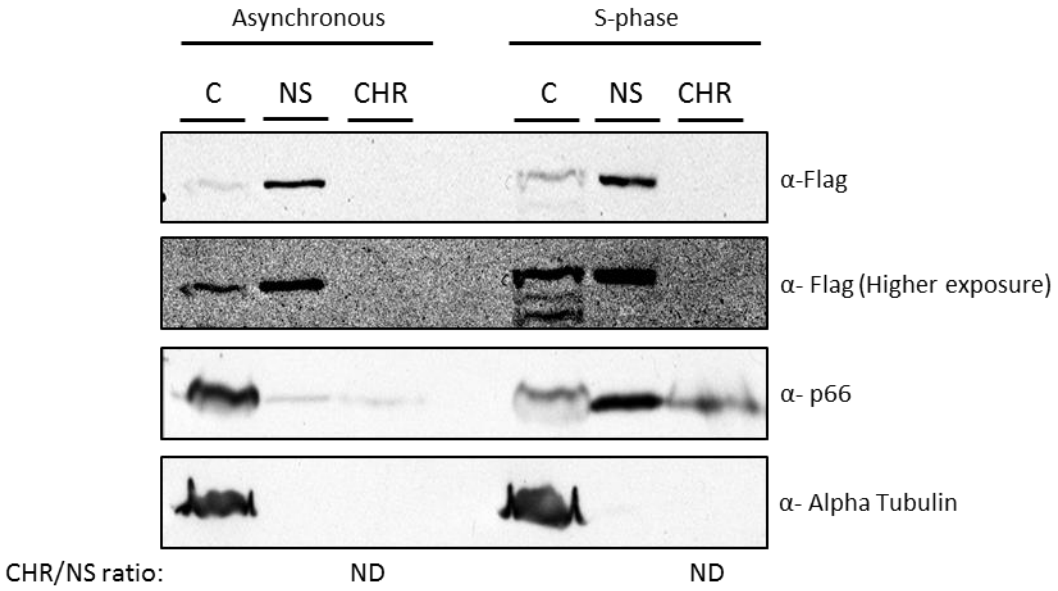

Figure 4.7 No interaction of Upf1 with chromatin was detected in the absence of residues 1-91

Flag-Upf1$^{resΔ1-91}$ FLP-IN HeLa cells were exposed to 0.5µg/ml doxycycline for 48 h (asynchronous) or S-phase enriched as described previously. Cells were then biochemically fractionated as described previously and samples representative of equal numbers of cells were separated by SDS-page and analysed by Western blotting with α-Flag antibodies. The purity of each fraction was determined with antibodies against alpha tubulin (cytoplasmic protein) or p66 (chromatin associated during S-phase). Movement of the polδ p66 subunit from cytoplasmic to nuclear fractions was used to indicate S-phase. Representative of 2 independent experiments. ND = No detectable Flag-Upf1 observed in chromatin fraction.

4.6.4 Alanine substitution analysis of PIKK consensus sites within the N-terminus of Upf1

The results above indicate that the N-terminal region comprising residues 1-91 contains some element which is important for chromatin association. Lingner and colleagues previously showed that knockdown of the classical checkpoint PIKK, ATR, resulted in a decreased level of chromatin-associated Upf1 (Azzalin and Lingner, 2006b). PIKKs are known to target S/TQ motifs, and so I chose to generate a series of phospho-mutants targeting these motifs within the first 91 residues of the protein.

The N-terminal 91 residues of Upf1 contain 4 S/TQ motifs (S10, T28, S42, T44) (Figure 4.8). Using site-directed mutagenesis of the relevant Upf1-containing plasmid, and subsequent cloning, I generated a series of HeLa FLP-IN Flag-Upf1^{res} cell lines, each of which lacked one of the N-terminal S/TQ motifs, in which the serine or threonine at each motif was replaced by alanine, to prevent the addition of a phosphate group at this position *in vivo.* This strategy generated three of the four potential mutants, as technical difficulties during cloning precluded the generation of T44A.

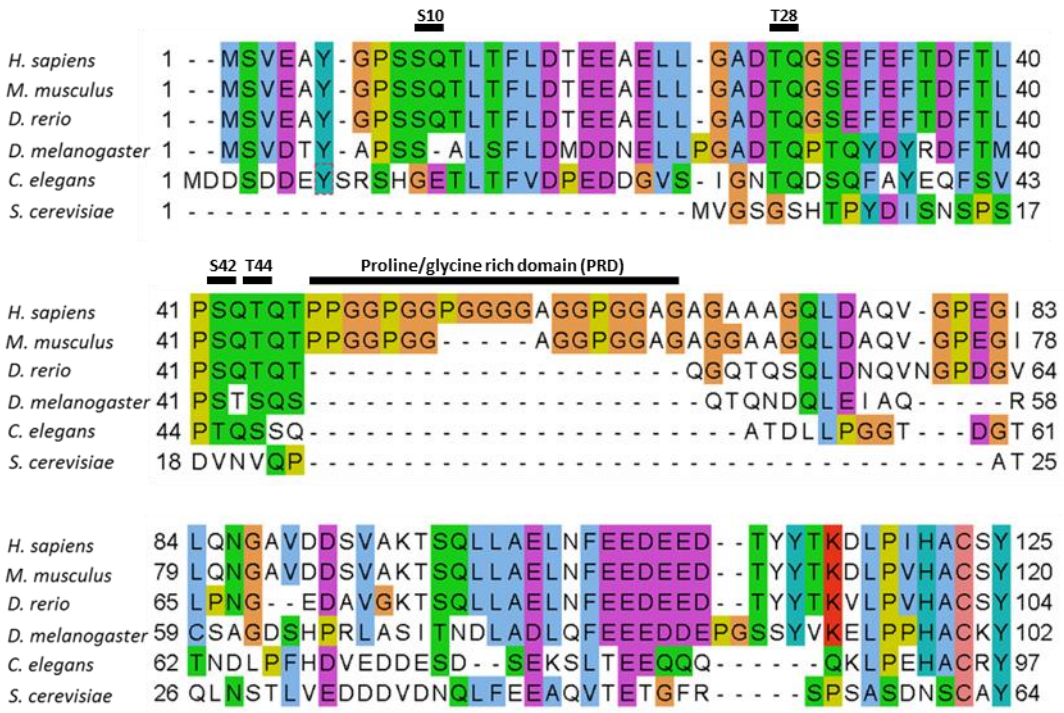

Figure 4.8 N-terminal conservation of Upf1 homologues

ClustalW2 multiple sequence alignment of the N-terminal ~100 amino acids of Upf1 homologues. Coloured blocks indicate conserved residues and the S/T-Q motifs at S10, T28, S42 and T44 are indicated. The proline/glycine rich domain (PRD) (residues 47-67) is also highlighted.

No defects in chromatin recruitment were observed when either serine 10 (Figure 4.9) or threonine 28 (Figure 4.10) was mutated, suggesting these motifs are not required for the association of Upf1 with chromatin. However, an S-phase specific increase in chromatin association of Upf1 was not observed when threonine 28 was mutated to alanine (Figure 4.10), despite this mutant still binding chromatin (see discussion). In contrast, strikingly, alanine substitution of serine 42 (Flag-Upf1^{resS42A}) resulted in the absence of detectable chromatin association in both asynchronous and S-phase cells (Figure 4.11), demonstrating that the presence of a serine at amino acid position 42 is essential for the recruitment of Upf1 to chromatin.

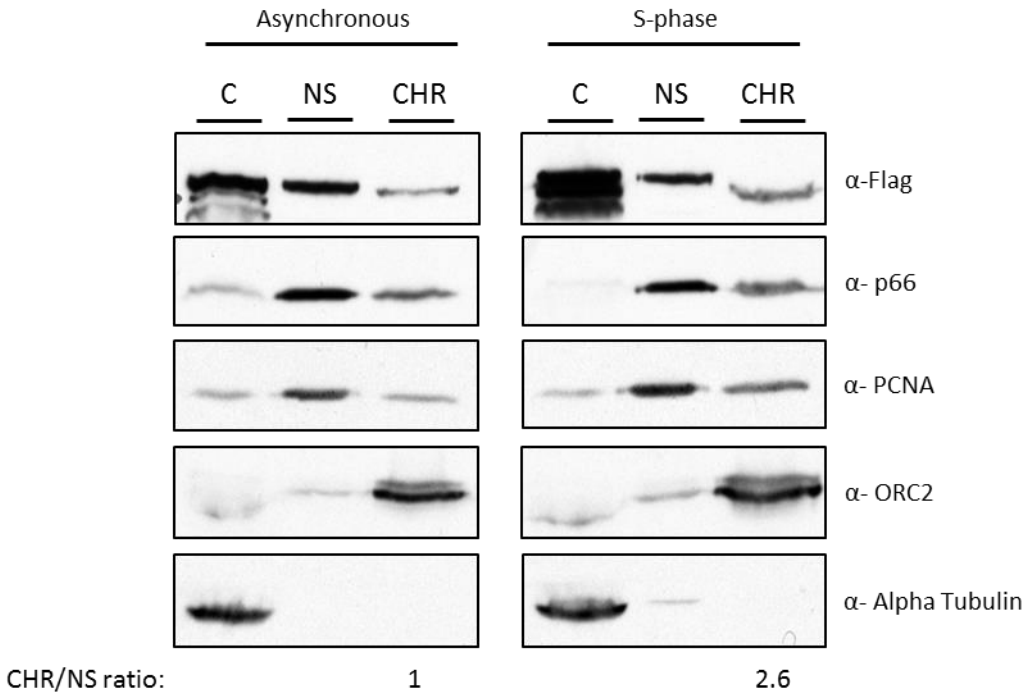

Figure 4.9 Mutation of Upf1 S10 does not affect chromatin recruitment

Flag-Upf1^{resS10A} FLP-IN HeLa cells were exposed to 0.5µg/ml doxycycline for 48 h (asynchronous) or S-phase enriched as described previously. Cells were then biochemically fractionated as described previously and samples representative of equal numbers of cells were separated by SDS-page and analysed by Western blotting with α-Flag antibodies. The purity of each fraction was determined with antibodies against alpha tubulin (cytoplasmic protein) or ORC2 (chromatin bound protein). Movement of the polδ p66 subunit and PCNA from cytoplasmic to nuclear fractions was used to indicate S-phase. Representative of 2 independent experiments.

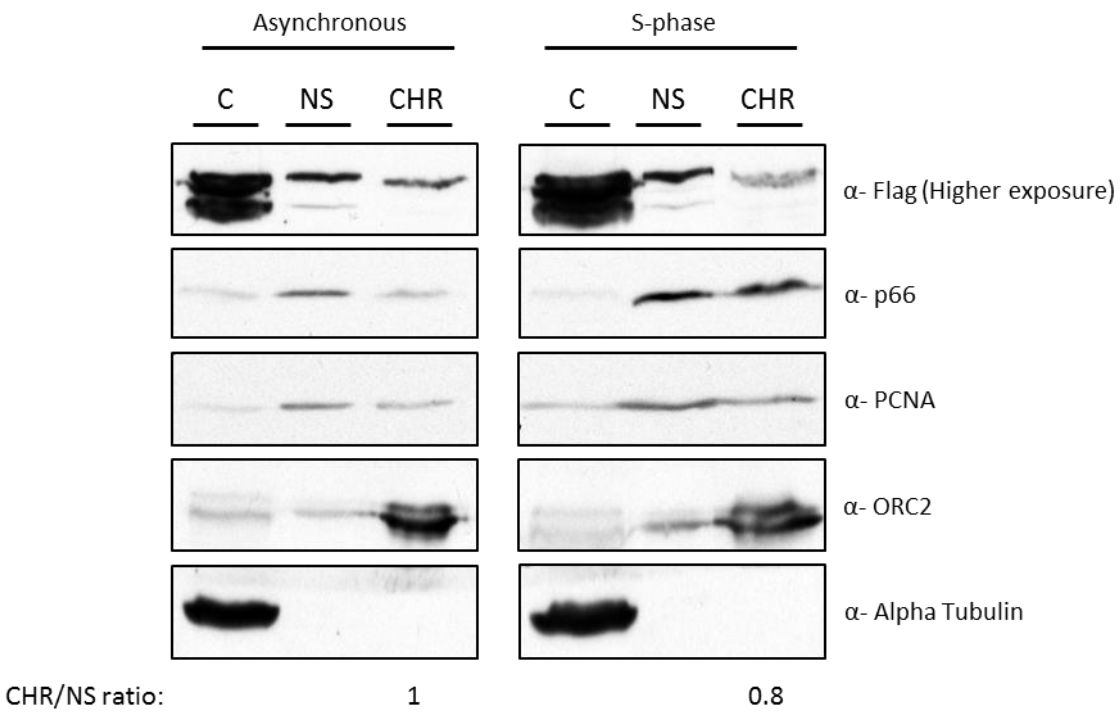

Figure 4.10 Mutation of Upf1 T28 reduces, but does not prevent the interaction of Upf1 with chromatin

Flag-Upf1^{resT28A} FLP-IN HeLa cells were exposed to 0.5µg/ml doxycycline for 48 h (asynchronous) or S-phase enriched as described previously. Cells were then biochemically fractionated as described previously and samples representative of equal numbers of cells were separated by SDS-page and analysed by Western blotting with α-Flag antibodies. The purity of each fraction was determined with antibodies against alpha tubulin (cytoplasmic protein) or ORC2 (chromatin bound protein). Movement of the polδ p66 subunit and PCNA from cytoplasmic to nuclear fractions was used to indicate S-phase. Representative of one experiment.

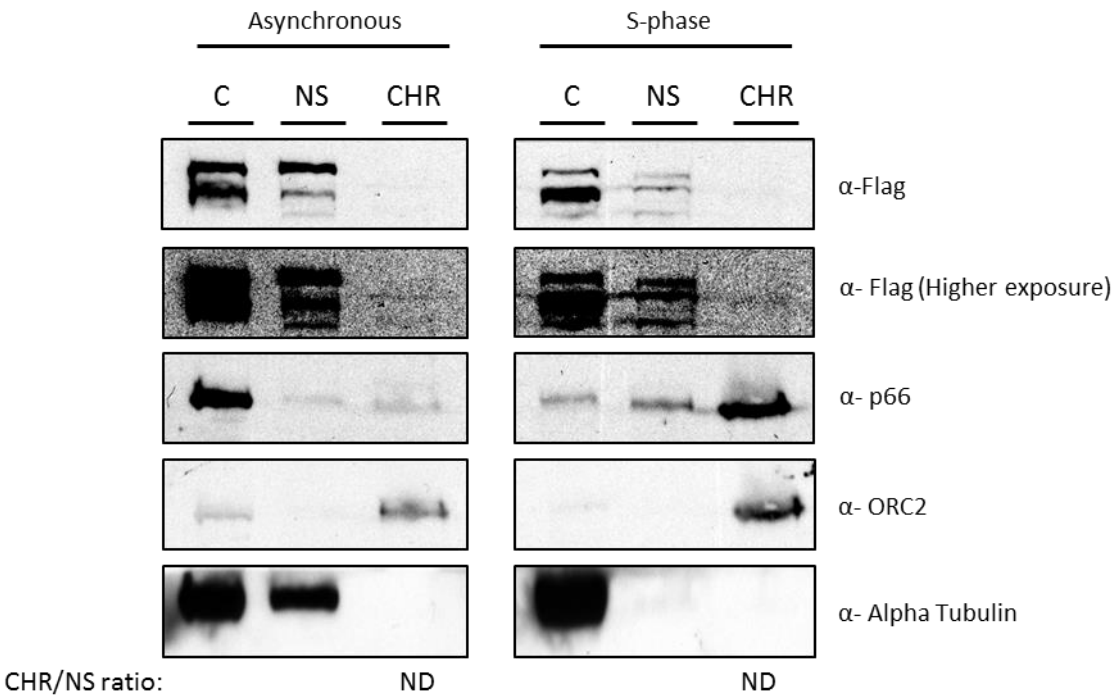

Figure 4.11 No interaction of Upf1 with chromatin was detected when S42 was mutated to alanine

Flag-Upf1^{resS42A} FLP-IN HeLa cells were exposed to 0.5µg/ml doxycycline for 48 h (asynchronous) or S-phase enriched as described previously. Cells were then biochemically fractionated as described previously and samples representative of equal numbers of cells were separated by SDS-page and analysed by Western blotting with α-Flag antibodies. The purity of each fraction was determined with antibodies against alpha tubulin (cytoplasmic protein) or ORC2 (chromatin bound protein). Movement of the polδ p66 subunit from cytoplasmic to nuclear fractions was used to indicate S-phase. Representative of 3 independent experiments. ND = No detectable Flag-Upf1 observed in chromatin fraction.

4.6.5 Role of phosphorylation at serine 42 in the recruitment of Upf1 to chromatin

In order to investigate a potential role for phosphorylation of serine 42 in chromatin recruitment of Upf1, a series of fragments corresponding to discrete domains of the protein were expressed as GST fusion proteins and purified from E.coli (this work was carried out by Dr. R Beniston) for use as *in vitro* substrates in PIKK protein kinase assays using an approach described by Ohno and colleagues (Yamashita et al., 2001). Because PIKKS have overlapping motif specificity (particularly *in vitro*), the individual fragments were tested as substrates using the PIKK, DNA-PK. Fragments were incubated with protein kinase in the presence of either unlabelled or γ^{32}P-ATP and analysed by autoradiography or mass spectrometry. Peptides originating from an N-terminal Upf1 fragment covering residues 1-101 were identified by mass spectrometry as containing a phospho-motif at S42 (Figure 4.12).

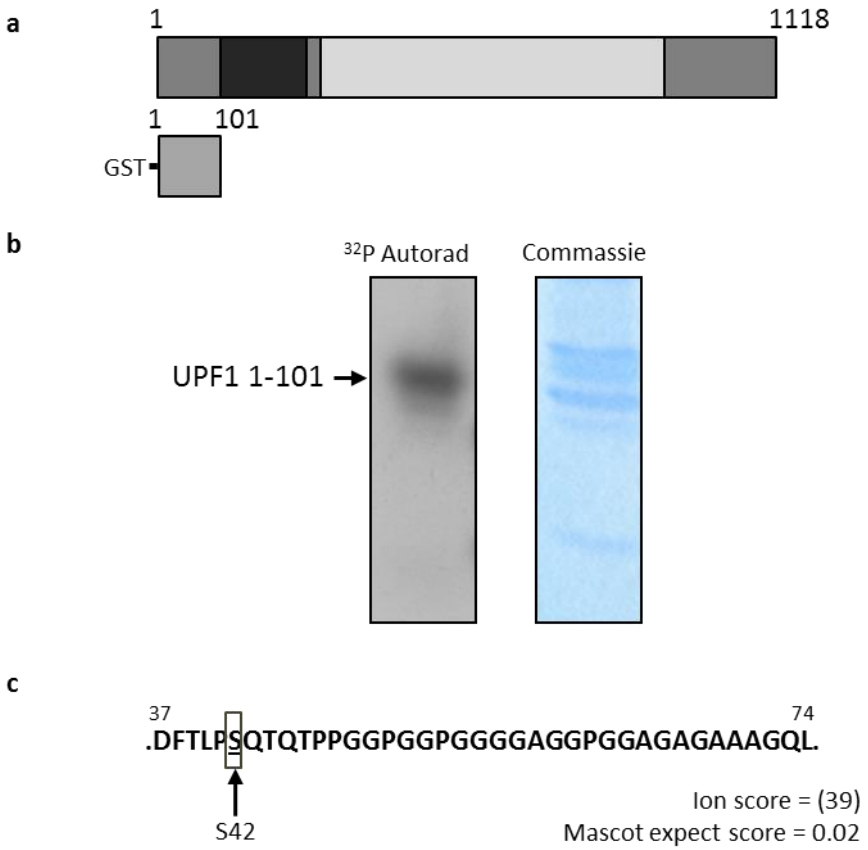

Figure 4.12 Upf1 S42 can be phosphorylated by DNA-PK *in vitro*

a) An N-terminal Upf1-GST fragment containing residues 1-101 was purified from *E.coli* before GST tag cleavage and incubation with DNA-PK in the presence of γ^{32}P-ATP. b) Autorad and collodial commassie gel of kinase reactions. Arrows indicate the 1-101 amino acid Upf1 fragment excised from the gel. c) Reactions were digested with Asp-N protease and resultant peptides analysed using a Brukker Maxxis UHR-TOF mass spectrometer. The Upf1 peptide fragment and identified phospho-motif is indicated. This work was performed by Dr R.Beniston.

On the basis of this data, I undertook an initial investigation into the possibility that phosphorylation of serine 42 was necessary for chromatin recruitment of Upf1. Site-directed mutagenesis of the relevant plasmid was undertaken to substitute a phospho-mimetic amino acid (S42E) at this site, and using the FLP-IN system, an additional cell line generated (Flag-Upf1^{resS42E}). Although time limitation precluded a

comprehensive analysis of the sub-cellular location of this mutant, an initial study utilising biochemical fractionation as above, indicated that this mutation resulted in significant levels of chromatin associated Upf1 (Figure 4.13). S-phase specific chromatin recruitment was enhanced with this mutation (3.8-fold) when compared to wild-type Upf1 (2.6-fold – figure 4.5), suggesting that phosphorylation of Upf1 at serine 42 may be relevant for this function.

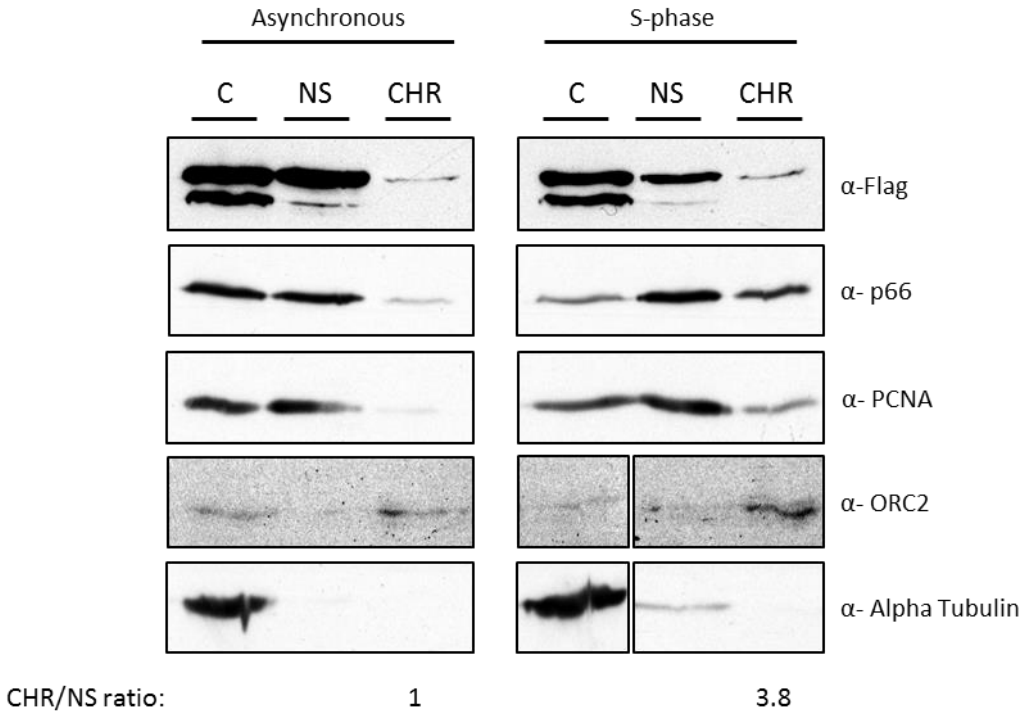

Figure 4.13 Phospho-mimetic substitution of S42 increases Upf1 chromatin recruitment

Flag-Upf1^{resS42E} FLP-IN HeLa cells were exposed to 0.5µg/ml doxycycline for 48 h (asynchronous) or S-phase enriched as described previously. Cells were then biochemically fractionated as described previously and samples representative of equal numbers of cells were separated by SDS-page and analysed by Western blotting with α-Flag antibodies. The purity of each fraction was determined with antibodies against alpha tubulin (cytoplasmic protein) or ORC2 (chromatin bound protein). Movement of the polδ p66 subunit and PCNA from cytoplasmic to nuclear fractions was used to indicate S-phase. The ORC2 and Alpha-tubulin panels are from the same Western blot and exposure conditions. Representative of 2 independent experiments.

4.7 The recruitment of Upf1 to chromatin is independent of the canonical NMD pathway

4.7.1 Mutation of sites involved in canonical NMD does not affect the recruitment of Upf1 to chromatin

In the previous section, I identified S42 as an essential amino acid required for chromatin association. Consequently, I wished to investigate more generally whether motifs or domains within Upf1 required for its recruitment to chromatin may be distinct from those required for its molecular interactions in its NMD role.

Specifically, I wanted to investigate whether the specific phosphorylation events required for canonical NMD are involved in the recruitment of Upf1 to chromatin. When this programme of work was initiated, a number of C-terminal phosphorylation sites had been implicated in regulation of Upf1 function in NMD. *In vitro* studies, using PIKK motif-containing 14mer peptides derived from Upf1, showed that three sites (S1078, S1096, S1116) were efficiently phosphorylated by the PIKK Smg1 (Yamashita et al., 2001). Ohno and colleagues developed a phospho-specific antibody against S1078, which cross-reacted with wild-type Upf1 extracted from cells, but not a mutant form lacking both S1078 and S1096 (Ohnishi et al., 2003). These data were interpreted to suggest that either or both S1078 and S1096 are phosphorylated during NMD *in vivo* (Ohnishi et al., 2003). In a separate study, mass spectrometric analysis of Upf1 from HeLa cells showed that both S1096 and S1116 were phosphorylated *in vivo* (R. Beniston and C. Smythe , unpublished), suggesting that the relevant site detected by the phospho-specific antibody was S1096. As the molecular cloning work to generate non-phosphorylatable mutants was underway, Okada-Katsuhata et al., 2012, showed that in addition to SMG1-mediated C-terminal

phosphorylation, phosphorylation at T28 could be detected with a phospho-site-specific antibody (Okada-Katsuhata et al., 2012), and that alanine substitution at this site resulted in reduced NMD efficiency. I therefore decided to generate the triply mutated form FLAG-Upf1$^{resT28A/S1096A/S1116A}$ (referred to as Flag-Upf1^{resAAA}), which would be predicted to be non-functional in the NMD pathway.

This mutant was used to generate another HeLa cell line using the FLP-IN system as before, and the cell line utilised to analyse the ability of this mutant to be recruited to chromatin. The subcellular distribution of this mutant was analysed by biochemical fractionation as before. In contrast to the result obtained with the S42 mutant, Flag-Upf1^{resAAA} was found to be associated with chromatin in asynchronous or S-phase enriched conditions (Figure 4.14), indicating that the recruitment of Upf1 to chromatin can occur independently of motifs that are essential for NMD.

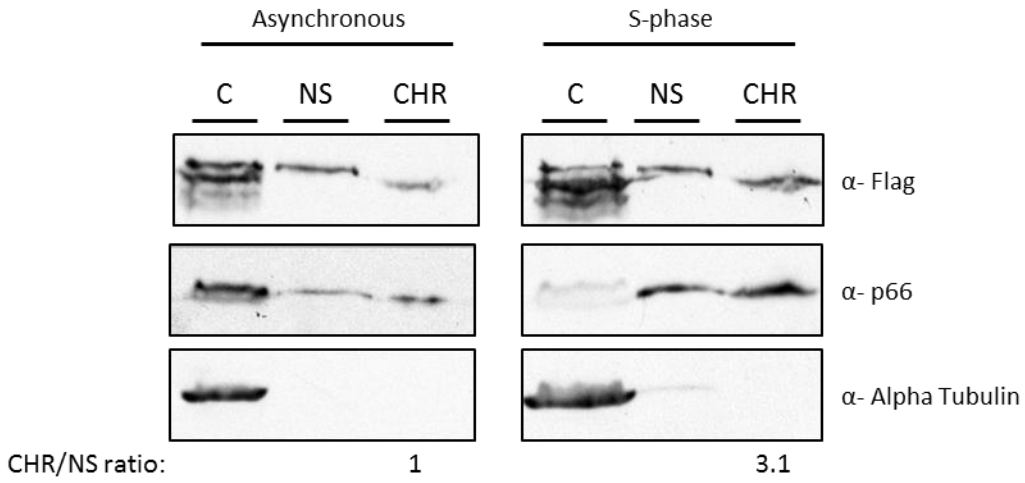

Figure 4.14 Mutation of Upf1 motifs required for canonical NMD does not affect chromatin recruitment

Flag-Upf1^{resAAA} FLP-IN HeLa cells were exposed to 0.5µg/ml doxycycline for 48 h (asynchronous) or S-phase enriched as described previously. Cells were then biochemically fractionated as described previously and samples representative of equal numbers of cells were separated by SDS-page and analysed by Western blotting with α-Flag antibodies. The purity of each fraction was determined with antibodies against alpha tubulin (cytoplasmic protein) and the movement of the polδ p66 subunit from cytoplasmic to nuclear fractions was used to indicate S-phase. Representative of 1 experiment

4.7.2 Mutation of a site involved in the recruitment of Upf1 to chromatin does not affect canonical NMD

Evidence presented in this study has suggested the recruitment of Upf1 to chromatin is independent of motifs, which when phosphorylated, are essential for NMD. It was important therefore, to address the reciprocal question, as to whether S42, a site essential for chromatin recruitment, is involved in the decay of PTC containing mRNA transcripts.

The role of Upf1 as an essential NMD component has been well established in *S.cerevisiae* and *C.elegans* (He et al., 1993; Pulak and Anderson, 1993) and depletion of Upf1 has been shown to inhibit NMD in human cells (Gehring et al., 2003). However, several Upf1-like helicases (Ighmbp2 and Senataxin) have recently been described and recent studies have demonstrated a variety of novel mechanisms, involving newly identified components, by which NMD may be effected (Brazao et al., 2012; Geissler et al., 2013; Lim et al., 2012). Knockdown of one novel component, regulator of differentiation 1 (Rod1), generates almost complete inhibition of NMD, comparable to knockdown of Upf2. Upf1 knockdown however, was shown to cause only partial inhibition of the decay of a PTC containing mRNA reporter in this study (Brazao et al., 2012), suggesting Upf1 may be partially dispensable for mammalian NMD.

4.7.2.1 Establishing the requirement for Upf1 in mammalian NMD

Prior to the functional analysis of S42 in NMD, based on the evidence presented above, I wished to establish the relative contribution of endogenous Upf1 to NMD in human cells.

HeLa cells were transfected with non-targeting control or Upf1 siRNA for 24 h, and then transiently transfected, simultaneously, with a plasmid containing a MUP gene, used to control RNA levels in subsequent analyses, and either a plasmid construct containing a wild-type β-globin gene (WT) or a variant containing a premature termination codon at residue 39 (NS39) (Figure 4.15a). Knockdown of Upf2, as a control for NMD inhibition, was attempted but was not successful. 24h after plasmid transfection, protein and RNA extracts were prepared from cells, and Upf1 knockdown confirmed by Western blot (Figure 4.15b) and relative β-globin mRNA levels determined by qPCR (Figure 4.15c). Using this protocol, relative levels of NS39 β-globin mRNA levels were significantly higher in Upf1 knockdown cells than those transfected with control siRNA. This data suggests that Upf1 is involved in NMD in HeLa cells, but the presence of Upf1 is not an absolute requirement, as significant depletion of endogenous Upf1 does not fully prevent the decay of PTC containing mRNA.

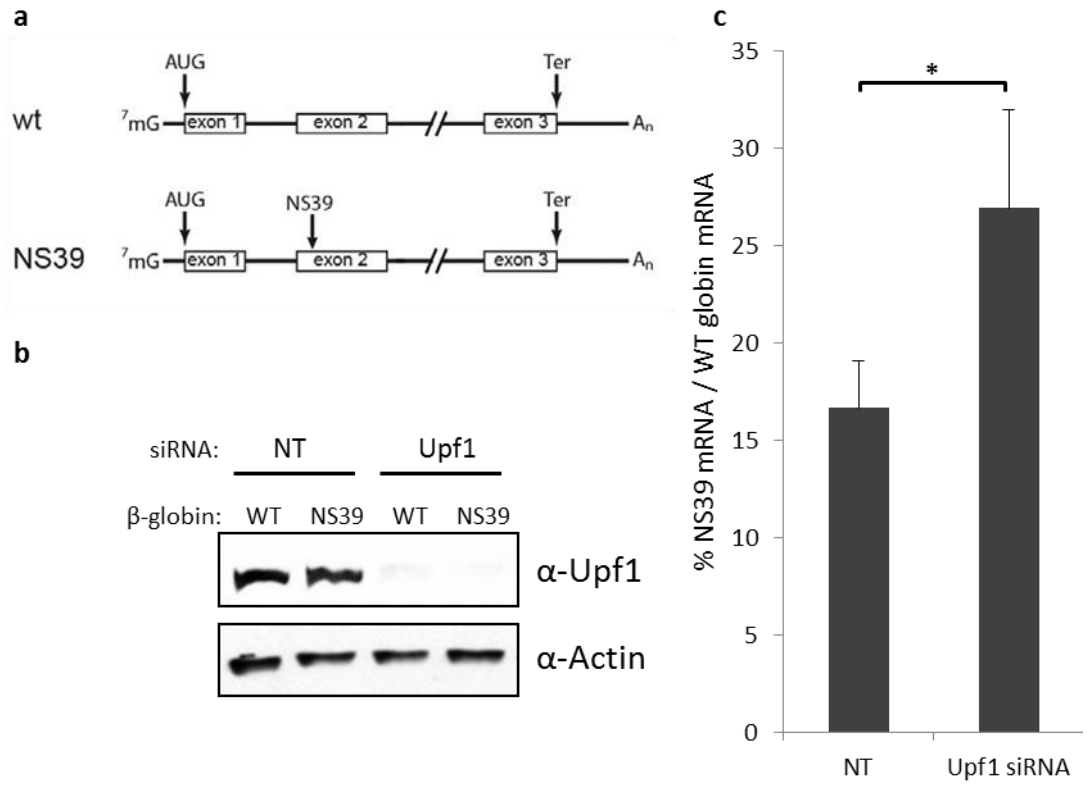

Figure 4.15 Upf1 knockdown causes a partial inhibition of NMD

a) The β-globin constructs used in this assay; either wt β-globin sequence (wt) or a PTC-containing variant (NS39). HeLa cells were transfected with non-targeting (NT) or Upf1 siRNA for 48 h before transfection with either wt or NS39 β-globin reporter constructs in (a) and a MUP control plasmid. RNA and protein extracts were prepared after an additional 24 h. b) Upf1 knockdown was assessed by western blotting with α-Upf1 antibodies or α-actin as a loading control. c) Relative β-globin mRNA levels were quantified by qPCR using the standard curve method and normalised to the MUP transfection control. n =3 *p<0.05

4.7.2.2 Analysis of phosphosite requirement for functional NMD

Taking into account the modest inhibition observed in the absence of endogenous Upf1, I then investigated whether S42, a site involved in chromatin recruitment, is involved in the decay of PTC containing mRNAs.

FLP-IN Flag-Upf1^{res}, Flag-Upf1^{resS42A} and Flag-Upf1^{resAAA} HeLa cell lines were transfected with non-targeting control or Upf1-specific siRNA for 24 h in the presence or absence of doxycycline. Cells were then transfected with β-globin/MUP plasmids as described previously (see 4.7.2.1) and RNA and protein extracts prepared. Knockdown of endogenous Upf1 and expression of Flag-Upf1^{res} mutants was confirmed by Western blot (Figure 4.16a) and relative β-globin mRNA levels determined by qPCR (Figure 4.16b). Upf1 knockdown again generated a modest increase in the levels of NS39 β-globin mRNA and expression of Flag-Upf1^{res} partially rescued this defect. Expression of Flag-Upf1^{resAAA}, predicted to be non-functional in NMD, did not rescue NMD in the absence of endogenous Upf1 when compared to cells transfected with a control siRNA ($p=0.002$). Interestingly, Flag-Upf1^{resS42A}, a Upf1 mutant unable to bind chromatin, rescued the ability of the cell to perform NMD ($p=0.516$), indicating a motif required for the S-phase specific recruitment of Upf1 to chromatin is not functionally required for NMD.

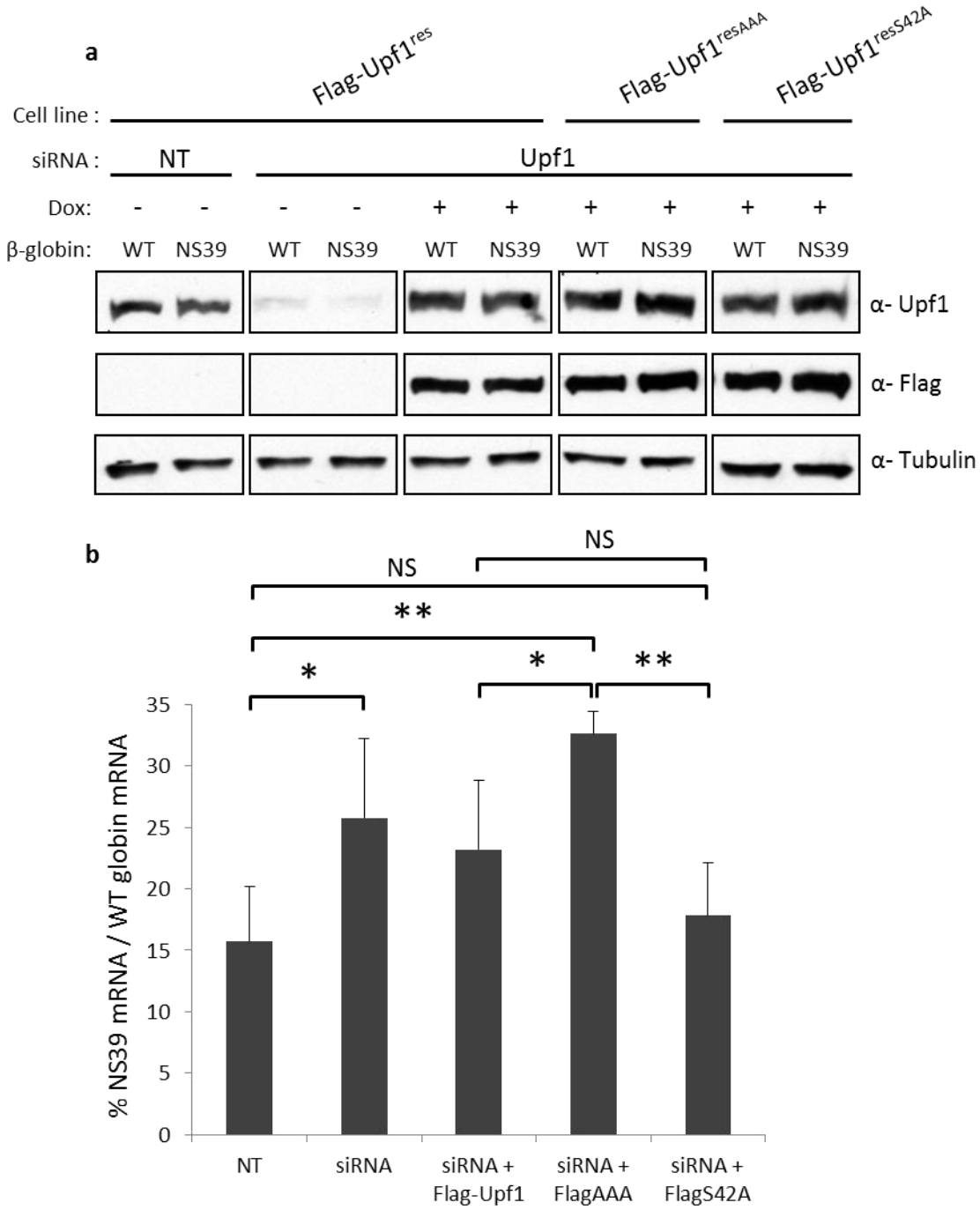

Figure 4.16 S42 is not required for the function of Upf1 in NMD

Flag-Upf1^{res}, Flag-Upf1^{resAAA} or Flag-Upf1^{res}S42A FLP-IN HeLa cells were transfected with non-targeting (NT) or Upf1 siRNA with or without doxycycline for 48 h before transfection with either wt or NS39 β-globin reporter constructs and a MUP control plasmid. RNA and protein extracts were prepared after an additional 24 h. a) Upf1 knockdown was assessed by western blotting with α-Upf1 or α-Flag antibodies. α-tubulin was used as a loading control. All panels are from the same western blot under the same exposure conditions.. b) Relative β-globin mRNA levels were quantified by qPCR using the standard curve method and normalised to the MUP transfection control. n =4 *p<0.05 **p<0.01

4.8 Discussion

Upf1 is essential for genomic stability in human cells and is recruited to chromatin during S-phase and in response to replication stress (Azzalin and Lingner, 2006b), proposing a role for Upf1 in DNA replication or repair. This recruitment to chromatin has been suggested to occur through interaction with DNA polymerase δ (Azzalin and Lingner, 2006b; Carastro et al., 2002), however I was unable to find evidence for a direct interaction between Upf1 and the p66 polδ subunit using the yeast two-hybrid system (Chapter 3). Upf1 chromatin recruitment may involve interactions with both DNA and/or chromatin bound proteins, therefore my aim in this section was to identify Upf1 structural motifs required for the S-phase recruitment to chromatin.

4.8.1 Generating an isogenic stable cell line expression system in HeLa cells

Early attempts to study the behaviour of transiently overexpressed Flag-Upf1 proved unsuccessful, and were attributed to Flag-Upf1 expression being in significant excess of endogenous Upf1. The population of Upf1 recruited to chromatin during S-phase represents a small fraction of the total protein within the cell (Azzalin and Lingner, 2006b), and therefore greatly increasing the levels of Upf1 might not necessarily increase the proportion of Upf1 engaged in this interaction. The excess of Flag-Upf1, resulting from transient overexpression, prevented the identification of known Upf1 interactors (this study and R. Beniston, unpublished), and thus transient over-expression was deemed not suitable to investigate Upf1 recruitment to chromatin. To address the issue of overexpression when studying these low-abundance interactions, I generated a library of isogenic stable FLP-IN cell lines and

demonstrated ectopic expression of Upf1^{res} to be broadly similar to levels of endogenous Upf1. As I planned to test the ability of Upf1 mutants to rescue knockdown of endogenous Upf1 in later experiments, I generated a FLP-IN HeLa cell line capable of expressing Flag-Upf1^{res}. In cells transfected with non-targeting siRNA and treated with doxycycline, I was able to distinguish ectopic expression of Flag-Upf1^{res} and demonstrated this mutant was resistant to siRNA mediated depletion, when challenged with a specific siRNA targeting the wild-type Upf1 sequence.

4.8.2 Identification of an N-terminal region essential for Upf1 chromatin recruitment

Having established a controlled Upf1 expression system *in vivo*, I then wanted to identify the Upf1 domains essential for chromatin recruitment. Using biochemical fractionation, I prepared cytoplasmic, soluble nuclear or chromatin-enriched fractions from asynchronous or S-phase enriched FLP-IN Flag-Upf1^{res} HeLa cells and demonstrated Flag-Upf1^{res} associated with chromatin in both asynchronous and S-phase enriched cells. This is consistent with data presented by Azzalin et al., 2006, and demonstrated that Flag-Upf1 expressed in the FLP-IN system behaves in a manner similar to endogenous Upf1 and responds to the cell cycle signalling events that cause chromatin recruitment.

The interaction of Upf1 with Upf2 is essential for NMD (Chakrabarti et al., 2011; Lykke-Andersen et al., 2000), however Upf2 has been shown to be dispensable for genomic stability (Azzalin and Lingner, 2006b). This suggested the CH domain of Upf1 (residues 115-272) required for this interaction (Kadlec et al., 2006), may also be dispensable for the recruitment of Upf1 to chromatin, but did not provide insight into

the role of the extreme N-terminus. In an initial investigation of Upf1 domains required for chromatin recruitment, I deleted the extreme N-terminal 91 amino acids and observed the nuclear accumulation of this mutant, and a complete absence of chromatin interaction. This mutant was able to bind Upf2 however, demonstrating motifs contained within the N-terminal 91 amino acids, and not the CH domain, are required for chromatin recruitment.

4.8.3 N-terminal Upf1 motifs may also be essential for nuclear export

On closer examination of this data, deletion of amino acids 1-91 also caused a decrease in cytoplasmic localisation of this mutant (Figure 4.7) when compared to Flag-Upf1^{res} (Figure 4.5), becoming largely localised to the nuclear soluble fraction (nucleoplasm). Previously, Mendell et al., 2002, investigating the nuclear-cytoplasmic shuttling of the mouse Upf1 homologue (termed Rent1), demonstrated that deletion of residues 55-416 caused nucleoplasmic accumulation of GFP-tagged Rent1, but the authors did not address the cause of this accumulation. Upf1 and Rent1 are 99.6% identical (BLAST search) and a possible explanation for their observation is that Upf1 becomes exported from the nucleus through interaction with Upf2-bound mRNAs during NMD, and therefore the absence of the CH domain in this mutant prevented nuclear export, resulting in net nuclear accumulation of Δ55-416Rent1. However, I also observed nuclear accumulation of Flag-Upf1$^{resΔ1-91}$, which contains the CH domain and which I showed remained capable of co-immunoprecipitating Upf2, suggesting that the failure in nuclear cytoplasmic shuttling is not a consequence of the absence of the CH domain. This effect does not appear to be dependent on the very extreme N-terminus, as deletion of residues 1-60 did not cause nuclear accumulation of Rent1 (Mendell et

al., 2002). Data from this study, taken with the results presented by Mendell and colleagues, suggests that residues 60-91 may be required for the nuclear export of Upf1/Rent1. This region does not contain a classical nuclear export sequence (Mendell et al., 2002), so it is a possibility that Upf1 is exported from the nucleus by an atypical mechanism, through interactions with currently unknown proteins.

The cytoplasmic shuttling of Upf1 was not the focus of this project, so I did not pursue this phenotype further. However, understanding the mechanism of nuclear-cytoplasmic shuttling of Upf1 may shed light on both the cellular location of NMD, and more importantly, into the mechanism of replication-dependent histone mRNA decay. In the current model, HD involves the nuclear recognition of replication stress, which then, through an unknown mechanism, causes the rapid decay of presumably cytoplasmic histone mRNAs (Kaygun and Marzluff, 2005a; Muller et al., 2007b; Sittman et al., 1983). ATR and DNA-PK have been shown to function during HD (Kaygun and Marzluff, 2005a; Muller et al., 2007b) and exposure to replication stress may cause ATR/DNA-PK signalling events that traffic Upf1 from sites of replication stress on chromatin into the cytoplasm to target histone mRNAs. However, recent data has suggested that HD may also occur exclusively in the nucleus (Choe et al., 2013; Rattray et al., 2013), therefore further study of this region may help to increase our understanding of how the nuclear export of Upf1 may be involved in NMD or the maintenance of genomic integrity through HD.

4.8.4 Identification of serine 42 as a critical residue for Upf1 chromatin recruitment

Lingner and colleagues (Azzalin and Lingner, 2006) demonstrated chromatin-bound Upf1 was hyperphosphorylated on S/T-Q motifs, and chromatin recruitment in response to replication stress requires ATR, suggesting phosphorylation mediates the interaction of Upf1 with chromatin. Analysis of the 91 amino acid region essential for chromatin recruitment identified the presence of four S/T-Q motifs (S10, T28, S42, T44), which are the consensus target sequences for PIKK kinases. Site-directed mutagenesis of each individual site, to prevent phosphorylation *in vivo*, demonstrated no defects in chromatin recruitment when S10 or T28 were mutated. However, mutation of T28 to alanine failed to generate an S-phase accumulation of Upf1 on chromatin (Figure 4.10); however time restrictions prevented further analysis of this mutant, therefore I am unable to draw any significant conclusions until further experimental repeats are performed.

Strikingly, mutation of S42 resulted in the absence of chromatin recruitment in asynchronous or S-phase enriched cells, demonstrating this motif is essential for chromatin recruitment. During production of these mutants, I was unable to mutate T44 due to the difficulties in the molecular cloning of Upf1 (see Materials and methods). Forming a dual SQTQ motif with S42, phosphorylation of either motif may be sufficient for Upf1 functions at chromatin, although it is possible, that both S42 and T44 are required for normal Upf1 function on chromatin.

4.8.5 S42, a residue required for Upf1 chromatin recruitment is not involved in NMD

I wanted to investigate whether the function of Upf1 at chromatin requires distinct structural motifs from those required for NMD, a process dispensable for genomic stability (Azzalin and Lingner, 2006b). The identification of S42 as a motif essential for the recruitment of Upf1 to chromatin raised the question of whether this residue was required generically for the all of the global functions of Upf1, or might be uniquely involved in its chromatin-associated functions. Similarly, it was important to establish whether well-established N- and C-terminal motifs required for NMD, were also important for the chromatin association of Upf1. Consistent with the recent work of several groups (Brazao et al., 2012; Geissler et al., 2013; Lim et al., 2012), I found that efficient siRNA-mediated knockdown of Upf1 reduced NMD efficiency, but did not eliminate it completely. Unlike the wild-type protein, ectopic expression of Flag-Upf1^{resAAA} failed to restore efficient NMD under these conditions, but importantly this mutant showed normal chromatin recruitment. In contrast, Flag-Upf1^{resS42A} efficiently restored NMD in siRNA treated cells, suggesting specific domains within Upf1 function in mutually exclusive cellular pathways.

4.8.6 Evidence for S42 as a Upf1 phosphorylation site

S42 is essential for the S-phase recruitment of Upf1 to chromatin, a process shown to be heavily regulated by PIKK mediated phosphorylation (Azzalin and Lingner, 2006b), suggesting phosphorylation of this residue may be necessary to bring about chromatin recruitment. Two preliminary lines of evidence support the possibility that S42 phosphorylation is required for chromatin association. Firstly, mass spectrometric

analysis of *in vitro* kinase assays using N-terminal Upf1 fragments identified S42 as being phosphorylated by the PIKK, DNA-PK (R. Beniston, unpublished). Secondly, an initial investigation into the effects of simulated phosphorylation at this motif *in vivo,* using a FLP-In cell line expressing the phospho-mimetic glutamic acid residue at position 42 demonstrated Flag-Upf1^{resS42E} is capable of interacting with chromatin, although this observation requires a more comprehensive study.

Further work will be required to establish whether phosphorylation at S42, and /or T44 are required for chromatin association. This is likely to include mass spectrometric analysis of chromatin-associated Upf1, together with a targeted, quantitative analysis of the extent of phosphorylation at S42 during S-phase with targeted knockdown of PIKK family members to identify the critical kinase required for Upf1 chromatin recruitment.

Upf1 binds to oligonucleotide sequences *in vitro* ((Li et al., 1992) Dehghani and Sanders, unpublished) but whether Upf1 is recruited to chromatin through direct association with DNA or through protein-protein interactions is not yet understood. Mass spectrometry based İnteractome studies, to determine the proteins which interact with Upf1 in the presence or absence of S42, may also provide candidate proteins which interact with Upf1 at chromatin.

4.8.7 The phosphorylation of S42 may generate structural changes to Upf1 N-terminal domains that allow interactions within the nucleus

Although Upf1 has been shown to be an essential gene for normal embryonic development in a number of model organisms, including *Danio*, *Drosophila* and mouse, this is believed to be the consequence of a requirement for NMD and, particularly,

SMD, which are essential for the regulation of developmentally expressed genes (Cho et al., 2012b; Kim et al., 2007), and not due to lack of genome stability during development. To date, Upf1 has only been reported to interact with chromatin and play some role in the maintenance of genomic stability in human cells (Azzalin and Lingner, 2006b; Azzalin et al., 2007). Therefore, what can be speculated as to the function of S42 in Upf1 chromatin recruitment and the maintenance of genomic stability? During early stages of this study, attempts to produce Upf1 cDNA through standard PCR were repeatedly unsuccessful, and analysis of the Upf1 coding sequence identified a 5' GC-rich (~95% GC) nucleotide region, preventing strand denaturation during PCR. This sequence is present only in the mouse and human Upf1 genes (BLAST search), and when translated forms a proline-glycine rich domain (PRD) unique to mammalian Upf1 (Figure 4.8). This repeat PPGGPGGPGG sequence (corresponding to amino acids 47-56 in human Upf1) fits the X-P-x-X-P domain criteria for an SH3 domain protein binding ligand (Aitio et al., 2010; Mayer, 2001) and sequences rich in alanine, glycine and proline have been proposed to function in structural flexibility, transcriptional repression, protein-protein and protein-RNA interactions (Cartegni et al., 1996; Catron et al., 1995; Steinert et al., 1991). This region therefore may facilitate, upon the correct stimulus, the interaction of Upf1 with currently unknown proteins or provide flexibility within this region to allow structural rearrangement of the N-terminus essential for the biochemical activity of Upf1.

4.8.8 *In silico* 3D prediction modelling of the N-terminal structure of Upf1 suggests a potential mechanism of chromatin recruitment

While not yet confirmed as a Upf1 phosphorylation motif *in vivo*, phospho-mimetic substitution of this site generated increased chromatin recruitment and

evidence, *in vitro,* has demonstrated at least one PIKK was capable of phosphorylating this motif (R.Beniston, unpublished). To investigate the potential effect of phosphorylation at this motif, I performed bioinformatic structural analysis of this region, with the aim of generating information as to how this site may contribute to the recruitment of Upf1 to chromatin. Attempts by other groups to resolve the complete crystal structure of Upf1 have proven unsuccessful thus far, with only the crystal structures described for the CH domain (amino acids 115-272) and helicase core (amino acids 295-914) (Cheng et al., 2007; Kadlec et al., 2006). The absence of crystal structures for the extreme N- and C-termini, most likely results from the relative lack of defined structure in these regions, and the potential to adopt multiple conformational states. To generate a model full-length protein structure, I submitted the sequence of human Upf1 to the I-TASSER 3D-structure prediction service, ranked as the top protein prediction server in recent Critical Assessment of protein Structure Prediction (CASP) experiments, which integrates published crystal structure data with protein prediction software and generate a 3D theoretical protein (Roy et al., 2010; Roy et al., 2012; Zhang, 2008).. Figure 4.17 shows the predicted 3D structure of a single Upf1 molecule, highlighting the highly conserved central helicase domain, Upf2 interacting CH domain, the N-terminus and C-terminal SQ domain. The CH domain is not bound to the helicase core in this model, as the presence of ATP or RNA, known to influence the binding of the CH domain to the helicase core, are not factored into the prediction (Chakrabarti et al., 2011).

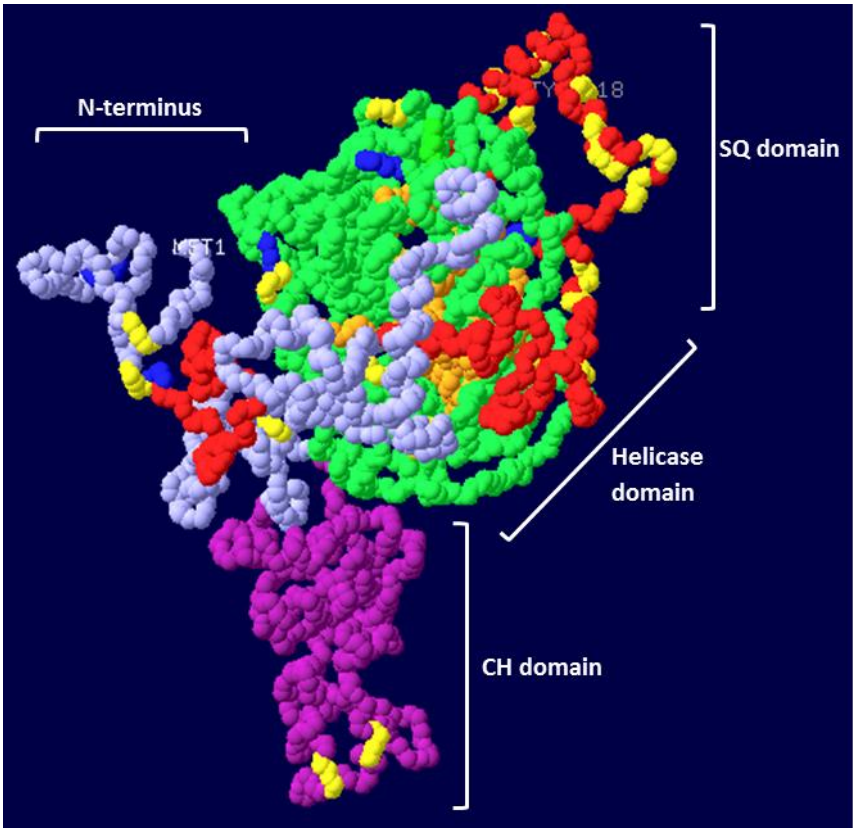

Figure 4.17 3D-structure prediction of full-length Upf1

The full-length Upf1 protein sequence was submitted to the I-TASSER 3D-structure prediction service and the resultant structure prediction processed using SwissView pdb viewer software. The Upf1 CH domain (purple), helicase domain (green), SQ domain and N-terminus are highlighted.

Closer analysis of the N-terminus (Figure 4.18a) highlights a compact structure, where the SQ motifs at S10 and S42 cluster immediately upstream of the PRD. In order to initiate the process of developing a working model for the function of serine 42 in the association of Upf1 with chromatin, I generated a phospho-mimetic mutation (S42E) at this motif *in silico*, analogous to the *in vivo* mutation described above, to introduce a negative charge representative of phosphorylation. When compared to the wild-type sequence (Figure 4.18b), introduction of a negative charge at this residue causes a large conformational change and an 'opening-out' of the N-terminal structure (Figure 4.18c). This S10/S42 cluster appears to be spatially distinct from T28, a motif

demonstrated to be phosphorylated by SMG1 during NMD responsible for the recruitment of SMG6 (Okada-Katsuhata et al., 2012). Importantly, phospho-mimetic substitution of either S10 or T28 did not generate this large conformational change (data not shown).

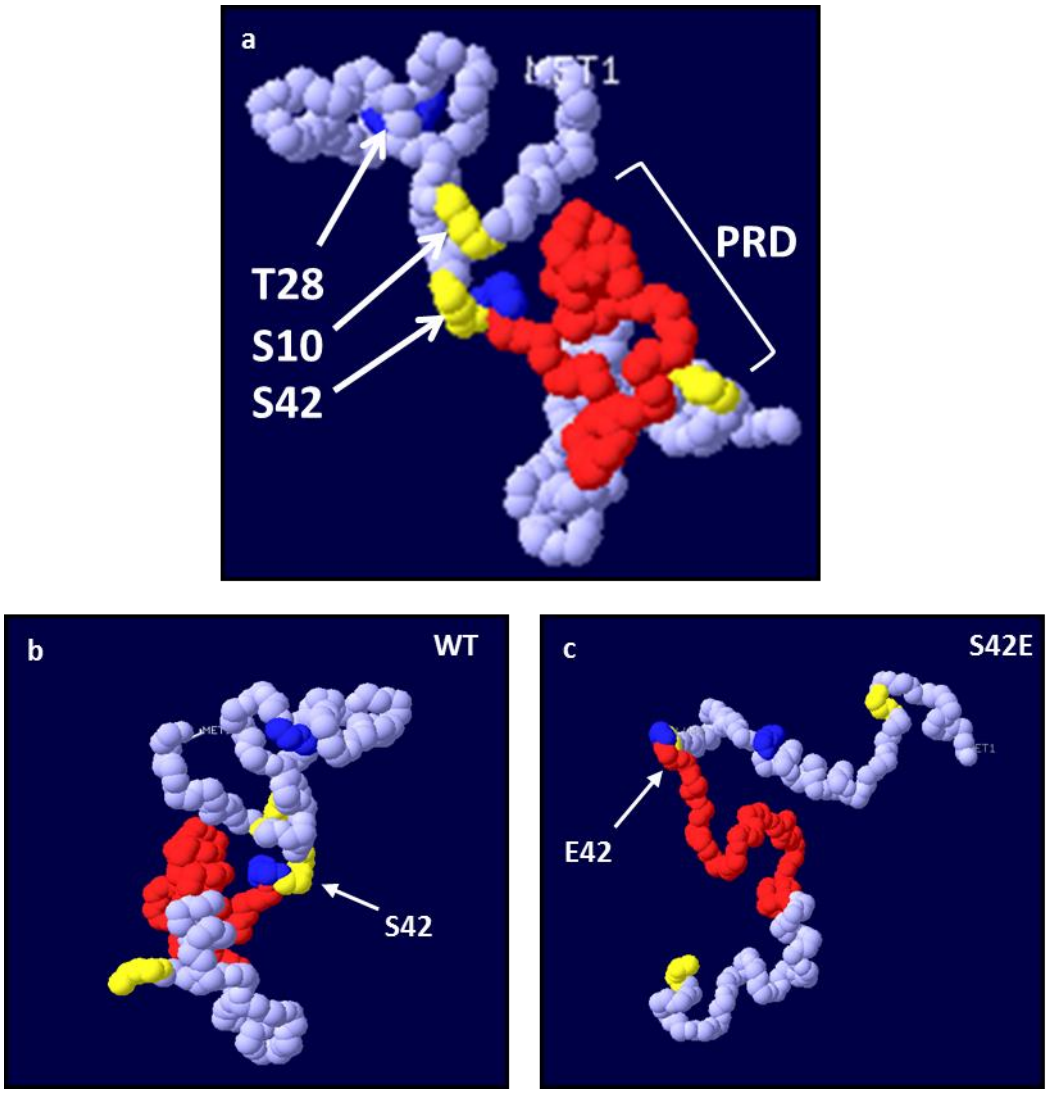

Figure 4.18 *In silico* phospho-mimetic substitution of S42 generates a large conformational change in the Upf1 N-terminus

a) The Upf1 N-terminal structure; highlighting the predicted positions of the S/T-Q motifs at S10, T28 and S42 and the PRD (red) b) A 180° lateral rotation of the image in (a), demonstrating the compact structure of the N-terminus. c) Predicted N-terminal structure after phospho-mimetic substitution of S42 to E42.

Interestingly, introduction of the phospho-mimetic mutation results in conversion of the PRD from a looped, closed conformation into an extended, linear configuration, using the I-TASSER modelling software. The proximity of this region immediately downstream of S42, a speculative Upf1 phosphorylation site, may generate morphological changes to the N-terminus that allow access to this region. While this region does not show any classical protein-protein interaction domains, it contains structural features similar those found in interaction surfaces (see earlier) and may facilitate the interaction of Upf1 with chromatin associated proteins, or directly with DNA.

Using bioinformatic analysis of the Upf1 3D structure, I propose the following speculative model for the recruitment of Upf1 to chromatin. Activation of PIKKs during replication stress may stimulate phosphorylation of Upf1 on S42 which induces a large conformational change within the N-terminus (Figure 4.18c). This could facilitate Upf1 loading onto chromatin either by, i) exposure of the PRD domain, allowing interaction with currently unknown chromatin-associated proteins, or, ii) the generation of a direct binding surface around S42 for a chromatin associated protein(s), analogous to the mechanism by which phospho-T28 acts in the recruitment of SMG6 during NMD, or iii) displacement of the N-terminus allows Upf1 helicase domains to directly interact with DNA.

In conclusion, in this chapter I investigated the S-phase recruitment of Upf1 to chromatin, and through generation of FLP-IN HeLa stable cell lines, performed structural and phospho-site analysis of the Upf1 extreme N-terminus and identified S42 as a critical motif required for Upf1 chromatin recruitment. I demonstrated S42

dependent recruitment of Upf1 to chromatin is functionally distinct from the role of Upf1 in NMD and provided preliminary evidence that phosphorylation of this motif may function in the recruitment of Upf1 to chromatin. Although yet to be proven, this suggests phosphorylation by nuclear PIKK proteins may specifically cause the S42 dependent recruitment of nuclear Upf1 onto chromatin, a process essential the S-phase specific functions of Upf1 in S-phase progression and genomic stability.

Chapter 5 Dissection of the S-phase specific functions of Upf1

5.1 Introduction

At the beginning of this study, in addition to roles in global mRNA surveillance, Upf1 had been shown to be involved in pathways essential for S-phase progression and genomic stability. The histone mRNA decay pathway, shown to involve Upf1, ensures the rapid decay of histone mRNAs in response to replication stress during S-phase, to prevent misregulation of histone protein levels and resultant genomic instability (Azzalin et al., 2007; Kaygun and Marzluff, 2005a; Muller et al., 2007b), however little is known of how Upf1 functions in this pathway. Azzalin and Lingner (2006), reported that shRNA-induced knockdown of Upf1 in HeLa cells caused an early S-phase cell cycle arrest, and these cells accumulated γH2AX, a marker of genomic instability. Upf1 was therefore proposed to function during DNA replication through S-phase specific recruitment to chromatin (Azzalin and Lingner, 2006a), and provide helicase activity at the replication fork through interaction with the p66 pol δ subunit (Carastro et al., 2002).

The role of Upf1 in the maintenance of genomic stability has been shown to be independent of the canonical NMD pathway, as knockdown of the core NMD component Upf2 does not affect the genomic integrity of the cell (Azzalin and Lingner, 2006b). NMD components have been demonstrated to bind telomeric DNA and knockdown of Upf1, SMG1 or SMG6 resulted in the loss of telomeric tracts and an accumulation of the lncRNA TERRA at telomeres (Azzalin et al., 2007). Interestingly, Upf1 knockdown also generated γH2AX foci at telomeres, and the requirement for polδ during lagging strand telomere DNA replication suggested Upf1 may also function

in the replication of a subset of telomeres *in vivo* (Azzalin et al., 2007; Chawla et al., 2011; Lormand et al., 2013).

In Chapter 4, I showed that S42 was essential for chromatin recruitment of Upf1, but was not required for NMD, while residues known to be important or implicated in the cyclical process of phosphorylation/dephosphorylation required for NMD (T28, S1096, S1116) were not required for chromatin recruitment. My objective here was to use the cell lines, HeLa- Flag-Upf1^{resS42A} and HeLa- Flag-Upf1^{resAAA}, generated in Chapter 4 to investigate the S-phase specific functions of Upf1 in two lines of study. Firstly, I aimed to investigate the proposed role of Upf1 in S-phase progression, through the interaction with the p66 polδ subunit, and investigate the significance of Upf1 nuclear interactions in the maintenance of genomic stability. In a second line of study, I aimed to perform a functional analysis of the role of Upf1 at telomeres.

5.2 Knockdown of endogenous Upf1 does not cause cell cycle arrest in HeLa cells

Upf1 knockdown was reported to cause an early S-phase arrest in HeLa cells (Azzalin and Lingner, 2006b), however this was not analysed further when similar experiments were performed subsequently by the same group (Azzalin et al., 2007). Therefore, I initially wished to clarify the requirement for Upf1 in cell cycle progression.

Flag-Upf1^{res} FLP-IN HeLa cells were transfected with non-targeting siRNA or Upf1 siRNA, with or without doxycycline, to investigate the effects on cell cycle progression of reducing Upf1 to very low levels, together with the consequences of concomitant expression of Flag-tagged Upf1. After incubation for three days, cells

were harvested and processed for flow cytometry as described in Materials and methods. Upf1 knockdown and expression of Flag-Upf1^{res} was confirmed by Western blot (Figure 5.1a) and the DNA content of cells determined by propidium iodide (PI) staining and analysis by flow cytometry (Figure 5.1b-e). Transfection of non-targeting siRNA in the presence or absence of Flag-Upf1^{res} did not disrupt the cell cycle profiles of these cells (Figure 5.1b and d). Efficient knockdown of endogenous Upf1 did not bring about any significant accumulation of early S-phase cells (Figure 5.1c) although a slight increase in the apparent proportion of cells in G2 was observed, which was not reversed in cells expressing Flag-Upf1^{res} (Figure 5.1d). These data indicate that, significant depletion of Upf1 had little or no effect on early S-phase progression, but may have resulted in a delay within G2/M, although this was not affected by expression of Flag-Upf1^{res}.

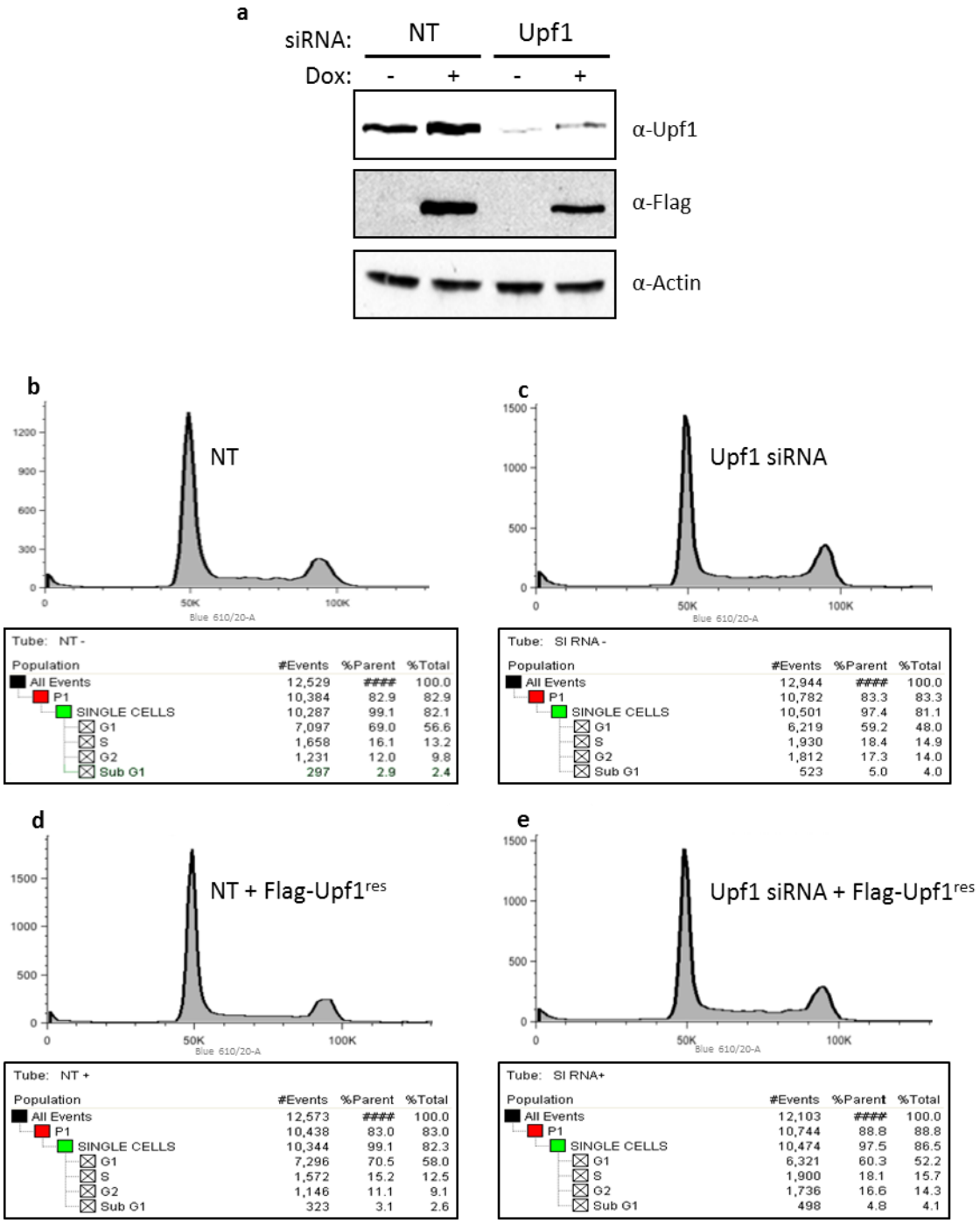

Figure 5.1 Upf1 knockdown does not generate an S-phase arrest in HeLa cells

Flag-Upf1^{res} FLP-IN HeLa cells were transfected with non-targeting siRNA or Upf1 siRNA, with or without 1µg/ml doxycycline for 72 h. Cells were then processed to generate cell lysates (a) or for flow cytometry (b-e) as described in Materials and methods. DNA was stained with PI and cells analysed by a BD LSRII flow cytometer. a) Western blot of Upf1 knockdown and Flag-Upf1^{res} expression. b-e) Cell cycle profiles of samples in (a), analysed using FlowJo software. The proportion of cells estimated to be in each phase of the cell cycle is indicated below each profile. Data is representative of two independent experiments.

5.3 Co-immunoprecipitation of Upf1 with the p66 subunit of DNA polymerase δ in HeLa cells

5.3.1 Endogenous Upf1 and p66 interact *in vivo*

Upf1 has been demonstrated to co-purify and co-immunoprecipitate with the p66 subunit of DNA polymerase δ (Carastro et al., 2002), and its association with components of DNA polymerase δ has been suggested as the mechanism by which Upf1 is recruited to chromatin (Azzalin and Lingner, 2006a; Carastro et al., 2002). I was unable to provide evidence in a yeast two-hybrid approach (Chapter 3) for a direct interaction between Upf1 and p66; in addition, transiently overexpressed Flag-Upf1 failed to immunoprecipitate p66 from HeLa cells (Chapter 4, and data not shown). Therefore I initially wanted to confirm that Upf1 and p66 do indeed interact *in vivo.*

I prepared nuclear extracts from asynchronous HeLa cells (see Materials and methods) and immunoprecipitated endogenous Upf1 or p66 using specific antibodies to each. The presence of both proteins in immunoprecipitated complexes was demonstrated by Western blot (Figure 5.2a-b), and endogenous Upf1 and p66 could be reciprocally co-immunoprecipitated, confirming this interaction occurs *in vivo*. It is important to note, that this interaction involves a very small fraction of both proteins, and was often not maintained even under low stringency wash conditions (data not shown), suggesting a weak or transient interaction. I was also unable to consistently detect PCNA, a processivity factor known to interact with polδ (Bruning and Shamoo, 2004; Podust et al., 1995), in immunoprecipitated complexes.

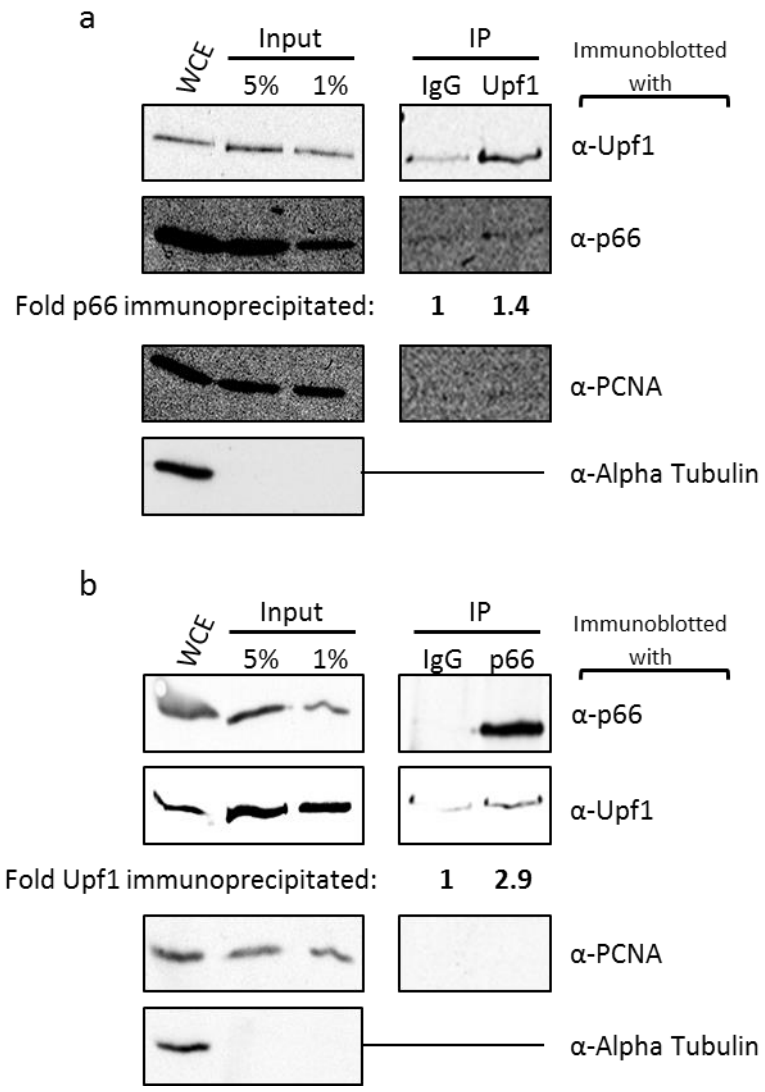

Figure 5.2 Co-immunoprecipitation of endogenous Upf1 and p66 in HeLa cells

a) Intact nuclei were prepared from asynchronous HeLa cells as described in Materials and methods, lysed with IP lysis buffer, and incubated overnight at 4°C with a) Upf1 or b) p66 antibodies. The following day Protein-G beads were added for 1 h at 4°C, before beads were collected and complexes eluted and analysed by SDS-PAGE. Western blot analysis was performed using α-Upf1, α-p66 or α-PCNA antibodies. Whole cell extract (WCE) and blotting for α-tubulin (cytoplasmic protein) were used to ensure purity of nuclear fractions. The Upf1 signal observed in IgG IP lanes reflects non-specific interactions between endogenous Upf1 and the IgG/ProteinG sepharose used. Quantification values indicate the fold amount of Upf1/p66 co-immunoprecipitated in each IP, normalised to the signal observed in the IgG control.

5.3.2 The Upf1-p66 interaction does not occur in S-phase enriched cells

As I initially performed these experiments in asynchronous cells, and the interaction between Upf1 and p66 had been proposed to be required for DNA replication (Azzalin and Lingner, 2006b), I wanted to investigate whether this interaction is elevated during S-phase.

I treated HeLa cells with 2mM hydroxyurea (HU) for 24 h to arrest a significant proportion of cells at the G_1/S boundary or within S-phase, before releasing them for 2-3 h to enrich for S-phase cells. Immunoprecipitations were performed as described previously. I was unable to demonstrate any interaction between endogenous Upf1 and p66 in this S-phase enriched cell population (data not shown), suggesting this interaction may not occur during global DNA replication.

5.3.3 Upf1 may interact with chromatin and p66 through a common motif

To investigate whether the interaction between Upf1 and p66 could be investigated in a mammalian cell system with the potential to identify interacting domains, I attempted to co-immunoprecipitate ectopically expressed, tagged forms of both proteins in HeLa cells.

Flag-Upf1^{res} FLP-IN HeLa cells were transiently transfected with an eGFP-p66 construct, previously shown to locate correctly to replication foci (Pohler et al., 2005), in the presence of doxycycline for 24 h, and incubated for an additional 24 h, or S-phase enriched as described previously. To increase the amount of immunoprecipitated Upf1-p66 complexes, I significantly increased the amount of cellular extract and antibody used in these immunoprecipitation experiments. Using

this approach, it was cost-prohibitive to generate nuclear extracts on the required scale and therefore whole cell extracts were used as the source of material for immunoprecipitation. The presence of both Flag-Upf1^{res}, endogenous p66 and the more slowly migrating eGFP-p66 band was confirmed in these lysates by Western blot (Figure 5.3).

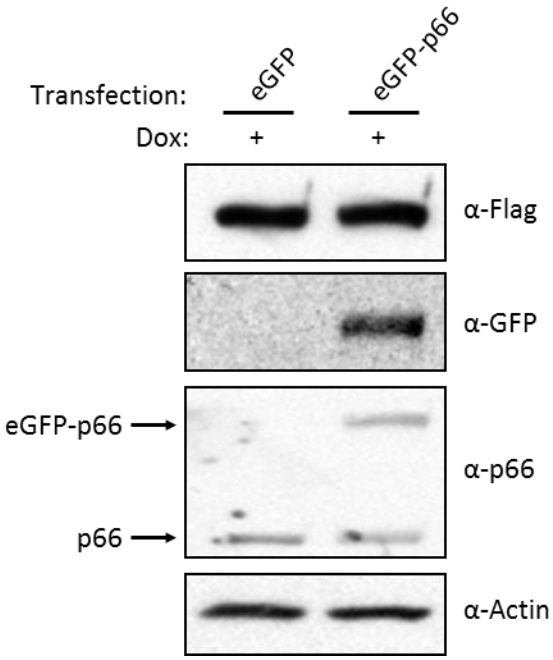

Figure 5.3 Co-expression of Flag-Upf1^{res} and eGFP-p66 in FLP-IN HeLa cells

Flag-Upf1^{res} FLP-IN HeLa cells were transfected with an eGFP-p66 construct and exposed to 0.5µg/ml doxycycline for 48 h. Whole cell extracts were then prepared as described in Materials and methods and expression analysed by Western blotting with α-Flag, α-GFP or α-p66 antibodies. α-actin was used as a loading control.

Immunoprecipitations were then performed using a Flag antibody, to specifically isolate ectopically expressed Flag-Upf1^{res}. The Flag-UPF1^{res} immunoprecipitates were probed for the presence of both forms of p66 using anti-p66 antibodies (Figure 5.4b). Unfortunately, technical restrictions prevented the identification of endogenous p66 with Flag-Upf1^{res} in these immunoprecipitations (data not shown). Faint bands corresponding to eGFP-p66 (Figure 5.4b, centre panel), were enriched in immunoprecipitates using anti-Flag antibodies compared to control IgG suggesting that, at least under these conditions, a small fraction of total eGFP-p66 may interact with Upf1. In cells enriched for S-phase (Figure 5.4b, left panel), the amount eGFP-p66 immunoprecipitated with Upf1 was reduced, consistent with the results obtained for the endogenous proteins (data not shown), suggesting this interaction is not enhanced during S-phase.

I wanted then to establish whether interaction with p66 is dependent upon S42, a motif demonstrated previously to be essential for recruitment of Upf1 to chromatin (Figure 4.11). FLP-IN HeLa cells expressing Flag-Upf1^{resS42A} were transiently transfected with an eGFP-p66 construct and immunoprecipitations performed as described previously. Interestingly, in contrast to data obtained from Flag-Upf1^{res} FLP-IN HeLa cells, eGFP-p66 could not be detected in Flag-Upf1 immunoprecipitates from with Flag-Upf1^{resS42A} FLP-IN cells (Figure 5.4b, right panel). This result suggests Upf1 interacts with p66, and requires the presence of S42, a motif shown to be essential for Upf1 chromatin recruitment.

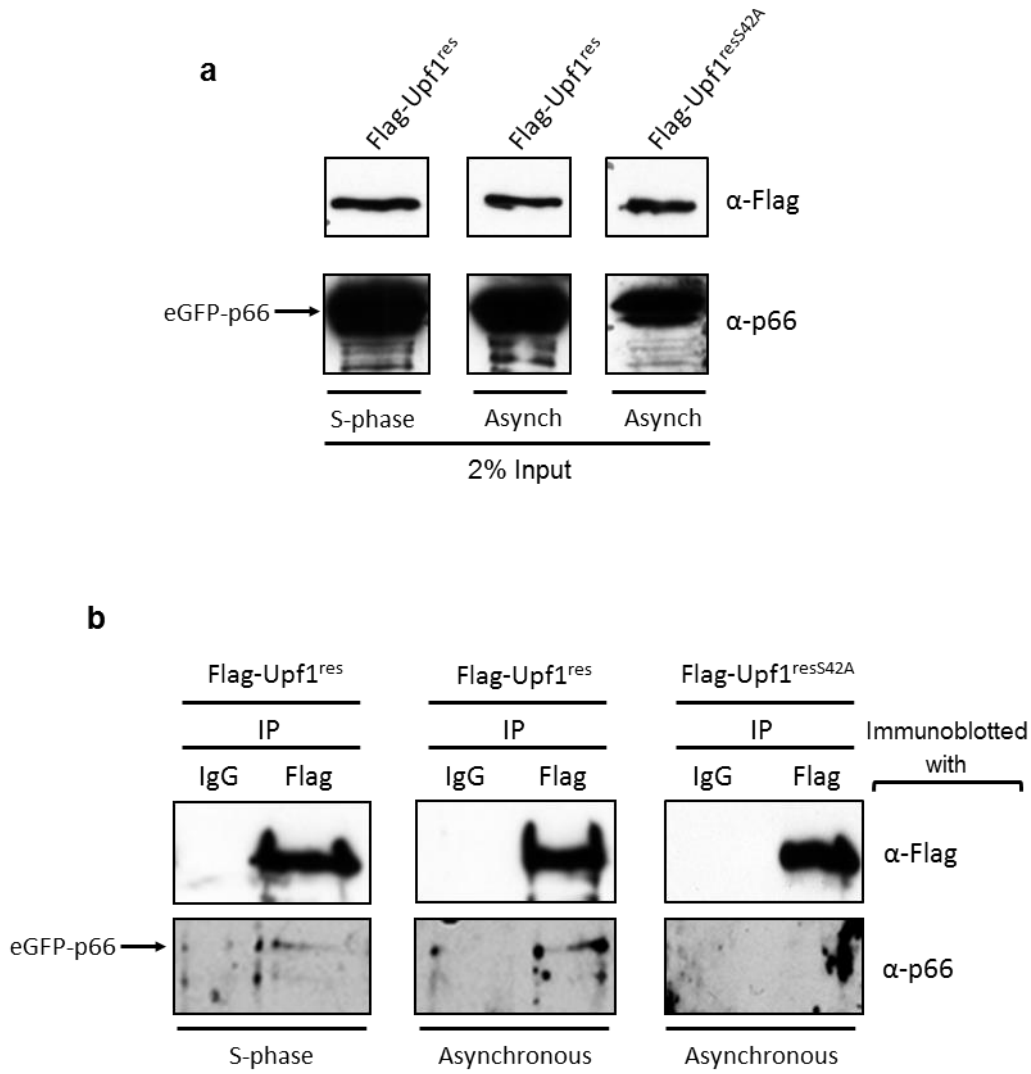

Figure 5.4 Flag-Upf1^{resS42A} could not be immunoprecipitated with ectopically expressed eGFP-p66

Flag-Upf1^{res} or Flag-Upf1^{resS42A} FLP-IN HeLa cells were transfected with an eGFP-p66 construct and exposed to 0.5µg/ml doxycycline for 48 h (Asynchronous). Alternatively for the final 24 h cells were S-phase enriched as described previously (S-phase). Whole cell extracts were then prepared as described in Materials and methods and samples incubated overnight with α-Flag antibodies. Protein-G beads were added for 1 h then complexes washed, eluted and separated by SDS-PAGE prior to Western blotting with α-Flag or α-p66 antibodies. a) 2% input of all immunoprecipitations b) Eluted proteins from immunoprecipitations. The p66 signal observed in IgG IP lanes reflects non-specific interactions between endogenous p66 and the IgG/ProteinG sepharose used.

5.4 The function of Upf1 in genomic stability involves motifs required for both chromatin recruitment and RNA decay

Azzalin and Lingner (2006) reported previously that depletion of Upf1 in the absence of exogenous genotoxic agents, utilising vectors generating short-hairpin RNAs targeting Upf1, resulted in early S-phase arrest. In addition, they reported the appearance of DNA double strand breaks following Upf1 depletion, as indicated by the accumulation of the phosphorylated form of the histone variant, H2AX (γH2AX), a downstream target of PIKK proteins during the DNA damage response (Azzalin and Lingner, 2006b). Circumstances that induce S-phase arrest, such as exposure to replication inhibitors, are known to bring about an increase in double strand break formation as a consequence of replication fork collapse, and an accumulation of γH2AX (Kurose et al., 2006).

However, in my hands, efficient knockdown of Upf1 by siRNA, failed to induce a significant S-phase arrest, although it did interfere with the efficiency of NMD (Chapter 4). These results raised questions regarding the significance of the reported role of Upf1 in cell cycle progression and genome integrity (Azzalin and Lingner, 2006b).

I set out to independently establish whether loss of Upf1 induced increased levels of double strand breaks, and if that was the case, to identify motifs within Upf1 essential for the maintenance of genomic stability.

5.4.1 Knockdown of endogenous Upf1 causes genomic instability in HeLa cells

Initially, HeLa cells were transiently transfected with non-targeting siRNA or Upf1 siRNA for three days and γH2AX levels determined by Western blot. Upf1

knockdown caused a dramatic increase in levels of γH2AX, compared to controls (Figure 5.5), demonstrating a significant DNA damage response in cells lacking Upf1.

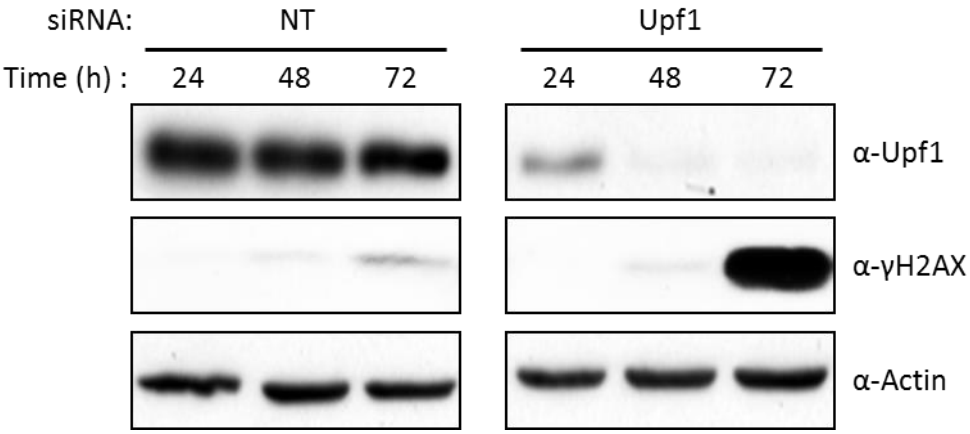

Figure 5.5 Upf1 knockdown activates a DNA damage response in HeLa cells

HeLa cells were transfected with non-targeting siRNA or Upf1 siRNA for 24-72 h before whole cell extracts prepared and analysed by Western blotting with α-Upf1 or α-γH2AX antibodies. α-actin was used as a loading control.

To confirm this effect was not an off-target effect of the siRNA used, I transiently transfected Flag-Upf1^{res} HeLa cells with non-targeting or Upf1 siRNA, with or without doxycycline, and assessed γH2AX levels. As before, siRNA-induced knockdown of Upf1 resulted in an increase in γH2AX levels, which was not observed in doxycycline-treated cells expressing Flag-Upf1^{res}. Thus, doxycycline-induced expression of Flag-Upf1^{res} was able to rescue the phenotype associated with Upf1 knockdown, preventing the expression of γH2AX signal (Figure 5.6), and supporting the notion that, despite having no effect on global S-phase progression, Upf1 is required to prevent the emergence of double strand breaks.

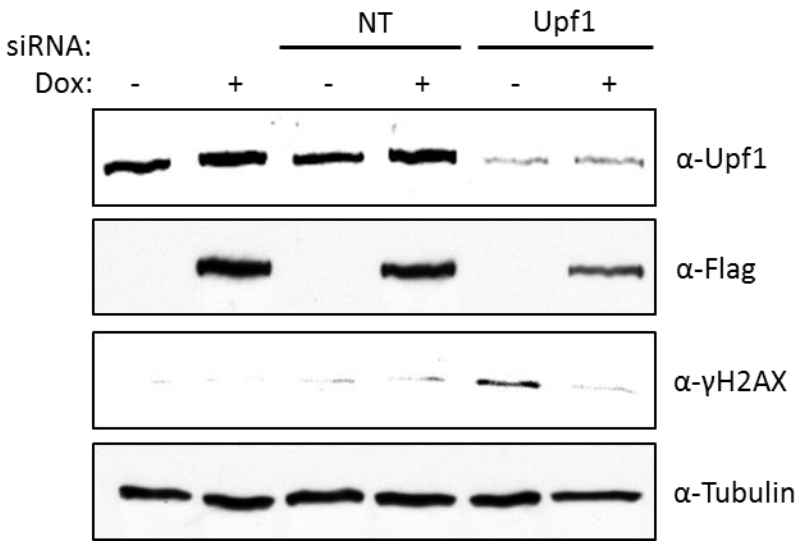

Figure 5.6 Expression of Flag-Upf1^{res} rescues the γH2AX signal induced by Upf1 knockdown

Flag-Upf1^{res} FLP-IN HeLa cells were un-transfected, or transfected with non-targeting siRNA or Upf1 siRNA for 72 h, and 1μg/ml doxycycline added where appropriate. Whole cell extracts were then prepared and analysed by Western blot using α-Upf1, α-Flag or α-γH2AX antibodies. α-tubulin was used as a loading control.

5.4.2 Upf1 chromatin recruitment is essential for Upf1-dependent genomic stability

The results described in Chapter 4 indicated that the N-terminal region of Upf1 comprising residues 1-91 is essential for chromatin association (Figure 4.7). I therefore investigated whether Flag-Upf1$^{resΔ1-91}$ FLP-IN cells were capable of rescuing the γH2AX phenotype associated with Upf1 knockdown. FLP-IN cells containing either Flag-Upf1$^{resΔ1-91}$ or Flag-Upf1^{res} were treated with doxycycline or not as appropriate, transfected with non-targeting or Upf1 siRNA, and levels of γH2AX determined. As before, Flag-Upf1^{res} expression blocked the appearance of significant levels of γH2AX (Figure 5.7b, compare lanes 3 and 4). In contrast, Upf1$^{resΔ1-91}$ was unable to rescue the γH2AX phenotype observed after Upf1 knockdown (Figure 5.7b, compare lanes 3 and 5). This data demonstrates that the N-terminal Upf1 residues 1-91, previously show to

be essential for chromatin recruitment, are required for Upf1-mediated prevention of genomic instability.

5.4.3 Upf1 motifs associated with RNA decay also are required for genomic stability

Canonical NMD has been demonstrated to be dispensable for genomic stability (Azzalin and Lingner, 2006b), and Upf1 phosphorylation site motifs either required or implicated in NMD are not involved in chromatin recruitment (Chapter 4). Therefore, I wished to establish the role, if any, of these motifs in the maintenance of genomic stability.

FLP-IN cells containing Flag-Upf1^{resAAA} were treated with doxycycline, transfected with non-targeting or Upf1 siRNA and γH2AX levels determined as before. Strikingly, expression of Flag-Upf1^{resAAA} in Upf1 knockdown cells generated a significantly higher level of γH2AX than Upf1 knockdown alone (Figure 5.7b, compare lanes 3 and 6). Expression of this mutant, even in the presence of endogenous Upf1, also generated a γH2AX signal (Figure 5.7a, lane 4). These data demonstrate that Upf1 motifs associated with NMD function, shown to be dispensable for chromatin recruitment, are essential for the maintenance of genomic stability.

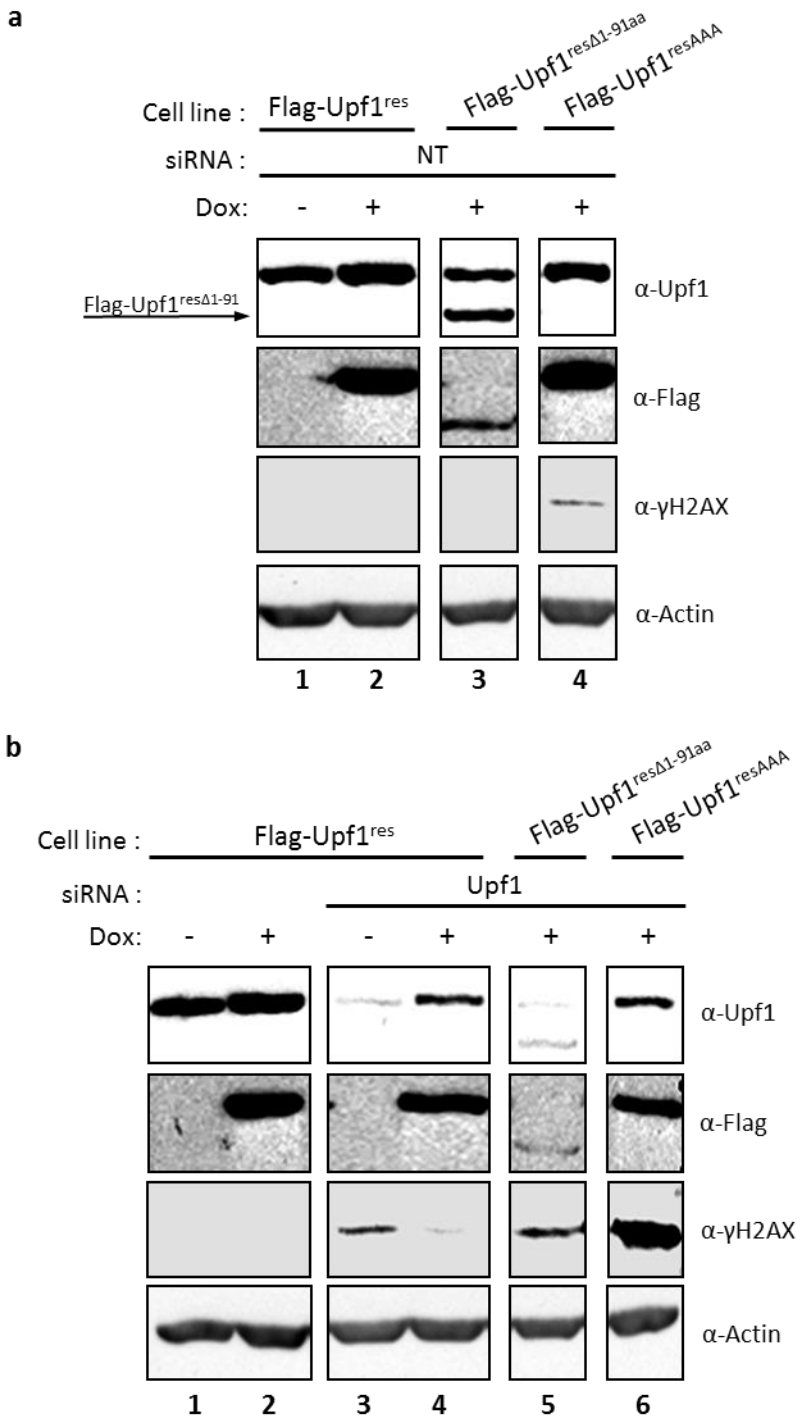

Figure 5.7 Upf1 mutants lacking motifs required for chromatin recruitment or NMD cannot rescue the γH2AX signal after Upf1 knockdown

Flag-Upf1^{res}, Flag-Upf1$^{resΔ1-91}$ or Flag-Upf1^{resAAA} FLP-IN HeLa cells were either un-transfected, or transfected with non-targeting siRNA or Upf1 siRNA with or without 1µg/ml doxycycline for 72 h. Whole cell extracts were then prepared and analysed by Western blot using α-Upf1, α-Flag or α-γH2AX antibodies. α-actin was used as a loading control. a) Cells transfected with non-targeting siRNA. b) Cells either un-transfected, or transfected with siRNA against Upf1. All panels are from the same western blot under the same exposure conditions.

5.5 Functional analysis of Upf1 dependent telomeric DNA replication

5.5.1 Upf1 knockdown causes the loss of a subset of telomeres in HeLa cells

Upf1 physical interacts with telomeres *in vivo* and was shown to be essential for leading, and to a lesser extent, lagging strand telomeric DNA replication (Azzalin et al., 2007; Chawla et al., 2011). Knockdown of SMG1 and SMG6 has been demonstrated to result in a loss of telomeres and accumulation of TERRA foci (Azzalin et al., 2007) suggesting that there may be mechanistic similarities between NMD and the Upf1-mediated maintenance of telomere integrity. I therefore wished to explore the functional role of Upf1 motifs essential for chromatin recruitment or NMD in the replication of telomeric DNA.

In a first step, Flag-Upf1^{res} FLP-IN HeLa cells were transfected with non-targeting siRNA or Upf1 siRNA, with or without doxycycline for 72 h. Cells were then incubated for an additional 4 h in the presence of colcemid, a compound which destabilises microtubules and prevents mitosis through failure to generate a mitotic spindle (Rieder and Palazzo, 1992). Samples of cells exposed to each condition were used to obtain mitotic spreads, prepared as described in Materials and Methods, and telomeric DNA labelled through hybridisation of a protein-nucleic acid (PNA) FISH (Fluorescent *In situ* Hybridisation) probe designed to specifically bind to telomeric sequences (Azzalin et al., 2007). Genomic DNA was counterstained with DAPI (4',6-Diamidino-2-Phenylindole, Dihydrochloride) and images acquired using a Deltavision confocal microscope. Representative microscopy images are displayed in Figure 5.8. Chromosomes from each experimental condition were analysed for loss of telomeres or telomere-free ends, as judged by the absence of a telomere associated fluorescent

signal associated with DAPI-stained chromosomes (see arrows, Figure 5.8a-e). Parallel samples were analysed for Upf1 knockdown and Flag-Upf1^{res} expression by Western blot (Figure 5.9a and b). Data for two independent experiments (expressed as percentage of telomere-free ends (%TFE) are shown in graphical (Figures 5.9a and b) and table form (Table 4). siRNA-mediated Upf1 knockdown resulted in a significant increase in numbers of telomere-free ends (compare Figure 5.8a and b, Figures 5.9a and 5.9b, lanes 1 and 2). Importantly, the appearance of TFEs induced by the loss of Upf1 expression was rescued by doxycycline-induced expression of Flag-Upf1^{res} (compare Figure 5.8a and c, Figures 5.9a and 5.9b, lanes 1 and 3) indicating an absence of a subset of telomeres in Upf1-depleted cells. Although not quantified, after knockdown of Upf1 I observed increased numbers of telomere fragments, regions of telomeric DNA not attached to a chromosome (Figure 5.8b, inset image).

5.5.2 Upf1 motifs required for both chromatin recruitment and RNA decay functions are required for maintenance of telomeric integrity

Upf1 has been shown to bind to telomeric chromatin *in vivo* (Chawla et al., 2011). In addition, a number of proteins, including SMG1 and SMG6, originally characterised by virtue of their role in NMD, have also been demonstrated to function at telomeres (Azzalin et al., 2007). SMG1 is capable of phosphorylating Upf1 at T28 *in vitro* (Ohnishi et al., 2003), and phosphorylation of this motif *in vivo* was significantly decreased by SMG1 knockdown (Okada-Katsuhata et al., 2012). Phosphorylation of this motif, presumably by SMG1, is necessary for the interaction of SMG6 with Upf1 and 5' RNA decay of PTC-containing transcripts during NMD (Okada-Katsuhata et al., 2012). This suggests the roles of Upf1, SMG1 and SMG6 in TERRA decay and telomere

replication may also involve signalling mechanisms more commonly associated with mRNA surveillance.

Data presented previously in this thesis has shown that a Upf1 mutant lacking S42 fails to associate with chromatin and is incapable of rescuing the appearance of double strand breaks, while mutants lacking the canonical residues required for cyclical phosphorylation/dephosphorylation during RNA decay in NMD, fail to rescue the appearance of double strand breaks, despite being capable of chromatin association. Therefore, I wished to compare the consequences, if any, of inducing the expression of each of these mutants, in the maintenance of telomere integrity.

Flag-Upf1^{resS42A} and Flag-Upf1^{resAAA} FLP-IN HeLa cell lines were transfected with Upf1 siRNA and expression of Flag-Upf1 mutants induced with doxycycline. Assessment of TFEs was performed as described previously, and expression of either Flag-Upf1^{resS42A} or Flag-Upf1^{resAAA} were unable to rescue telomere loss in the absence of endogenous Upf1 (Figure 5.8d and e, Figures 5.9a and 5.9b, compare lane 2 to lanes 4 and 5). This data indicates that although these Upf1 motifs are functionally distinct for Upf1 chromatin recruitment and NMD function, they are both essential for the role of Upf1 in maintenance of telomere integrity.

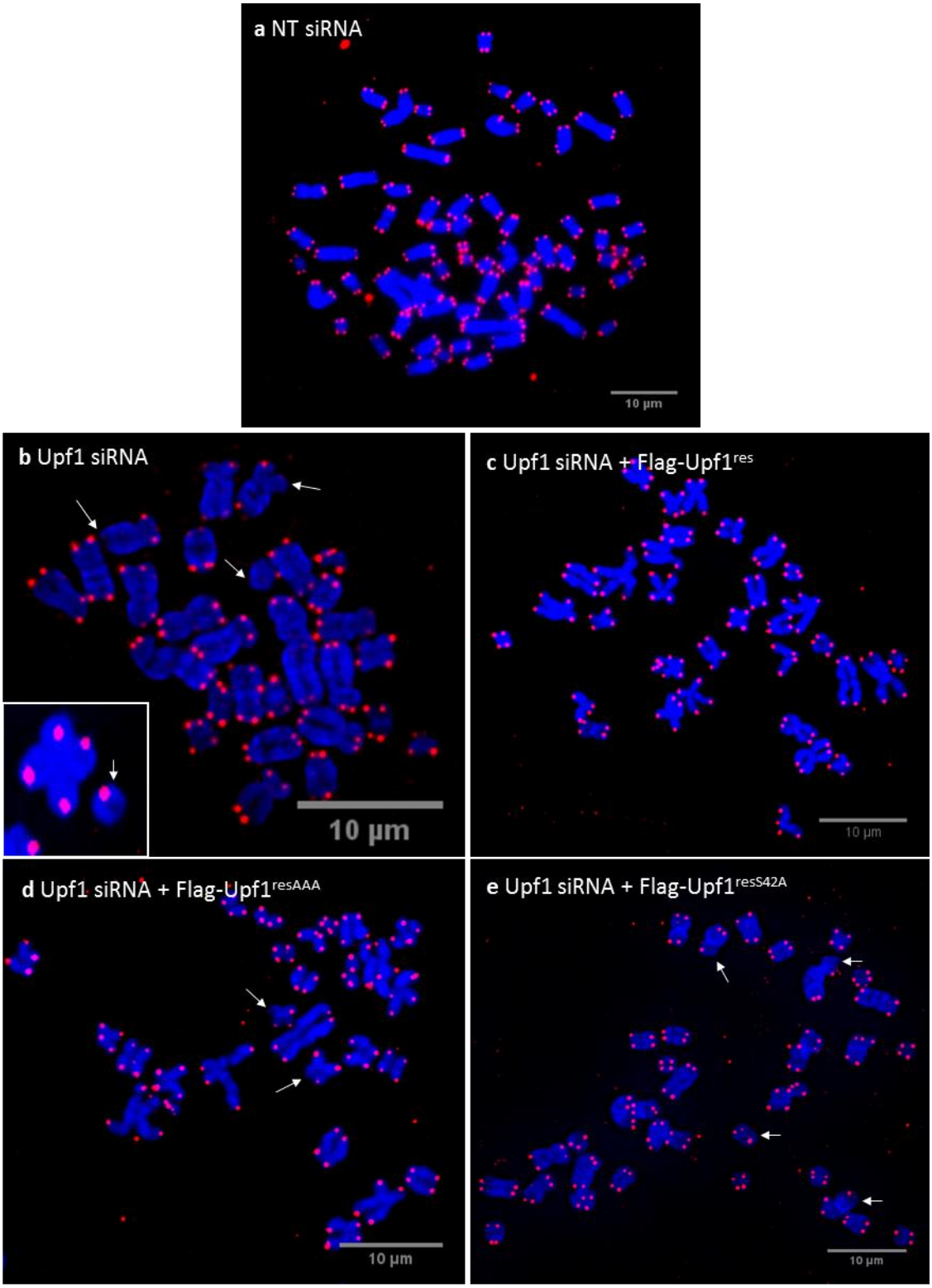

Figure 5.8 Telomere loss after Upf1 knockdown and rescue by Flag-Upf1^{res} mutants in HeLa cells

Flag-Upf1^{res}, Flag-Upf1^{resS42A} or Flag-Upf1^{resAAA} FLP-IN HeLa cells were transfected with non-targeting siRNA or Upf1 siRNA with or without 1µg/ml doxycycline for 72 h. Telomeric sequences (red) were identified by FISH as described in Materials and methods. DAPI is shown in blue. Arrows indicate telomere free ends (TFEs). b) Indent – arrow indicating a telomere fragment.

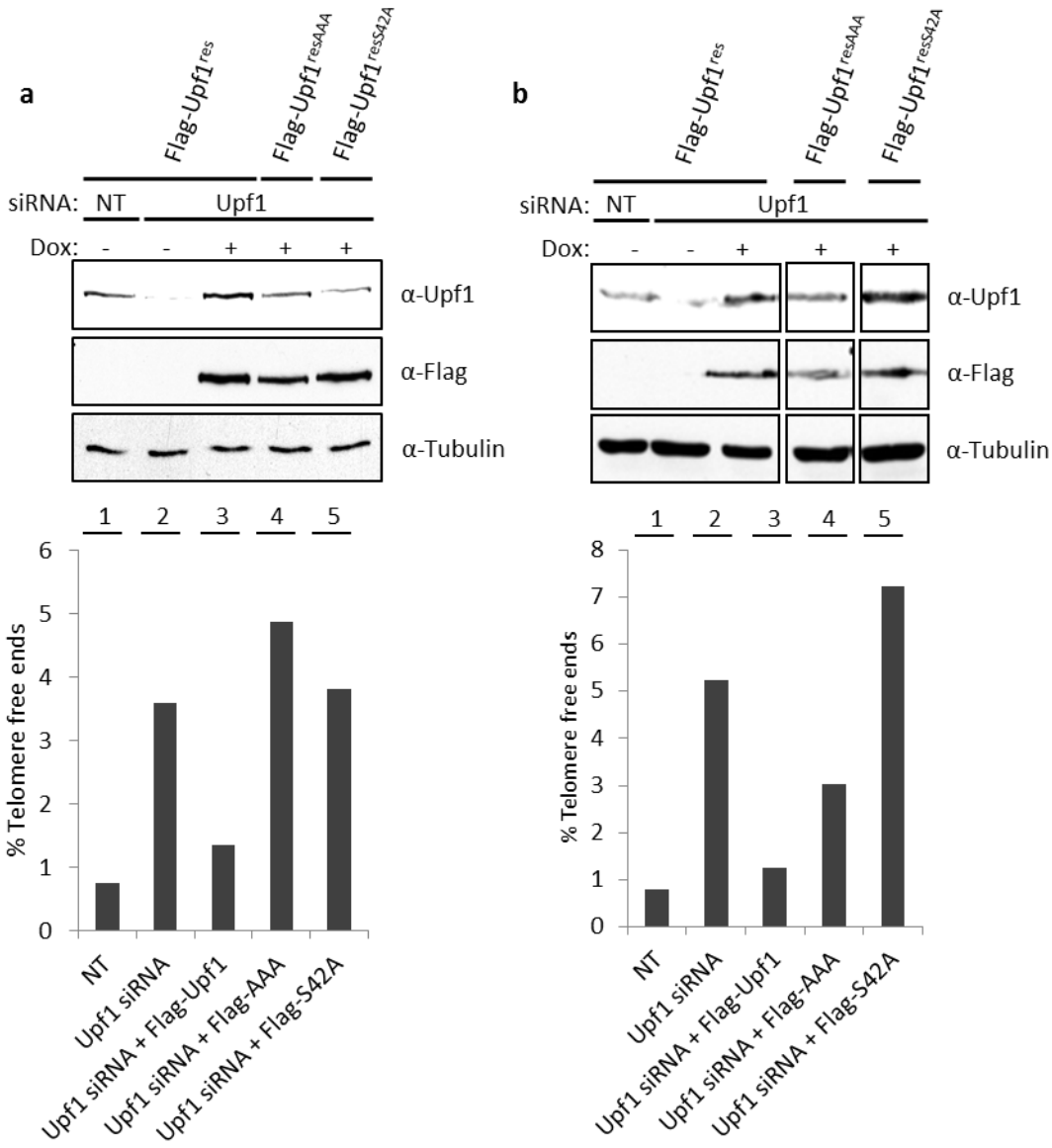

Figure 5.9 Quantification of telomere-free ends in Upf1-knockdown cells and rescue by Flag-Upf1^{res} mutants

Flag-Upf1^{res}, Flag-Upf1^{resAAA} or Flag-Upf1^{resS42A} FLP-IN HeLa cells were transfected with non-targeting siRNA or Upf1 siRNA, with or without 1µg/ml doxycycline for 72 h. Telomere free ends were identified by FISH and quantified as described in Materials and methods. a) and b) Western blots (upper) and % TFEs (lower) from two independent experiments. All panels are from the same western blot under the same exposure conditions.

siRNA +/- expression	Chromosomes counted	%TFEs
NT	993	0.78
Upf1 siRNA	2325	4.43
Upf1 siRNA + Flag-Upf1^{res}	1299	1.31
Upf1 siRNA + Flag-Upf1^{resAAA}	1150	3.96
Upf1 siRNA + Flag-Upf1^{resS42A}	1451	5.03

Table 4 Quantification of telomere free ends (TFEs) in Figure 5.9

Summary of two independent experiments, displaying total number of chromosomes counted and % telomere free ends.

5.6 Discussion

The DNA/RNA helicase Upf1 has traditionally been demonstrated primarily responsible for the surveillance of a broad class of mRNA transcripts. However, Azzalin and Lingner, presented evidence that Upf1 has S-phase specific functions involved in DNA replication and genomic stability (Azzalin and Lingner, 2006b). The initial aim of this chapter was to investigate the functions of chromatin-associated Upf1 in DNA replication and genomic stability.

5.6.1 Upf1 is not required for S-phase progression

Upf1 was proposed to be an essential component required for S-phase progression, on the basis of flow cytometry data following short-hairpin- induced Upf1 knockdown. This was reported to induce an early S-phase arrest in HeLa cells (Azzalin and Lingner, 2006b). I did not observe this phenotype using siRNA-mediated knockdown of Upf1 in this study (Figure 5.1). The reasons for this discrepancy are unknown. I cannot exclude the possibility that minor technical differences between approaches resulted in variations in Upf1 knockdown efficiency that may have contributed to this discrepancy. Only a small fraction of total Upf1 interacts with chromatin during S-phase (Azzalin and Lingner, 2006 and Chapter 4) and therefore trace amounts of endogenous Upf1 in knockdown cells may have been sufficient to facilitate S-phase progression in my experiments. As low levels of Flag-Upf1^{res} expression were demonstrated to be capable of rescuing phenotypes arising from Upf1 knockdown (see below), I cannot discount this possibility.

However, early S-phase arrest was not observed by the same group when similar experiments were performed in subsequent work (Azzalin et al., 2007),

suggesting that the original data may have been mis-interpreted. Closer analysis of the cell cycle data presented by Azzalin and Lingner, (2006), suggests the early S-phase arrest reported may have been an artefact accidentally generated during processing of the flow cytometry data. The cell cycle profile obtained by them from Upf1-knockdown cells resembled a normal unperturbed cell cycle, albeit with an apparent rightwards shift in the predominant 2n peak, corresponding to a possible small increase in the total DNA content of these cells. However, a similar shift was also observed in the 4n peak which those authors attributed to the presence of a significant proportion of polyploid cells, and the complete absence of a G2/M population.

An alternative interpretation of their data is that either variability in cell numbers between samples resulted in apparent differences in DNA content, or that there was an undetected change in the flow pressure between samples during the analysis, both circumstances which can result in “profile drift” (Mark Jones, personal communication).

The results reported here, together with subsequent data from the Azzalin group (Azzalin et al, 2007) provide strong evidence that Upf1 knockdown does not generate an early S-phase arrest, and Upf1 is not required for global S-phase progression.

siRNA-mediated knockdown of Upf1 undertaken in this work did result in an increase in the proportion of cells in G2/M phase of the cell cycle. These data are consistent with observations reported here and elsewhere that Upf1 depletion results in a DNA damage response associated with a failure to maintain telomere integrity, as discussed below (Chawla et al., 2011).

5.6.2 Upf1 and p66 interact in HeLa cells, but are not primarily involved in genomic DNA replication

Upf1 was shown to co-purify to almost complete homogeneity with p66 from bovine thymus extracts (Carastro et al., 2002), being separated only after 4 fractionation steps using Heparin-Sepharose chromatography. This data suggests a strong binding interaction between these two components. I found no evidence for a direct interaction using the yeast two-hybrid (Chapter 3) or studies using transiently overexpressed Flag-Upf1 (Chapter 4), so in this section of work I performed an investigation of the interaction between Upf1 and p66 in FLP-IN HeLa cells. The rationale behind this approach was that this system could be utilised, in principle, to demonstrate functionality of a tagged derivative of Upf1, and could serve as the basis for a strategy to identify Upf1 mutants with phenotypes associated with a role in genomic stability.

Endogenous Upf1 and p66 co-immunoprecipitated in nuclear extracts from asynchronous HeLa cells (Figure 5.2), although this reflected an extremely small fraction of both proteins. Consistent with the notion that p66 is solely involved in DNA replication, while Upf1 appears to play a role in a range of surveillance pathways in multiple cellular locations, Upf1 was more easily detected in p66 immunoprecipitates than p66 in Upf1 immunoprecipitates (Figure 5.2). These immunoprecipitation experiments were also very sensitive to wash conditions used in processing steps (data not shown), and I could not consistently identify PCNA in these complexes. Repeated attempts to optimise wash conditions through titration of both detergent and salt concentration did not significantly increase the amount of either protein co-immunoprecipitated (data not shown). A potential refinement to the current protocol

would be to induce chemical cross-links within cells, forming covalent bonds between cysteine residues on neighbouring proteins. This may stabilise these weak interactions during immunoprecipitation, a technique utilised previously to demonstrate interaction of Upf1 with CBP80 (Hwang et al., 2010).

In an attempt to generate a genetically tractable system for the analysis of the Upf1-p66 interaction, I expressed tagged forms of each protein simultaneously in FLP-IN HeLa cells and demonstrated Flag-Upf1^{res} co-immunoprecipitated ectopically expressed GFP-p66 (Figure 5.4b). Using this approach, I demonstrated that S42 in Upf1, a residue required for chromatin recruitment, is also required for the interaction with GFP-p66 (Figure 5.4b).

It cannot be concluded from this data that an interaction with p66 is the mechanism by which Upf1 associates with chromatin. As discussed previously (Chapter 4) purified Upf1 has been shown to bind directly to oligonucleotides and act as both a DNA, as well as an RNA helicase (Li et al., 1992) Dehghani and Sanders, unpublished), and it is conceivable that changes in the conformation of the N-terminal region of Upf1 induced by the S42A mutation precludes a direct association with DNA. Further studies, involving a comparative biochemical analysis of DNA binding and helicase activity of wild-type, S42A, and potentially S42E mutants, together with a differential proteomic analysis of the interactomes of the nuclear forms of Upf1 may help to provide mechanistic evidence of the role of p66 in Upf1 chromatin recruitment.

At least two explanations can be proposed to explain the very low stoichiometry of association detected between Upf1 and p66 from HeLa cells. One possibility is that Upf1 and p66 do not interact directly, and form a weak association as

constituent parts of a larger replication complex that fails to survive extraction conditions used. Upf1 has been demonstrated to co-immunoprecipitate the p125 polδ subunit (Azzalin and Lingner, 2006b), and therefore Upf1 may interact with p66 indirectly through an interaction with alternative polδ subunits. However, Upf1 does not co-purify with the p125 subunit in bovine thymus extracts or co-immunoprecipitate the p50 subunit in HeLa cells (Carastro et al., 2002), suggesting p66 is the most likely candidate subunit by which Upf1 interacts with polδ.

A second potential explanation is that a direct interaction does occur, possibly involving the association of the N-terminal region of Upf1 with p66; however while necessary, these elements may not be sufficient for stable association. An additional, post-translational modification(s) of either or both p66 and Upf1 may be required, but might be expected to be a regulated, and possibly rare, event in HeLa cells.

Given that Upf1 had been proposed to act at, or close to, replication forks, (Azzalin and Lingner, 2006a, b; Muller et al., 2007a) a reasonable initial hypothesis was that the extent of interaction may be elevated during S-phase. When immunoprecipitations were performed using extracts generated from S phase-enriched cells, the interaction between Upf1 and p66 was reduced or absent (Figure 5.4a and data not shown). This result was initially surprising, however taken together with the absence of early S-phase arrest in Upf1-depleted cells (discussed above), and the effects of Upf1 mutants on telomere integrity (discussed below), it suggests the interaction between Upf1 and p66 does not occur throughout S-phase and is a rare event, at least in HeLa tissue culture cell models, posing the question as to why Upf1 co-purified with p66 in bovine thymus extracts (Carastro et al., 2002).

The thymus gland is an immune tissue involved in the maturation of T-cells (Nishino et al., 2006), which undergo rapid clonal cell divisions upon antigen recognition (Mueller et al., 1989). As a result, it is unusual in that it contains significant quantities of somatic cells that express high levels of telomerase (Liu et al., 2001), necessary to prevent rapid telomere shortening and cellular senescence (Reviewed in Shay and Wright, 2005). Interestingly, tissue-specific TERRA expression in mice has been shown to be the highest in the thymus gland (Schoeftner and Blasco, 2008). High level expression of TERRA in these tissues correlates with the need to suppress high levels of telomerase activity during normal DNA replication (Redon et al., 2010). Assuming the same is true in the bovine thymus, the proposed requirement for Upf1 in TERRA degradation for both telomere replication and end processing during late S-phase will be much greater in this tissue than in HeLa cells, shown to express relatively low levels of TERRA (Azzalin et al., 2007; Schoeftner and Blasco, 2008).

Upf1 has been proposed to interact with polδ at telomeres to displace TERRA ahead of the progressing replication fork during lagging strand DNA synthesis (Azzalin et al., 2007). Upf1 knockdown, however, generated only mild defects at lagging strands, with defects occurring predominantly at leading strand telomeres (Chawla et al., 2011). Leading strand synthesis uses the $(AATCCC)_n$ telomeric strand as a template during semi-conservative DNA replication. The TERRA molecule $(UUAGGG)_n$ also referred to as the G-rich strand) is transcribed from, and hybridises with, this strand during early S-phase (See Figure 1.6) (Schoeftner and Blasco, 2008). The 5'-3' RNA helicase activity of Upf1 was proposed to displace TERRA from the $(AATCCC)_n$ strand in

late S-phase, allowing polε-mediated leading strand synthesis (Chawla et al., 2011), suggesting the primary function of Upf1 at telomeres does not involve polδ.

However, minor defects detected at lagging strands in these cells (Chawla et al., 2011) suggested secondary Upf1 functions involving polδ contribute to telomere integrity. C-rich TERRA transcripts $(CCCUAA)_n$, originating from the $(TTAGGG)_n$ telomeric DNA strand are almost undetectable in cells (Azzalin et al., 2007; Schoeftner and Blasco, 2008). However, it is possible that trace amounts of this C-rich TERRA hybridises with the $(TTAGGG)_n$ telomeric strand and prevents lagging strand DNA synthesis. Therefore, albeit at a much lower frequency than at leading strands, Upf1 may interact with polδ, via p66, to degrade C-rich TERRA and facilitate lagging strand synthesis in late S-phase, explaining the very weak interaction observed in asynchronous HeLa cells (Figure 5.2). Proportionately higher levels of both G- and C-rich TERRA in bovine thymus may require extensive Upf1-dependent regulation at both leading and lagging strands. Interactions with polδ, and potentially polε, in this tissue will therefore be significantly higher than in HeLa cells, allowing the co-purification of Upf1 and p66 from this tissue.

Thus, a role for Upf1 in global DNA replication appears unlikely, as Upf1 knockdown did not generate an early S-phase arrest (Figure 5.1) and the weak interaction with p66 was absent in S-phase enriched cells (Figure 5.2). TERRA degradation is known to occur in late S-phase (Porro et al., 2010). The relatively crude method of S-phase enrichment used in this study, not designed to generate late S-phase cells, may have inadvertently enriched for a population of cells in which this interaction is rare or absent. If Upf1 is required to displace TERRA transcripts late in S-

phase, then a reasonable prediction would be that Upf1 is targeted to either leading or lagging strand polymerases in late S-phase. The use of an alternative cell synchronisation method, such as timed release from a double thymidine block (Reviewed in Ma and Boon, 2011), would allow this interaction to be assessed at specific S-phase stages to confirm or refute this hypothesis.

5.6.3 Upf1-dependent genomic stability is dependent upon motifs required for both chromatin recruitment and RNA decay

When this work was initiated, the loss of genomic stability in Upf1-knockdown cells, as demonstrated by the detection of γH2AX, was suggested to be the consequence of a failure of global S-phase progression, dependent on the interaction of Upf1 with chromatin (Azzalin and Lingner, 2006a, b). However, as discussed above, I was unable to reproduce these findings. However, I demonstrated that Upf1 knockdown *did* induce significant levels of γH2AX, confirming that, irrespective of global S-phase progression, depletion of Upf1 in HeLa cells resulted in genomic instability (Figure 5.6). This effect was rescued by expression of Flag-Upf1^{res}, demonstrating this was not an off-target effect of the siRNA. The appearance of double strand breaks, as indicated by increased levels of γH2AX, might be expected to bring about the activation of one or more cell cycle checkpoints, and affect the cell cycle profile observed in Upf1-depleted cells. I observed an increase in the G2/M fraction in Upf1-depleted cells compared to controls (9.8% to 14%, Figure 5.1), however it was not clear whether this was a direct consequence of Upf1 depletion, as expression of Flag-Upf1^{res} failed to restore the cell cycle distribution to that of control cells. The significance of this observation remains unclear, although it is conceivable

that the induced levels of Flag-Upf1 (Figure 5.1a) were insufficient to rescue this phenotype.

I also investigated whether Upf1 recruitment to chromatin, proposed to target Upf1 to sites of DNA replication, was required for the Upf1-dependent maintenance of genomic stability. Unfortunately, due to time restrictions, I was unable to perform a comprehensive analysis of the specific role of S42, a motif identified as essential for chromatin recruitment. However, I was able to assess the ability of Flag-Upf1$^{resΔ1-91}$, which I also demonstrated was unable to associate with chromatin, to rescue the effects of Upf1 knockdown on genomic stability. Unlike full-length Flag-Upf1^{res}, expression of this mutant in Upf1-knockdown cells did not prevent the accumulation of γH2AX; indicating motifs located within the N-terminal 91 amino acids are required for both Upf1 chromatin recruitment, and function in the maintenance of genomic stability. Flag-Upf1$^{resΔ1-91}$ was expressed at relatively low levels in this experiment, and this could be proposed as a reason why this mutant failed to rescue the effect of Upf1 knockdown. However, comparable levels of Flag-Upf1^{res} expression rescued this phenotype in previous experiments, suggesting the lack of the N-terminal 91 amino acids, rather than the expression level of this mutant, was the reason for the failure to prevent the accumulation of γH2AX.

The NMD pathway has been shown not to be involved in the maintenance of genomic stability, as deletion of core components essential for NMD (such as Upf2) have no effect on genomic integrity (Azzalin and Lingner, 2006b). However, the helicase function of Upf1 *is* required for genomic integrity, as expression of the K509Q mutant lacking helicase activity did not rescue telomere replication in the absence of

Upf1, a phenotype demonstrated previously to generate γH2AX foci at telomeres (Chawla et al., 2011).

As described previously, during the process of NMD, cycles of Upf1 phosphorylation and dephosphorylation have been shown to be essential for remodelling of RNA-containing macromolecular complexes and RNA decay (Chapter 1) where phospho-Upf1 serves as a scaffold for recruitment of mRNA decapping, deadenylation and exonucleolytic decay factors (Lejeune et al., 2003; Ohnishi et al., 2003; Okada-Katsuhata et al., 2012). In contrast, the precise role of phosphorylation of chromatin-associated Upf1 for the maintenance of genomic integrity is unclear.

In the work presented in Chapter 4, I generated a Upf1 mutant unable to function in NMD, as it lacks both N- and C-terminal essential phosphorylation sites required for recruitment of components essential for RNA decay. The availability of this mutant allowed me to directly investigate whether the lack of availability of phosphorylation sites required for Upf1 NMD functions were required for genomic stability. Expression of Flag-Upf1^{resAAA} in cells depleted of Upf1 resulted in very high levels of γH2AX. Expression of this mutant in cells that retained normal levels of endogenous wild-type Upf1 also generated levels of γH2AX greater than that observed in control cells, suggesting that Flag-Upf1^{resAAA} acts in a dominant-negative fashion (Figure 5.7, lanes 6 and 10). These results demonstrate that Upf1 phosphorylation site motifs required for NMD function are also essential for the maintenance of genomic stability.

In conclusion, Upf1 regions and/or sites demonstrated previously to be essential for chromatin recruitment, and NMD function, are both essential for the

maintenance of genomic stability. The 91 amino acid region deleted in Flag-Upf1$^{resΔ1-91}$ encompasses multiple candidate PIKK phosphorylation sites (S/TQ motifs, S10, T28, S42, T44) in addition to the PRD, and from these data, I cannot distinguish whether the failure of this mutant to maintain genomic integrity is as a consequence of a failure in S42-mediated chromatin association, T28 phosphorylation, or the lack of other N-terminal motifs. It will be important to identify the specific N-terminal motif(s) that contribute to this phenotype, and investigate whether S42 is essential for the maintenance of genomic stability. The finding that Flag-Upf1^{resS42E} is associated with chromatin suggests a model in which phosphorylation at this site (or perhaps at T44) by a PIKK promotes chromatin association, which is likely to be required for the maintenance of genomic stability. The genomic instability in cells expressing Flag-Upf1^{resAAA} suggests that there is likely to be significant overlap in the basic mechanism governing Upf1 function in maintaining genomic integrity and its role in RNA decay pathways. Because Upf1 undergoes cycles of phosphorylation and dephosphorylation to facilitate helicase progression and RNA decay during NMD, it will be important to investigate the effects of combined and individual phospho-mimetic mutants on genomic stability; a similar requirement would predict that expression of the phospho-mimetic mutant Flag-Upf1^{resEEE}, like its un-phosphorylatable counterpart Flag-Upf1^{resAAA} would result in loss of genomic stability.

5.6.4 Functional analysis of Upf1 at telomeres

Upf1 has been shown to bind to telomeric DNA and is involved in the degradation of TERRA (Azzalin et al., 2007). While the work described in this thesis was underway, Chawla and colleagues reported that Upf1 was directly involved in the

replication of telomeric DNA tracts, and required the ATPase/helicase activity of Upf1 (Chawla et al., 2011). I therefore chose to explore the functional role of Upf1 motifs essential for chromatin recruitment and RNA decay in the maintenance of telomere integrity.

Upf1 knockdown caused a significant loss of telomeres (Figure 5.10), at a frequency consistent with data obtained by Azzalin and colleagues (Azzalin et al., 2007; Chawla et al., 2011). I also observed an increased frequency of telomere fragments in these cells, regions of telomeric DNA that have broken away from a chromosome (Figure 5.8b, inset image). Telomeres have been reported to resemble genomic fragile sites (Sfeir et al., 2009) and RNA-DNA hybrids have been reported to cause replication fork collapse, and double strand break formation at genomic regions (Alzu et al., 2012). While I did not quantify these abnormalities, they suggest that double strand breaks may form at telomeres when TERRA-DNA hybrids cannot be resolved, and therefore Upf1 may function to prevent site fragility at a subset of telomeres. This could explain the loss of telomeric tracts observed in Upf1 knockdown cells, and quantification of these abnormalities, and their prevalence in the presence of Upf1 mutants, would be an interesting line of further study.

Importantly, telomere loss was rescued by Flag-Upf1^{res} expression, confirming a direct involvement of Upf1 in telomere replication. Interestingly, telomere loss was not rescued in Upf1 knockdown cells expressing Flag-Upf1^{resS42A} (Figure 5.9); demonstrating Upf1 function in telomere replication is predicated on the ability of Upf1 to interact with chromatin. Confirmation that Flag-Upf1^{resS42A} does not interact

specifically at telomeres could be achieved by chromatin immunoprecipitation (ChIP) assays to further support this data.

The PIKK ATR has been reported to regulate both the association of Upf1 with chromatin (Azzalin and Lingner, 2006b) and the interaction of Upf1 with telomeric DNA (Chawla et al., 2011). However, in the former case, ATR depletion was shown to partially reduce the extent of Upf1 association with chromatin only after treatment with ionising radiation, which appears to increase the levels of chromatin-associated Upf1, compared to those observed during normal S-phase progression (Azzalin and Lingner, 2006). Thus the significance of this observation with respect to Upf1-chromatin association during normal S-phase progression is not clear. In the latter case, ATR depletion reduced Upf1 association with telomeric DNA by about 50%. To date, the sites of phosphorylation of Upf1 by ATR have not been identified either *in vitro* or *in vivo*. However the data presented here indicate that, should ATR be found to be responsible for mediating the recruitment of Upf1 to chromatin during S-phase, then it must do so via phosphorylation of a site(s) distinct from those canonical sites (T28, S1096, S1116) already implicated in RNA decay mechanisms. One attractive possibility is that more than one PIKK is involved in the process of chromatin recruitment, and that this is achieved via the phosphorylation of S42. Quantitative analysis of the phosphorylation state of S42 (and possibly T44) on chromatin-associated Upf1 following knockdown of distinct PIKKs implicated in genomic stability will be required to test this hypothesis.

This result did not provide evidence for the specific function of Upf1 at telomeres however. Accumulation of TERRA and telomere loss observed in cells

depleted of Upf1, SMG1 or SMG6, but not Upf2, suggests that a Upf1-mediated RNA decay pathway, in part, may also contribute to telomere replication (Azzalin et al., 2007). In agreement with these findings, data presented in this study support the hypothesis that NMD-like functions of Upf1 are involved in both genomic stability and telomere homeostasis (Figures 5.7 and 5.9). However, contrary to as presented by Azzalin and Lingner., 2006, knockdown of endogenous Upf1 did not generate an S-phase arrest in this study (Figure 6.1), highlighting the need to re-examine other previously described observations. While suggested to be not required for genomic stability and telomere homeostasis (Azzalin and Lingner, 2006b), it will be important for me to re-examine the role of Upf2 in these processes, to clarify whether the mechanisms involved in NMD are also fundamental to the role of Upf1 in the nucleus.

Flag-Upf1^{resAAA} was unable to rescue telomere loss in the absence of endogenous Upf1 (Figure 5.9) suggesting phosphorylation of T28, S1096 or S1116 in isolation or in combination may regulate recruitment of factors required for RNA decay. TERRA transcripts bound to telomeres have been shown to lack a poly-A tail (Porro et al., 2010), and knockdown of SMG7 did not generate significant telomere loss (Azzalin et al., 2007). This implies, indirectly, that TERRA transcripts may not necessarily be degraded from the 3' end and the interaction of SMG5:7 with phospho-S1096 (Okada-Katsuhata et al., 2012) may be dispensable at telomeres. SMG1 has been demonstrated to mediate the interaction of SMG6 with Upf1 through phosphorylation of T28 during NMD (Okada-Katsuhata et al., 2012) and TERRA has been proposed to be degraded by the SMG6 PIN domain (Azzalin et al., 2007). The generation of distinct cell lines expressing either N-terminal (T28) or C terminal (S1096,

S1116) unphosphorylatable mutants will be necessary to test whether TERRA degradation involves redundant or non-redundant processes.

5.6.5 Multiple PIKKs may target distinct Upf1 motifs to target TERRA degradation

The data discussed above suggest a model where both SMG1 and ATR may contribute to the function of Upf1 at telomeres. ATR may become activated and phosphorylate Upf1 in response to replication fork stall at TERRA foci, or by TERRA inhibition of the RPA-POT1 switch during end processing (Flynn et al., 2011), causing Upf1 recruitment to these telomeric regions. Additional phosphorylation by SMG1 may then occur at T28 and potentially C-terminal motifs, stimulating Upf1 helicase activity (Fiorini et al., 2012) and remodelling of the TERRA molecule, allowing nucleolytic degradation through interactions with SMG6. However, small molecule mediated inhibition of DNA-PK kinase activity was recently shown to bring about an increase in TERRA foci (Le et al., 2013), suggesting multiple PIKKs may contribute to this process.

5.6.6 A loss of genomic stability in Upf1 knockdown cells may arise from a failure of telomere replication

A source of the genomic instability generated by Upf1 knockdown may represent a failure to degrade TERRA at telomeres during late S-phase. Stretches of RPA-bound ssDNA during end processing or replication fork stall at unresolved TERRA foci are predicted to activate a DNA damage response (Luke and Lingner, 2009).

Upf1 knockdown was reported to induce γH2AX foci at telomeres (Chawla et al., 2011) and the failure of Flag-Upf1$^{resΔ1\text{-}91}$ to rescue γH2AX accumulation in Upf1 knockdown cells may be a result of the inability of this mutant to be recruited to sites of TERRA-induced replication stress at telomeres. Flag-Upf1^{resS42A}, also lacking

chromatin interaction, was shown to be unable to rescue telomere loss induced by Upf1 knockdown. The telomere loss and accumulation of γH2AX at telomeres demonstrated by Chawla and colleagues, (2011), correlates with the similar phenotypes I observed when Upf1 mutants lacking chromatin interaction were expressed in Upf1 depleted cells. Taken together, these data suggest the maintenance of telomere integrity, and ultimately genomic stability, may be dependent upon the interactions of Upf1 with chromatin.

The dominant negative effect on genomic stability demonstrated by Flag-Upf1^{resAAA} may be the consequence of this mutant binding telomeric DNA at TERRA foci, but which subsequently is unable to undertake Upf1-mediated RNA decay functions, in the absence of either N- or C-terminal PIKK phosphorylation sites required for the recruitment of additional decay factors. The physical presence of this non-functional Upf1 mutant at these sites may prevent activity of wild-type Upf1 or other functionally related helicases and cause a prolonged DNA damage response, evidenced by increased levels of γH2AX.

5.7 Upf1 functions during S-phase to regulate a subset of telomeres

Upf1 was proposed to function in DNA replication through interactions with polδ, however in this chapter I have demonstrated Upf1 knockdown does not generate a cell cycle arrest and the interaction with the p66 polδ subunit does not appear to occur in S-phase enriched cells. Therefore I conclude that Upf1 does not function in global DNA replication, and the genomic instability in the absence of Upf1 reflects failures in telomere homeostasis. Upf1 motifs associated with both chromatin recruitment and RNA decay were demonstrated to be essential for telomere

replication during S-phase, suggesting the basis for a mechanism of PIKK-dependent Upf1-mediated regulation of telomere integrity in the nucleus.

Chapter 6 General discussion and future perspectives

The aim of this study was to investigate the role of Upf1 in DNA replication and genomic stability during S-phase. HeLa cells in which Upf1 was knocked down had previously been demonstrated to be unable to replicate DNA and accumulated markers of genomic instability (Azzalin and Lingner, 2006b). Upf1 was therefore proposed to be essential for DNA replication (Azzalin and Lingner, 2006a), acting as a replicative helicase, associated with pol δ, via the p66 subunit with which it had been shown previously to co-purify and co-immunoprecipitate (Carastro et al., 2002). These functions of Upf1 were demonstrated to be independent of the canonical NMD pathway (Azzalin and Lingner, 2006b), suggesting the role of Upf1 in S-phase may be distinct from its role in the regulation of mRNAs containing premature termination codons.

Subsequently, Upf1 was also implicated in the intra- S phase checkpoint linking replication origin firing with histone supply via regulation of histone mRNA levels (Muller et al., 2007b) and it was suggested that Upf1, acting at the replication fork, might be the focus for signalling pathways to co-ordinate DNA replication and histone mRNA decay (Azzalin and Lingner, 2006a; Kaygun and Marzluff, 2005a; Muller et al., 2007a). One potential implication of these observations was that regions or domains of Upf1 that are responsible for ensuring an interaction with p66 might be functionally distinguishable from those required for NMD. The long-term aim therefore was to develop approaches aimed at understanding how regulation of Upf1 facilitates its apparently pleiotropic functions.

There were three lines of study: investigation of the interaction between Upf1 and the p66 polδ subunit; characterisation of Upf1 motifs essential for S-phase chromatin recruitment, and, finally the analysis of Upf1 interactions and functions during S-phase.

I attempted to investigate the interaction with p66 in the yeast two-hybrid system, with the aim of identifying unique Upf1 motifs required for this interaction. Unfortunately I was unable to recapitulate this interaction using this system. Because the association of Upf1 with chromatin has been proposed to be regulated by ATR (Azzalin and Lingner, 2006b), a PIKK kinase activated by replication stress (Mordes and Cortez, 2008), I attempted to establish whether elevated levels of replication stress might result in a detectable interaction between p66 and Upf1 in the yeast two-hybrid system. No interaction could be detected. Subsequently, I was unable to determine whether appropriate signalling could be generated in the yeast system, and concluded that the yeast two-hybrid was not suitable for the study of this interaction.

Through the generation of a library of stable HeLa FLP-IN cell lines, capable of expressing tagged-Upf1 mutants, I identified Upf1 S42 as an essential amino acid residue required for the interaction of Upf1 with chromatin during S-phase. I have provided evidence that phosphorylation at this motif may target Upf1 to chromatin, although this requires *in vivo* confirmation by identification of the relevant phosphorylated form of Upf1 *in vivo*.

In my hands, Upf1 knockdown did not cause S-phase cellular arrest and interaction with p66 was not increased in S-phase enriched cells, leading to the conclusion that Upf1 does not function to sustain global DNA replication. This

conclusion then raised questions as to the role of Upf1 at chromatin during S-phase, if not global DNA replication.

6.1 Upf1 may undergo nuclear-specific signalling events during telomere replication

Upf1 motifs required for NMD were shown to be dispensable for chromatin recruitment, demonstrating the mechanism by which Upf1 is recruited to chromatin must be distinct from that which targets Upf1 to perform NMD. However, the function of Upf1 in the maintenance of telomere integrity was shown to be dependent upon Upf1 chromatin recruitment and, perhaps surprisingly, motifs required for NMD. Similarly, these motifs were essential for the role of Upf1 in the maintenance of genomic stability, suggesting the genomic instability arising from Upf1 knockdown in the absence of extrinsic genotoxic stress is likely to represent, at least in part, a failure of Upf1-dependent processes at telomeres. These data presented a potential mechanism by which Upf1 is capable of differentially functioning in both cytoplasmic mRNA surveillance and the nuclear, S-phase specific events essential for the maintenance of genomic stability.

6.2 Multiple PIKK-mediated phosphorylation events may target, and then activate Upf1 at telomeres

SMG1 is found both in the nucleus and cytoplasm (Brumbaugh et al., 2004), consistent with the function of SMG1 in the decay of cytoplasmic PTC mRNAs (Yamashita et al., 2001). Upf1 motifs (T28 and S1096) are phosphorylated by SMG1 during NMD (Okada-Katsuhata et al., 2012) and the majority of phospho-Upf1 in the cell has been demonstrated to be cytoplasmic (Pal et al., 2001). ATR however, shown to regulate the recruitment of Upf1 to chromatin after replication stress (Azzalin and

Lingner, 2006b), is thought to function exclusively in the nucleus (Abraham, 2001). Therefore, the nuclear and cytoplasmic compartments present distinct signalling environments to Upf1 proteins, potentially allowing different Upf1 phosphorylation events in either location. Combined phosphorylation of both sets of motifs on a single Upf1 molecule, within the nucleus, may be a mechanism of targeting Upf1 to participate in RNA processing functions that are common to both NMD and telomere maintenance and I propose the following model.

The presence of stretches of RPA-bound ssDNA generated at telomeres by TERRA-induced replication fork stall, or inhibition of telomere protection, is likely to be recognised by, and bring about the activation of ATR. Nuclear Upf1 may then be phosphorylated, potentially at S42, causing recruitment to these regions through binding to DNA and/ or pol δ/ε.

Upf1 interactions with chromatin appear to be Upf2-independent, and Upf2 knockdown did not generate significant telomere defects in earlier studies (Azzalin et al., 2007). This suggests stimulation of Upf1 helicase activity, demonstrated to be essential for telomere replication (Chawla et al., 2011), occurs through the displacement of the CH domain by interactions with DNA, pol δ/ε or currently unknown telomeric proteins.

Through initiation of a sequence of events similar to the post-EJC stages of NMD, nuclear SMG1 then may additionally phosphorylate telomere-bound Upf1 at T28, or in combination with S1096 and S1116, to further stimulate helicase activity and recruit SMG6, the proposed nuclease involved in TERRA decay (Azzalin et al., 2007;

Huntzinger et al., 2008). The subsequent remodelling, displacement and decay of TERRA at telomeres then may allow appropriate replication of these regions.

6.3 Upf1 may also have non-telomeric functions on chromatin during S-phase

My data, consistent with previous studies (Azzalin and Lingner, 2006b) demonstrated a small fraction of Upf1 is recruited to chromatin during S-phase. This recruitment has been reported to be initiated in late G_1 (Azzalin and Lingner, 2006b) and peak during S-phase. The function of Upf1 at telomeres will be required in late S/G_2 and therefore a key question that needs to be addressed is why, if Upf1 recruited to telomeres in late S-phase, Upf1 is also recruited to chromatin throughout S-phase.

Knockdown of Upf1 was demonstrated to cause γH2AX foci at telomeres, however non-telomeric γH2AX foci were also present in these cells (Chawla et al., 2011). Upf1 therefore may be involved in the resolution of DNA damage at genomic regions. However, a wide range of well-characterised DNA helicases (RECQL1, BLM, WRN, RECQL4 and RECQL5) function in the resolution of DNA damage at genomic sites (Reviewed in Brosh, 2013).

An unexplored possibility is that Upf1 may function to degrade TERRA at *genomic* DNA regions during S-phase. Interstitial telomere sequences, stretches of $(TTAGGG/AATCCC)_n$ DNA located in non-telomeric, genomic loci have been reported in mammalian cells (Azzalin et al., 1997; Lin and Yan, 2008) and are bound by shelterin components (Mignon-Ravix et al., 2002). It is plausible therefore, that TERRA also hybridises with these 'mini-telomeres' during S-phase and presents physical barriers to replication forks, similar to the R-loops generated at other RNA polymerase II transcribed regions (McIvor et al., 2010). Upf1 may be recruited to these genomic sites

during S-phase, to resolve these specific RNA-DNA hybrids and allow replication fork progression.

6.4 The role of Upf1 in histone mRNA decay (HD) may be coupled to interactions with chromatin

I did not investigate the role of Upf1 in Histone mRNA decay (HD) in this study, so cannot discount the possibility that interaction of Upf1 with chromatin during S-phase is linked to this process.

The discovery that the majority of histone mRNAs degraded during HD were CBP80-bound (Choe et al., 2013) suggests these are immature mRNAs, which have not undergone pioneer round translation in the cytoplasm. While it is plausible that these mRNAs are specifically degraded in the cytoplasm as they leave the nucleus, data from Rattray and colleagues demonstrated alternative splicing of HBP/SLBP in response to replication stress may cause nuclear retention of histone mRNAs (Rattray et al., 2013).

Certain PTC-containing transcripts have been demonstrated to be retained at their site of transcription on DNA by Upf1 and SMG6 and not subjected to intron splicing (de Turris et al., 2011), therefore cannot be degraded by EJC-dependent mechanisms. Histone mRNAs also lack introns, so it is a possibility that upon replication stress, alternative splicing of HBP/SLBP and PIKK dependent Upf1 phosphorylation/SMG6 recruitment causes the retention, and decay, of histone mRNAs as they are transcribed.

6.5 Cyclin-cdk and/ or cdc7/ASK activity may regulate Upf1 chromatin recruitment

The functions of Upf1 in telomere regulation and HD do not explain why Upf1 interacts with chromatin in the apparent absence of replication stress. The recruitment

of Upf1 to chromatin in late G_1 demonstrated by Azzalin et al., 2006, suggests Upf1 chromatin recruitment occurs prior *to* S-phase entry (Azzalin and Lingner, 2006b). One possibility is the recruitment of Upf1 to chromatin, in the absence of replication stress, may be a PIKK-independent, cell cycle-regulated event. Strikingly, the recruitment of Upf1 to chromatin follows the pattern of cyclin E expression, which together with cdk2, phosphorylate key proteins to cause entry into S-phase, and the activity profile of cdc7/ASK, required for the initiation of DNA replication through the firing of licensed replication origins (Reviewed in Hochegger et al., 2008; and Jares et al., 2000).

The Upf1 region surrounding S42 (TLPSQTQTPP) does not display a classical cdk2 consensus motif (S/T-P-X-K/R) (Ubersax and Ferrell, 2007), but phosphorylation of this site in late G_1 induced directly or indirectly by cyclin-E/cdk2 or cdc7/ASK, both of which target serine/threonine containing consensus motifs (Pines, 1995; Sato et al., 1997) may cause nuclear Upf1 to interact with chromatin.

The recruitment of Upf1 to chromatin as cells begin to replicate their genome may sequester a population of Upf1 within the nucleus, preventing its cytoplasmic export. While not actively participating in DNA replication, a readily available pool of Upf1 in close proximity to regions of DNA replication would allow signalling events associated with replication arrest to be rapidly transduced onto the population of nuclear histone mRNAs or TERRA foci at telomeres.

The functions of Upf1 in cytoplasmic mRNA surveillance are largely governed by two factors, the phospho-status of Upf1, and the relative amount of proteins required for specific surveillance pathways. NMD becomes down-regulated during development, where increased expression of Staufen1 preferentially targets Upf1 to

interact with Staufen1-bound mRNAs, instead of NMD targets (Gong et al., 2009). Histone gene expression steadily increases in late G_1, prior to a dramatic increase in expression as cells enter S-phase (Azzalin and Lingner, 2006b; Harris et al., 1991). HBP/SLBP expression also increases during S-phase, to allow the efficient processing of these high levels of histone mRNA. Upf1 has been demonstrated to co-immunoprecipitate HBP/SLBP (Kaygun and Marzluff, 2005a), and high levels of HBP/SLBP-bound histone mRNA present in the nucleus during S-phase may bias the interaction of nuclear phospho-Upf1 with HBP/SLBP over NMD proteins.

The function of Upf1 in S-phase specific pathways may be governed by signalling events that alter the affinity of Upf1 for its respective nuclear interactions. Upf1 may be loosely tethered to chromatin after phosphorylation of S42. In response to replication stress, PIKK-mediated phosphorylation of additional N-terminal motifs may generate conformational changes in the N-terminal structure that increase the affinity of Upf1 for proteins such as HBP/SLBP or telomere components. Conformational changes in Upf1 structure have been demonstrated previously to modulate the affinity of Upf1 for nucleotides during NMD (Chakrabarti et al., 2011; Chamieh et al., 2008) and as I did not investigate chromatin recruitment in response to replication stress, this possibility needs to be explored further.

Interestingly, both histone mRNAs and chromatin-bound TERRA share common characteristics. Histone mRNAs lack introns and TERRA is non-coding, therefore both will not be degraded by an EJC-dependent mechanism, they are both non-polyadenylated and their decay is regulated by Upf1 and ATR/DNA-PK in response to S-phase specific stimuli. It is entirely possible therefore the distinct roles of Upf1 in HD

and telomere regulation are also temporally regulated during S-phase. The CyclinA-dependent degradation of HBP/SLBP at the end of S-phase may remove the bias for chromatin associated Upf1 to perform histone mRNA decay, allowing replication stress originating from TERRA hybrids to cause Upf1 recruitment to telomeres. Upf1 may therefore perform a biphasic function at chromatin during S-phase, regulated by both cyclin/cdc7 expression and replication stress-dependent PIKK activity.

In conclusion, this study has demonstrated Upf1 is not involved in global DNA replication, but performs specific functions within the nucleus during S-phase that are separable from cytoplasmic mRNA surveillance. The identification of a novel Upf1 motif (S42) has highlighted the role of Upf1 chromatin recruitment in telomere replication and the maintenance of genomic stability in human cells.

6.6 Future perspectives

Chromatin bound Upf1 was demonstrated to be phosphorylated on S/T-Q motifs (Azzalin and Lingner, 2006b) and the SQ motif found at serine 42 is a consensus motif for PIKK phosphorylation. ATR and SMG1 are known to contribute to Upf1 phosphorylation and chromatin recruitment *in vivo* (Azzalin and Lingner, 2006b; Kashima et al., 2006). The discovery that DNA-PK can phosphorylate Upf1 *in vitro* at serine 42 (R.Beniston, unpublished) is of interest, as DNA-PK has been implicated in both the regulated decay of TERRA at telomeres and replication dependent histone mRNA decay, two processes dependent upon Upf1 (Le et al., 2013; Muller et al., 2007b). Future work to establish whether S42 is phosphorylated will be required, either by mass-spectrometric analysis of chromatin-bound Upf1, or via the generation of an S42 phospho-specific antibody. As it was not technically possible to perform

alanine substitution mutagenesis of T44 in this study, it will be important to determine the requirement of T44 in Upf1 chromatin recruitment and understand whether S42 alone, or in combination with this adjacent motif, is required for chromatin interactions.

Phospho-mimetic substitution of S42 generated significantly increased Upf1 chromatin association. It would be of great interest to study the effects of phospho-mimetic forms of Upf1 motifs in both chromatin recruitment and telomere function. While dependent upon S42, it is not clear whether modification of this motif facilitates the binding of Upf1 directly to DNA, or promotes the interaction of Upf1 with chromatin-associated proteins. Distinguishing these scenarios will be challenging and require a combination of *in vivo* proteomic approaches to identify differential protein interactions depending on the phospho-status of S42, and *in vitro* DNA binding assays under conditions that either simulate, or preserve phosphorylation at S42.

I have demonstrated that the Upf1 function at telomeres involves multiple motifs, and this raises many questions as to the specific mechanism of action. The loss of telomeres that arises after Upf1 knockdown was not rescued by Flag-Upf1^{resAAA}, suggesting both N- and C-terminal phosphorylation events may contribute to the function of Upf1 at telomeres. It will be necessary to establish individual FLP-IN cell lines containing alanine substitutions at each of the residues T28, S1096 or S1116, and to determine the consequences on telomere loss to identify the essential motifs required for this process. As discussed previously, it is conceivable that cycles of phosphorylation and dephosphorylation of Upf1 are required for maintenance of telomere integrity. It follows that in this case, FLP-IN cells expressing the relevant

phospho-mimetic mutant might also be expected to interfere with maintenance of telomere integrity.

Although an interaction between Upf1 and the p66 polδ subunit was demonstrated here and previously, the majority of TERRA within the cell is found at telomeric leading strands (Schoeftner and Blasco, 2008), which are replicated by DNA polymerase ε. Therefore an obvious future experiment would be to examine whether Upf1 interacts with polε, to understand how Upf1 performs its primary function in leading strand telomere synthesis (Chawla et al., 2011).

The telomere defects observed in Upf1 knockdown cells were relatively rare, and not universal to all chromosomes. It would be interesting to identify whether these are fragile telomeric sites, common to a subset of chromosomes. This could be performed using CO-FISH, where chromosomal and telomeric FISH probes are hybridised to the same metaphase, identifying the chromosomes experiencing telomere loss (Speicher et al., 1996).

HeLa cells have been reported to express relatively low levels of TERRA (Schoeftner and Blasco, 2008), therefore the demand for Upf1-dependent TERRA degradation will be low in HeLa cells. A refinement to the current protocol would be to analyse the function of Upf1 at telomeres in a high TERRA background. This could be achieved two ways; either using a cell line that has been demonstrated to express high levels of TERRA, such as mouse NS1 cells (Schoeftner and Blasco, 2008); or utilising the FLP-IN HeLa cell lines generated by this study in combination with transient transfection of plasmid constructs expressing TERRA.

A critical future experiment will be the identification of the specific kinase(s) required for the S-phase functions of Upf1. SMG1, ATR and DNA-PK have been proposed as candidate kinases involved in Upf1 functions at telomeres (Azzalin et al., 2007; Chawla et al., 2011; Le et al., 2013; Muller et al., 2007b) and this study). Knockdown of individual PIKKs using RNA interference or chemically induced inhibition of PIKK activity will shed light on the role of PIKKs in this process. It will also be very interesting to explore the role of cyclin-cdks and cdc7/ASK in the recruitment of Upf1 to chromatin, and how this may regulate the role of Upf1 in HD or telomere regulation during S-phase.

My findings have given new insights into the mechanism by which Upf1 is recruited to chromatin and how this recruitment may be essential for the S-phase specific functions of Upf1 required to maintain genomic stability.

References

Abraham, R.T. (2001). Cell cycle checkpoint signaling through the ATM and ATR kinases. Genes Dev *15*, 2177-2196.

Abraham, R.T. (2004). PI 3-kinase related kinases: 'big' players in stress-induced signaling pathways. DNA Repair (Amst) *3*, 883-887.

Aguilera, A., and Gomez-Gonzalez, B. (2008). Genome instability: a mechanistic view of its causes and consequences. Nat Rev Genet *9*, 204-217.

Aitio, O., Hellman, M., Kazlauskas, A., Vingadassalom, D.F., Leong, J.M., Saksela, K., and Permi, P. (2010). Recognition of tandem PxxP motifs as a unique Src homology 3-binding mode triggers pathogen-driven actin assembly. Proc Natl Acad Sci U S A *107*, 21743-21748.

Ajamian, L., Abrahamyan, L., Milev, M., Ivanov, P.V., Kulozik, A.E., Gehring, N.H., and Mouland, A.J. (2008). Unexpected roles for UPF1 in HIV-1 RNA metabolism and translation. RNA *14*, 914-927.

Alzu, A., Bermejo, R., Begnis, M., Lucca, C., Piccini, D., Carotenuto, W., Saponaro, M., Brambati, A., Cocito, A., Foiani, M*., et al.* (2012). Senataxin associates with replication forks to protect fork integrity across RNA-polymerase-II-transcribed genes. Cell *151*, 835-846.

Anastasaki, C., Longman, D., Capper, A., Patton, E.E., and Caceres, J.F. (2011). Dhx34 and Nbas function in the NMD pathway and are required for embryonic development in zebrafish. Nucleic Acids Res *39*, 3686-3694.

Aparicio, O.M. (2013). Location, location, location: it's all in the timing for replication origins. Genes Dev *27*, 117-128.

Applequist, S.E., Selg, M., Raman, C., and Jack, H.M. (1997). Cloning and characterization of HUPF1, a human homolog of the Saccharomyces cerevisiae nonsense mRNA-reducing UPF1 protein. Nucleic Acids Res *25*, 814-821.

Arias-Palomo, E., Yamashita, A., Fernandez, I.S., Nunez-Ramirez, R., Bamba, Y., Izumi, N., Ohno, S., and Llorca, O. (2011). The nonsense-mediated mRNA decay SMG-1 kinase is regulated by large-scale conformational changes controlled by SMG-8. Genes Dev *25*, 153-164.

Arora, R., Brun, C.M., and Azzalin, C.M. (2012). Transcription regulates telomere dynamics in human cancer cells. RNA *18*, 684-693.

Artandi, S.E., and DePinho, R.A. (2010). Telomeres and telomerase in cancer. Carcinogenesis *31*, 9-18.

Atkin, A.L., Altamura, N., Leeds, P., and Culbertson, M.R. (1995). The majority of yeast UPF1 co-localizes with polyribosomes in the cytoplasm. Mol Biol Cell *6*, 611-625.

Avery, P., Vicente-Crespo, M., Francis, D., Nashchekina, O., Alonso, C.R., and Palacios, I.M. (2011). Drosophila Upf1 and Upf2 loss of function inhibits cell growth and causes animal death in a Upf3-independent manner. RNA *17*, 624-638.

Azzalin, C.M., and Lingner, J. (2006a). The double life of UPF1 in RNA and DNA stability pathways. Cell Cycle *5*, 1496-1498.

Azzalin, C.M., and Lingner, J. (2006b). The human RNA surveillance factor UPF1 is required for S phase progression and genome stability. Curr Biol *16*, 433-439.

Azzalin, C.M., Mucciolo, E., Bertoni, L., and Giulotto, E. (1997). Fluorescence in situ hybridization with a synthetic (T2AG3)n polynucleotide detects several intrachromosomal telomere-like repeats on human chromosomes. Cytogenet Cell Genet *78*, 112-115.

Azzalin, C.M., Reichenbach, P., Khoriauli, L., Giulotto, E., and Lingner, J. (2007). Telomeric repeat containing RNA and RNA surveillance factors at mammalian chromosome ends. Science *318*, 798-801.

Bachant, J., Jessen, S.R., Kavanaugh, S.E., and Fielding, C.S. (2005). The yeast S phase checkpoint enables replicating chromosomes to bi-orient and restrain spindle extension during S phase distress. J Cell Biol *168*, 999-1012.

Bailey, S.M., Cornforth, M.N., Kurimasa, A., Chen, D.J., and Goodwin, E.H. (2001). Strand-specific postreplicative processing of mammalian telomeres. Science *293*, 2462-2465.

Balk, B., Maicher, A., Dees, M., Klermund, J., Luke-Glaser, S., Bender, K., and Luke, B. (2013). Telomeric RNA-DNA hybrids affect telomere-length dynamics and senescence. Nat Struct Mol Biol *20*, 1199-1205.

Banerjee, S., Yang, S., and Foster, C.B. (2012). A luciferase reporter assay to investigate the differential selenium-dependent stability of selenoprotein mRNAs. J Nutr Biochem *23*, 1294-1301.

Battle, D.J., and Doudna, J.A. (2001). The stem-loop binding protein forms a highly stable and specific complex with the 3' stem-loop of histone mRNAs. RNA *7*, 123-132.

Bertuch, A., and Lundblad, V. (1998). Telomeres and double-strand breaks: trying to make ends meet. Trends Cell Biol *8*, 339-342.

Bhattacharya, A., Czaplinski, K., Trifillis, P., He, F., Jacobson, A., and Peltz, S.W. (2000). Characterization of the biochemical properties of the human Upf1 gene product that is involved in nonsense-mediated mRNA decay. RNA *6*, 1226-1235.

Blake, D.J., Weir, A., Newey, S.E., and Davies, K.E. (2002). Function and genetics of dystrophin and dystrophin-related proteins in muscle. Physiol Rev *82*, 291-329.

Brazao, T.F., Demmers, J., van Ijcken, W., Strouboulis, J., Fornerod, M., Romao, L., and Grosveld, F.G. (2012). A new function of ROD1 in nonsense-mediated mRNA decay. FEBS Lett *586*, 1101-1110.

Brosh, R.M., Jr. (2013). DNA helicases involved in DNA repair and their roles in cancer. Nat Rev Cancer *13*, 542-558.

Brown, E.J., and Baltimore, D. (2000). ATR disruption leads to chromosomal fragmentation and early embryonic lethality. Genes Dev *14*, 397-402.

Brumbaugh, K.M., Otterness, D.M., Geisen, C., Oliveira, V., Brognard, J., Li, X., Lejeune, F., Tibbetts, R.S., Maquat, L.E., and Abraham, R.T. (2004). The mRNA surveillance protein hSMG-1 functions in genotoxic stress response pathways in mammalian cells. Mol Cell *14*, 585-598.

Bruning, J.B., and Shamoo, Y. (2004). Structural and thermodynamic analysis of human PCNA with peptides derived from DNA polymerase-delta p66 subunit and flap endonuclease-1. Structure *12*, 2209-2219.

Bruno, I.G., Karam, R., Huang, L., Bhardwaj, A., Lou, C.H., Shum, E.Y., Song, H.W., Corbett, M.A., Gifford, W.D., Gecz, J.*, et al.* (2011). Identification of a microRNA that activates gene expression by repressing nonsense-mediated RNA decay. Mol Cell *42*, 500-510.

Burnette, W.N. (1981). "Western blotting": electrophoretic transfer of proteins from sodium dodecyl sulfate--polyacrylamide gels to unmodified nitrocellulose and radiographic detection with antibody and radioiodinated protein A. Anal Biochem *112*, 195-203.

Canman, C.E., Lim, D.S., Cimprich, K.A., Taya, Y., Tamai, K., Sakaguchi, K., Appella, E., Kastan, M.B., and Siliciano, J.D. (1998). Activation of the ATM kinase by ionizing radiation and phosphorylation of p53. Science *281*, 1677-1679.

Carastro, L.M., Tan, C.K., Selg, M., Jack, H.M., So, A.G., and Downey, K.M. (2002). Identification of delta helicase as the bovine homolog of HUPF1: demonstration of an interaction with the third subunit of DNA polymerase delta. Nucleic Acids Res *30*, 2232-2243.

Cartegni, L., Maconi, M., Morandi, E., Cobianchi, F., Riva, S., and Biamonti, G. (1996). hnRNP A1 selectively interacts through its Gly-rich domain with different RNA-binding proteins. J Mol Biol *259*, 337-348.

Casper, A.M., Nghiem, P., Arlt, M.F., and Glover, T.W. (2002). ATR regulates fragile site stability. Cell *111*, 779-789.

Catron, K.M., Zhang, H., Marshall, S.C., Inostroza, J.A., Wilson, J.M., and Abate, C. (1995). Transcriptional repression by Msx-1 does not require homeodomain DNA-binding sites. Mol Cell Biol *15*, 861-871.

Cha, R.S., and Kleckner, N. (2002). ATR homolog Mec1 promotes fork progression, thus averting breaks in replication slow zones. Science *297*, 602-606.

Chakrabarti, S., Jayachandran, U., Bonneau, F., Fiorini, F., Basquin, C., Domcke, S., Le Hir, H., and Conti, E. (2011). Molecular mechanisms for the RNA-dependent ATPase activity of Upf1 and its regulation by Upf2. Mol Cell *41*, 693-703.

Chamieh, H., Ballut, L., Bonneau, F., and Le Hir, H. (2008). NMD factors UPF2 and UPF3 bridge UPF1 to the exon junction complex and stimulate its RNA helicase activity. Nat Struct Mol Biol *15*, 85-93.

Chang, J.C., and Kan, Y.W. (1979). beta 0 thalassemia, a nonsense mutation in man. Proc Natl Acad Sci U S A *76*, 2886-2889.

Chawla, R., Redon, S., Raftopoulou, C., Wischnewski, H., Gagos, S., and Azzalin, C.M. (2011). Human UPF1 interacts with TPP1 and telomerase and sustains telomere leading-strand replication. EMBO J *30*, 4047-4058.

Chen, C.Y., and Shyu, A.B. (2003). Rapid deadenylation triggered by a nonsense codon precedes decay of the RNA body in a mammalian cytoplasmic nonsense-mediated decay pathway. Mol Cell Biol *23*, 4805-4813.

Cheng, J., Fogel-Petrovic, M., and Maquat, L.E. (1990). Translation to near the distal end of the penultimate exon is required for normal levels of spliced triosephosphate isomerase mRNA. Mol Cell Biol *10*, 5215-5225.

Cheng, J., and Maquat, L.E. (1993). Nonsense codons can reduce the abundance of nuclear mRNA without affecting the abundance of pre-mRNA or the half-life of cytoplasmic mRNA. Mol Cell Biol *13*, 1892-1902.

Cheng, Z., Muhlrad, D., Lim, M.K., Parker, R., and Song, H. (2007). Structural and functional insights into the human Upf1 helicase core. EMBO J *26*, 253-264.

Chiu, S.Y., Lejeune, F., Ranganathan, A.C., and Maquat, L.E. (2004). The pioneer translation initiation complex is functionally distinct from but structurally overlaps with the steady-state translation initiation complex. Genes Dev *18*, 745-754.

Cho, H., Han, S., Choe, J., Park, S.G., Choi, S.S., and Kim, Y.K. (2012a). SMG5-PNRC2 is functionally dominant compared with SMG5-SMG7 in mammalian nonsense-mediated mRNA decay. Nucleic Acids Res.

Cho, H., Kim, K.M., Han, S., Choe, J., Park, S.G., Choi, S.S., and Kim, Y.K. (2012b). Staufen1-Mediated mRNA Decay Functions in Adipogenesis. Mol Cell.

Cho, H., Kim, K.M., and Kim, Y.K. (2009). Human proline-rich nuclear receptor coregulatory protein 2 mediates an interaction between mRNA surveillance machinery and decapping complex. Mol Cell *33*, 75-86.

Choe, J., Kim, K.M., Park, S., Lee, Y.K., Song, O.K., Kim, M.K., Lee, B.G., Song, H.K., and Kim, Y.K. (2013). Rapid degradation of replication-dependent histone mRNAs largely occurs on mRNAs bound by nuclear cap-binding proteins 80 and 20. Nucleic Acids Res *41*, 1307-1318.

Chow, T.T., Zhao, Y., Mak, S.S., Shay, J.W., and Wright, W.E. (2012). Early and late steps in telomere overhang processing in normal human cells: the position of the final RNA primer drives telomere shortening. Genes Dev *26*, 1167-1178.

Cimprich, K.A., and Cortez, D. (2008). ATR: an essential regulator of genome integrity. Nat Rev Mol Cell Biol *9*, 616-627.

Clerici, M., Mourao, A., Gutsche, I., Gehring, N.H., Hentze, M.W., Kulozik, A., Kadlec, J., Sattler, M., and Cusack, S. (2009). Unusual bipartite mode of interaction between the nonsense-mediated decay factors, UPF1 and UPF2. EMBO J *28*, 2293-2306.

Correa-Cerro, L.S., Wassif, C.A., Waye, J.S., Krakowiak, P.A., Cozma, D., Dobson, N.R., Levin, S.W., Anadiotis, G., Steiner, R.D., Krajewska-Walasek, M.*, et al.* (2005). DHCR7 nonsense mutations and characterisation of mRNA nonsense mediated decay in Smith-Lemli-Opitz syndrome. J Med Genet *42*, 350-357.

Cortez, D., Guntuku, S., Qin, J., and Elledge, S.J. (2001). ATR and ATRIP: partners in checkpoint signaling. Science *294*, 1713-1716.

Cui, Y., Hagan, K.W., Zhang, S., and Peltz, S.W. (1995). Identification and characterization of genes that are required for the accelerated degradation of mRNAs containing a premature translational termination codon. Genes Dev *9*, 423-436.

Culbertson, M.R., Underbrink, K.M., and Fink, G.R. (1980). Frameshift suppression Saccharomyces cerevisiae. II. Genetic properties of group II suppressors. Genetics *95*, 833-853.

Cusanelli, E., Romero, C.A., and Chartrand, P. (2013). Telomeric noncoding RNA TERRA is induced by telomere shortening to nucleate telomerase molecules at short telomeres. Mol Cell *51*, 780-791.

Czaplinski, K., Weng, Y., Hagan, K.W., and Peltz, S.W. (1995). Purification and characterization of the Upf1 protein: a factor involved in translation and mRNA degradation. RNA *1*, 610-623.

Dahlseid, J.N., Lew-Smith, J., Lelivelt, M.J., Enomoto, S., Ford, A., Desruisseaux, M., McClellan, M., Lue, N., Culbertson, M.R., and Berman, J. (2003). mRNAs encoding telomerase components and regulators are controlled by UPF genes in Saccharomyces cerevisiae. Eukaryot Cell *2*, 134-142.

De Bont, R., and van Larebeke, N. (2004). Endogenous DNA damage in humans: a review of quantitative data. Mutagenesis *19*, 169-185.

de Klein, A., Muijtjens, M., van Os, R., Verhoeven, Y., Smit, B., Carr, A.M., Lehmann, A.R., and Hoeijmakers, J.H. (2000). Targeted disruption of the cell-cycle checkpoint gene ATR leads to early embryonic lethality in mice. Curr Biol *10*, 479-482.

de Lange, T. (2005a). Shelterin: the protein complex that shapes and safeguards human telomeres. Genes Dev *19*, 2100-2110.

De Lange, T. (2005b). Telomere-related genome instability in cancer. Cold Spring Harb Symp Quant Biol *70*, 197-204.

de Lange, T. (2009). How telomeres solve the end-protection problem. Science *326*, 948-952.

de Turris, V., Nicholson, P., Orozco, R.Z., Singer, R.H., and Muhlemann, O. (2011). Cotranscriptional effect of a premature termination codon revealed by live-cell imaging. RNA *17*, 2094-2107.

Dean, F.B., Lian, L., and O'Donnell, M. (1998). cDNA cloning and gene mapping of human homologs for Schizosaccharomyces pombe rad17, rad1, and hus1 and cloning of homologs from mouse, Caenorhabditis elegans, and Drosophila melanogaster. Genomics *54*, 424-436.

DeLisle, A.J., Graves, R.A., Marzluff, W.F., and Johnson, L.F. (1983). Regulation of histone mRNA production and stability in serum-stimulated mouse 3T6 fibroblasts. Mol Cell Biol *3*, 1920-1929.

Denchi, E.L., and de Lange, T. (2007). Protection of telomeres through independent control of ATM and ATR by TRF2 and POT1. Nature *448*, 1068-1071.

Denning, G., Jamieson, L., Maquat, L.E., Thompson, E.A., and Fields, A.P. (2001). Cloning of a novel phosphatidylinositol kinase-related kinase: characterization of the human SMG-1 RNA surveillance protein. J Biol Chem *276*, 22709-22714.

Dostie, J., and Dreyfuss, G. (2002). Translation is required to remove Y14 from mRNAs in the cytoplasm. Curr Biol *12*, 1060-1067.

Eberle, A.B., Lykke-Andersen, S., Muhlemann, O., and Jensen, T.H. (2009). SMG6 promotes endonucleolytic cleavage of nonsense mRNA in human cells. Nat Struct Mol Biol *16*, 49-55.

Ellis, N.A. (1997). DNA helicases in inherited human disorders. Curr Opin Genet Dev *7*, 354-363.

Enomoto, S., Glowczewski, L., Lew-Smith, J., and Berman, J.G. (2004). Telomere cap components influence the rate of senescence in telomerase-deficient yeast cells. Mol Cell Biol *24*, 837-845.

Falck, J., Coates, J., and Jackson, S.P. (2005). Conserved modes of recruitment of ATM, ATR and DNA-PKcs to sites of DNA damage. Nature *434*, 605-611.

Fang, Y., Bateman, J.F., Mercer, J.F., and Lamande, S.R. (2013). Nonsense-mediated mRNA decay of collagen -emerging complexity in RNA surveillance mechanisms. J Cell Sci *126*, 2551-2560.

Farnung, B.O., Brun, C.M., Arora, R., Lorenzi, L.E., and Azzalin, C.M. (2012). Telomerase efficiently elongates highly transcribing telomeres in human cancer cells. PLoS One *7*, e35714.

Fernandez, I.S., Yamashita, A., Arias-Palomo, E., Bamba, Y., Bartolome, R.A., Canales, M.A., Teixido, J., Ohno, S., and Llorca, O. (2011). Characterization of SMG-9, an essential component of the nonsense-mediated mRNA decay SMG1C complex. Nucleic Acids Res *39*, 347-358.

Fiorini, F., Boudvillain, M., and Le Hir, H. (2012). Tight intramolecular regulation of the human Upf1 helicase by its N- and C-terminal domains. Nucleic Acids Res.

Flynn, R.L., Centore, R.C., O'Sullivan, R.J., Rai, R., Tse, A., Songyang, Z., Chang, S., Karlseder, J., and Zou, L. (2011). TERRA and hnRNPA1 orchestrate an RPA-to-POT1 switch on telomeric single-stranded DNA. Nature *471*, 532-536.

Franks, T.M., Singh, G., and Lykke-Andersen, J. (2010). Upf1 ATPase-dependent mRNP disassembly is required for completion of nonsense- mediated mRNA decay. Cell *143*, 938-950.

Freire, R., Murguia, J.R., Tarsounas, M., Lowndes, N.F., Moens, P.B., and Jackson, S.P. (1998). Human and mouse homologs of Schizosaccharomyces pombe rad1(+) and Saccharomyces cerevisiae RAD17: linkage to checkpoint control and mammalian meiosis. Genes Dev *12*, 2560-2573.

Frischmeyer-Guerrerio, P.A., Montgomery, R.A., Warren, D.S., Cooke, S.K., Lutz, J., Sonnenday, C.J., Guerrerio, A.L., and Dietz, H.C. (2011). Perturbation of thymocyte development in nonsense-mediated decay (NMD)-deficient mice. Proc Natl Acad Sci U S A *108*, 10638-10643.

Frischmeyer, P.A., and Dietz, H.C. (1999). Nonsense-mediated mRNA decay in health and disease. Hum Mol Genet *8*, 1893-1900.

Fukuhara, N., Ebert, J., Unterholzner, L., Lindner, D., Izaurralde, E., and Conti, E. (2005). SMG7 is a 14-3-3-like adaptor in the nonsense-mediated mRNA decay pathway. Mol Cell *17*, 537-547.

Gaba, A., Jacobson, A., and Sachs, M.S. (2005). Ribosome occupancy of the yeast CPA1 upstream open reading frame termination codon modulates nonsense-mediated mRNA decay. Mol Cell *20*, 449-460.

Gao, Q., Das, B., Sherman, F., and Maquat, L.E. (2005). Cap-binding protein 1-mediated and eukaryotic translation initiation factor 4E-mediated pioneer rounds of translation in yeast. Proc Natl Acad Sci U S A *102*, 4258-4263.

Gatfield, D., Unterholzner, L., Ciccarelli, F.D., Bork, P., and Izaurralde, E. (2003). Nonsense-mediated mRNA decay in Drosophila: at the intersection of the yeast and mammalian pathways. EMBO J *22*, 3960-3970.

Gehring, N.H., Neu-Yilik, G., Schell, T., Hentze, M.W., and Kulozik, A.E. (2003). Y14 and hUpf3b form an NMD-activating complex. Mol Cell *11*, 939-949.

Geissler, V., Altmeyer, S., Stein, B., Uhlmann-Schiffler, H., and Stahl, H. (2013). The RNA helicase Ddx5/p68 binds to hUpf3 and enhances NMD of Ddx17/p72 and Smg5 mRNA. Nucleic Acids Res *41*, 7875-7888.

Gilson, E., and Geli, V. (2007). How telomeres are replicated. Nat Rev Mol Cell Biol *8*, 825-838.

Gingras, A.C., Raught, B., and Sonenberg, N. (2001). Regulation of translation initiation by FRAP/mTOR. Genes Dev *15*, 807-826.

Glavan, F., Behm-Ansmant, I., Izaurralde, E., and Conti, E. (2006). Structures of the PIN domains of SMG6 and SMG5 reveal a nuclease within the mRNA surveillance complex. EMBO J *25*, 5117-5125.

Glover, T.W., Arlt, M.F., Casper, A.M., and Durkin, S.G. (2005). Mechanisms of common fragile site instability. Hum Mol Genet *14 Spec No. 2*, R197-205.

Glover, T.W., Berger, C., Coyle, J., and Echo, B. (1984). DNA polymerase alpha inhibition by aphidicolin induces gaps and breaks at common fragile sites in human chromosomes. Hum Genet *67*, 136-142.

Gomez, D.E., Armando, R.G., Farina, H.G., Menna, P.L., Cerrudo, C.S., Ghiringhelli, P.D., and Alonso, D.F. (2012). Telomere structure and telomerase in health and disease (review). Int J Oncol *41*, 1561-1569.

Gong, C., Kim, Y.K., Woeller, C.F., Tang, Y., and Maquat, L.E. (2009). SMD and NMD are competitive pathways that contribute to myogenesis: effects on PAX3 and myogenin mRNAs. Genes Dev *23*, 54-66.

Griffith, J.D., Comeau, L., Rosenfield, S., Stansel, R.M., Bianchi, A., Moss, H., and de Lange, T. (1999). Mammalian telomeres end in a large duplex loop. Cell *97*, 503-514.

Gudikote, J.P., and Wilkinson, M.F. (2002). T-cell receptor sequences that elicit strong down-regulation of premature termination codon-bearing transcripts. EMBO J *21*, 125-134.

Hall-Jackson, C.A., Cross, D.A., Morrice, N., and Smythe, C. (1999). ATR is a caffeine-sensitive, DNA-activated protein kinase with a substrate specificity distinct from DNA-PK. Oncogene *18*, 6707-6713.

Han, M., Chang, M., Kim, U.J., and Grunstein, M. (1987). Histone H2B repression causes cell-cycle-specific arrest in yeast: effects on chromosomal segregation, replication, and transcription. Cell *48*, 589-597.

Harley, C.B., Futcher, A.B., and Greider, C.W. (1990). Telomeres shorten during ageing of human fibroblasts. Nature *345*, 458-460.

Harris, M.E., Bohni, R., Schneiderman, M.H., Ramamurthy, L., Schumperli, D., and Marzluff, W.F. (1991). Regulation of histone mRNA in the unperturbed cell cycle: evidence suggesting control at two posttranscriptional steps. Mol Cell Biol *11*, 2416-2424.

Harvey, A.C., Jackson, S.P., and Downs, J.A. (2005). Saccharomyces cerevisiae histone H2A Ser122 facilitates DNA repair. Genetics *170*, 543-553.

He, F., Peltz, S.W., Donahue, J.L., Rosbash, M., and Jacobson, A. (1993). Stabilization and ribosome association of unspliced pre-mRNAs in a yeast upf1- mutant. Proc Natl Acad Sci U S A *90*, 7034-7038.

Hochegger, H., Takeda, S., and Hunt, T. (2008). Cyclin-dependent kinases and cell-cycle transitions: does one fit all? Nat Rev Mol Cell Biol *9*, 910-916.

Hodgkin, J., Papp, A., Pulak, R., Ambros, V., and Anderson, P. (1989). A new kind of informational suppression in the nematode Caenorhabditis elegans. Genetics *123*, 301-313.

Hoefig, K.P., Rath, N., Heinz, G.A., Wolf, C., Dameris, J., Schepers, A., Kremmer, E., Ansel, K.M., and Heissmeyer, V. (2013). Eri1 degrades the stem-loop of oligouridylated histone mRNAs to induce replication-dependent decay. Nat Struct Mol Biol *20*, 73-81.

Hosoda, N., Kim, Y.K., Lejeune, F., and Maquat, L.E. (2005). CBP80 promotes interaction of Upf1 with Upf2 during nonsense-mediated mRNA decay in mammalian cells. Nat Struct Mol Biol *12*, 893-901.

Huang, L., Lou, C.H., Chan, W., Shum, E.Y., Shao, A., Stone, E., Karam, R., Song, H.W., and Wilkinson, M.F. (2011). RNA homeostasis governed by cell type-specific and branched feedback loops acting on NMD. Mol Cell *43*, 950-961.

Hubscher, U., Maga, G., and Spadari, S. (2002). Eukaryotic DNA polymerases. Annu Rev Biochem *71*, 133-163.

Humphries, R.K., Ley, T.J., Anagnou, N.P., Baur, A.W., and Nienhuis, A.W. (1984). Beta O-39 thalassemia gene: a premature termination codon causes beta-mRNA deficiency without affecting cytoplasmic beta-mRNA stability. Blood *64*, 23-32.

Huntzinger, E., Kashima, I., Fauser, M., Sauliere, J., and Izaurralde, E. (2008). SMG6 is the catalytic endonuclease that cleaves mRNAs containing nonsense codons in metazoan. RNA *14*, 2609-2617.

Hwang, J., Sato, H., Tang, Y., Matsuda, D., and Maquat, L.E. (2010). UPF1 association with the cap-binding protein, CBP80, promotes nonsense-mediated mRNA decay at two distinct steps. Mol Cell *39*, 396-409.

Iborra, F.J., Jackson, D.A., and Cook, P.R. (2001). Coupled transcription and translation within nuclei of mammalian cells. Science *293*, 1139-1142.

Ishigaki, Y., Li, X., Serin, G., and Maquat, L.E. (2001). Evidence for a pioneer round of mRNA translation: mRNAs subject to nonsense-mediated decay in mammalian cells are bound by CBP80 and CBP20. Cell *106*, 607-617.

Isken, O., Kim, Y.K., Hosoda, N., Mayeur, G.L., Hershey, J.W., and Maquat, L.E. (2008). Upf1 phosphorylation triggers translational repression during nonsense-mediated mRNA decay. Cell *133*, 314-327.

Isken, O., and Maquat, L.E. (2007). Quality control of eukaryotic mRNA: safeguarding cells from abnormal mRNA function. Genes Dev *21*, 1833-1856.

Ivanov, P.V., Gehring, N.H., Kunz, J.B., Hentze, M.W., and Kulozik, A.E. (2008). Interactions between UPF1, eRFs, PABP and the exon junction complex suggest an integrated model for mammalian NMD pathways. EMBO J *27*, 736-747.

J. Sambrook, E.F.F.a.T.M. (1989). Molecular Cloning: A Laboratory Manual (Fourth Edition): (Cold Spring Harbor, NY: Cold Spring Harbor Laboratory Press).

Jares, P., Donaldson, A., and Blow, J.J. (2000). The Cdc7/Dbf4 protein kinase: target of the S phase checkpoint? EMBO Rep *1*, 319-322.

Jazayeri, A., Falck, J., Lukas, C., Bartek, J., Smith, G.C., Lukas, J., and Jackson, S.P. (2006). ATM- and cell cycle-dependent regulation of ATR in response to DNA double-strand breaks. Nat Cell Biol *8*, 37-45.

Jin, H., Suh, M.R., Han, J., Yeom, K.H., Lee, Y., Heo, I., Ha, M., Hyun, S., and Kim, V.N. (2009). Human UPF1 participates in small RNA-induced mRNA downregulation. Mol Cell Biol *29*, 5789-5799.

Johnson, J.K., Waddell, N., and Chenevix-Trench, G. (2012). The application of nonsense-mediated mRNA decay inhibition to the identification of breast cancer susceptibility genes. BMC Cancer *12*, 246.

Jolly, L.A., Homan, C.C., Jacob, R., Barry, S., and Gecz, J. (2013). The UPF3B gene, implicated in intellectual disability, autism, ADHD and childhood onset schizophrenia regulates neural progenitor cell behaviour and neuronal outgrowth. Hum Mol Genet.

Kadlec, J., Guilligay, D., Ravelli, R.B., and Cusack, S. (2006). Crystal structure of the UPF2-interacting domain of nonsense-mediated mRNA decay factor UPF1. RNA *12*, 1817-1824.

Karlseder, J., Broccoli, D., Dai, Y., Hardy, S., and de Lange, T. (1999). p53- and ATM-dependent apoptosis induced by telomeres lacking TRF2. Science *283*, 1321-1325.

Kashima, I., Yamashita, A., Izumi, N., Kataoka, N., Morishita, R., Hoshino, S., Ohno, M., Dreyfuss, G., and Ohno, S. (2006). Binding of a novel SMG-1-Upf1-eRF1-eRF3 complex (SURF) to the exon junction complex triggers Upf1 phosphorylation and nonsense-mediated mRNA decay. Genes Dev *20*, 355-367.

Kataoka, N., Diem, M.D., Kim, V.N., Yong, J., and Dreyfuss, G. (2001). Magoh, a human homolog of Drosophila mago nashi protein, is a component of the splicing-dependent exon-exon junction complex. EMBO J *20*, 6424-6433.

Kataoka, N., and Dreyfuss, G. (2004). A simple whole cell lysate system for in vitro splicing reveals a stepwise assembly of the exon-exon junction complex. J Biol Chem *279*, 7009-7013.

Kaygun, H., and Marzluff, W.F. (2005a). Regulated degradation of replication-dependent histone mRNAs requires both ATR and Upf1. Nat Struct Mol Biol *12*, 794-800.

Kaygun, H., and Marzluff, W.F. (2005b). Translation termination is involved in histone mRNA degradation when DNA replication is inhibited. Mol Cell Biol *25*, 6879-6888.

Khanna, K.K., and Lavin, M.F. (1993). Ionizing radiation and UV induction of p53 protein by different pathways in ataxia-telangiectasia cells. Oncogene *8*, 3307-3312.

Kim, K.M., Cho, H., Choi, K., Kim, J., Kim, B.W., Ko, Y.G., Jang, S.K., and Kim, Y.K. (2009). A new MIF4G domain-containing protein, CTIF, directs nuclear cap-binding protein CBP80/20-dependent translation. Genes Dev *23*, 2033-2045.

Kim Sh, S.H., Kaminker, P., and Campisi, J. (2002). Telomeres, aging and cancer: in search of a happy ending. Oncogene *21*, 503-511.

Kim, V.N., Yong, J., Kataoka, N., Abel, L., Diem, M.D., and Dreyfuss, G. (2001). The Y14 protein communicates to the cytoplasm the position of exon-exon junctions. EMBO J *20*, 2062-2068.

Kim, Y.K., Furic, L., Desgroseillers, L., and Maquat, L.E. (2005). Mammalian Staufen1 recruits Upf1 to specific mRNA 3'UTRs so as to elicit mRNA decay. Cell *120*, 195-208.

Kim, Y.K., Furic, L., Parisien, M., Major, F., DesGroseillers, L., and Maquat, L.E. (2007). Staufen1 regulates diverse classes of mammalian transcripts. EMBO J *26*, 2670-2681.

Koseoglu, M.M., Dong, J., and Marzluff, W.F. (2010). Coordinate regulation of histone mRNA metabolism and DNA replication: cyclin A/cdk1 is involved in inactivation of histone mRNA metabolism and DNA replication at the end of S phase. Cell Cycle *9*, 3857-3863.

Krakoff, I.H., Brown, N.C., and Reichard, P. (1968). Inhibition of ribonucleoside diphosphate reductase by hydroxyurea. Cancer Res *28*, 1559-1565.

Kumagai, A., and Dunphy, W.G. (2000). Claspin, a novel protein required for the activation of Chk1 during a DNA replication checkpoint response in Xenopus egg extracts. Mol Cell *6*, 839-849.

Kurose, A., Tanaka, T., Huang, X., Traganos, F., Dai, W., and Darzynkiewicz, Z. (2006). Effects of hydroxyurea and aphidicolin on phosphorylation of ataxia telangiectasia mutated on Ser 1981 and histone H2AX on Ser 139 in relation to cell cycle phase and induction of apoptosis. Cytometry A *69*, 212-221.

Labib, K., and Hodgson, B. (2007). Replication fork barriers: pausing for a break or stalling for time? EMBO Rep *8*, 346-353.

Laemmli, U.K. (1970). Cleavage of structural proteins during the assembly of the head of bacteriophage T4. Nature *227*, 680-685.

Larionov, A., Krause, A., and Miller, W. (2005). A standard curve based method for relative real time PCR data processing. BMC Bioinformatics *6*, 62.

Le Hir, H., Izaurralde, E., Maquat, L.E., and Moore, M.J. (2000). The spliceosome deposits multiple proteins 20-24 nucleotides upstream of mRNA exon-exon junctions. EMBO J *19*, 6860-6869.

Le, P.N., Maranon, D.G., Altina, N.H., Battaglia, C.L., and Bailey, S.M. (2013). TERRA, hnRNP A1, and DNA-PKcs Interactions at Human Telomeres. Front Oncol *3*, 91.

LeBlanc, J.J., and Beemon, K.L. (2004). Unspliced Rous sarcoma virus genomic RNAs are translated and subjected to nonsense-mediated mRNA decay before packaging. J Virol *78*, 5139-5146.

Leeds, P., Peltz, S.W., Jacobson, A., and Culbertson, M.R. (1991). The product of the yeast UPF1 gene is required for rapid turnover of mRNAs containing a premature translational termination codon. Genes Dev *5*, 2303-2314.

Leeds, P., Wood, J.M., Lee, B.S., and Culbertson, M.R. (1992). Gene products that promote mRNA turnover in Saccharomyces cerevisiae. Mol Cell Biol *12*, 2165-2177.

Lees-Miller, S.P., Sakaguchi, K., Ullrich, S.J., Appella, E., and Anderson, C.W. (1992). Human DNA-activated protein kinase phosphorylates serines 15 and 37 in the amino-terminal transactivation domain of human p53. Mol Cell Biol *12*, 5041-5049.

Lehner, B., and Sanderson, C.M. (2004). A protein interaction framework for human mRNA degradation. Genome Res *14*, 1315-1323.

Lejeune, F., Ishigaki, Y., Li, X., and Maquat, L.E. (2002). The exon junction complex is detected on CBP80-bound but not eIF4E-bound mRNA in mammalian cells: dynamics of mRNP remodeling. EMBO J *21*, 3536-3545.

Lejeune, F., Li, X., and Maquat, L.E. (2003). Nonsense-mediated mRNA decay in mammalian cells involves decapping, deadenylating, and exonucleolytic activities. Mol Cell *12*, 675-687.

Lejeune, F., Ranganathan, A.C., and Maquat, L.E. (2004). eIF4G is required for the pioneer round of translation in mammalian cells. Nat Struct Mol Biol *11*, 992-1000.

Lew, J.E., Enomoto, S., and Berman, J. (1998). Telomere length regulation and telomeric chromatin require the nonsense-mediated mRNA decay pathway. Mol Cell Biol *18*, 6121-6130.

Li, M., Fu, W., Wo, L., Shu, X., Liu, F., and Li, C. (2013). miR-128 and its target genes in tumorigenesis and metastasis. Exp Cell Res.

Li, X., Tan, C.K., So, A.G., and Downey, K.M. (1992). Purification and characterization of delta helicase from fetal calf thymus. Biochemistry *31*, 3507-3513.

Lim, S.C., Bowler, M.W., Lai, T.F., and Song, H. (2012). The Ighmbp2 helicase structure reveals the molecular basis for disease-causing mutations in DMSA1. Nucleic Acids Res *40*, 11009-11022.

Lin, K.W., and Yan, J. (2008). Endings in the middle: current knowledge of interstitial telomeric sequences. Mutat Res *658*, 95-110.

Linde, L., and Kerem, B. (2011). Nonsense-mediated mRNA decay and cystic fibrosis. Methods Mol Biol *741*, 137-154.

Liu, K., Hodes, R.J., and Weng, N. (2001). Cutting edge: telomerase activation in human T lymphocytes does not require increase in telomerase reverse transcriptase (hTERT) protein but is associated with hTERT phosphorylation and nuclear translocation. J Immunol *166*, 4826-4830.

Loh, B., Jonas, S., and Izaurralde, E. (2013). The SMG5-SMG7 heterodimer directly recruits the CCR4-NOT deadenylase complex to mRNAs containing nonsense codons via interaction with POP2. Genes Dev *27*, 2125-2138.

Long, A.A., Mahapatra, C.T., Woodruff, E.A., 3rd, Rohrbough, J., Leung, H.T., Shino, S., An, L., Doerge, R.W., Metzstein, M.M., Pak, W.L.*, et al.* (2010). The nonsense-mediated decay pathway maintains synapse architecture and synaptic vesicle cycle efficacy. J Cell Sci *123*, 3303-3315.

Lopez-Contreras, A.J., and Fernandez-Capetillo, O. (2010). The ATR barrier to replication-born DNA damage. DNA Repair (Amst) *9*, 1249-1255.

Lormand, J.D., Buncher, N., Murphy, C.T., Kaur, P., Lee, M.Y., Burgers, P., Wang, H., Kunkel, T.A., and Opresko, P.L. (2013). DNA polymerase delta stalls on telomeric lagging strand templates independently from G-quadruplex formation. Nucleic Acids Res.

Luke, B., and Lingner, J. (2009). TERRA: telomeric repeat-containing RNA. EMBO J *28*, 2503-2510.

Luke, B., Panza, A., Redon, S., Iglesias, N., Li, Z., and Lingner, J. (2008). The Rat1p 5' to 3' exonuclease degrades telomeric repeat-containing RNA and promotes telomere elongation in Saccharomyces cerevisiae. Mol Cell *32*, 465-477.

Lykke-Andersen, J. (2002). Identification of a human decapping complex associated with hUpf proteins in nonsense-mediated decay. Mol Cell Biol *22*, 8114-8121.

Lykke-Andersen, J., Shu, M.D., and Steitz, J.A. (2000). Human Upf proteins target an mRNA for nonsense-mediated decay when bound downstream of a termination codon. Cell *103*, 1121-1131.

Lykke-Andersen, J., Shu, M.D., and Steitz, J.A. (2001). Communication of the position of exon-exon junctions to the mRNA surveillance machinery by the protein RNPS1. Science *293*, 1836-1839.

Ma, H.T., and Poon, R.Y. (2011). Synchronization of HeLa cells. Methods Mol Biol *761*, 151-161.

Maderazo, A.B., Belk, J.P., He, F., and Jacobson, A. (2003). Nonsense-containing mRNAs that accumulate in the absence of a functional nonsense-mediated mRNA decay pathway are destabilized rapidly upon its restitution. Mol Cell Biol *23*, 842-851.

Maicher, A., Kastner, L., Dees, M., and Luke, B. (2012). Deregulated telomere transcription causes replication-dependent telomere shortening and promotes cellular senescence. Nucleic Acids Res *40*, 6649-6659.

Malik, V., Rodino-Klapac, L.R., Viollet, L., and Mendell, J.R. (2010). Aminoglycoside-induced mutation suppression (stop codon readthrough) as a therapeutic strategy for Duchenne muscular dystrophy. Ther Adv Neurol Disord *3*, 379-389.

Maquat, L.E. (2005). Nonsense-mediated mRNA decay in mammals. J Cell Sci *118*, 1773-1776.

Maquat, L.E., Tarn, W.Y., and Isken, O. (2010). The pioneer round of translation: features and functions. Cell *142*, 368-374.

Martadinata, H., and Phan, A.T. (2009). Structure of propeller-type parallel-stranded RNA G-quadruplexes, formed by human telomeric RNA sequences in K+ solution. J Am Chem Soc *131*, 2570-2578.

Martin, F., Schaller, A., Eglite, S., Schumperli, D., and Muller, B. (1997). The gene for histone RNA hairpin binding protein is located on human chromosome 4 and encodes a novel type of RNA binding protein. EMBO J *16*, 769-778.

Martinez, P., Thanasoula, M., Munoz, P., Liao, C., Tejera, A., McNees, C., Flores, J.M., Fernandez-Capetillo, O., Tarsounas, M., and Blasco, M.A. (2009). Increased telomere fragility and fusions resulting from TRF1 deficiency lead to degenerative pathologies and increased cancer in mice. Genes Dev *23*, 2060-2075.

Marzluff, W.F., and Duronio, R.J. (2002). Histone mRNA expression: multiple levels of cell cycle regulation and important developmental consequences. Curr Opin Cell Biol *14*, 692-699.

Mascarenhas, R., Dougherty, J.A., and Schoenberg, D.R. (2013). SMG6 Cleavage Generates Metastable Decay Intermediates from Nonsense-Containing beta-Globin mRNA. PLoS One *8*, e74791.

Matsuoka, S., Huang, M., and Elledge, S.J. (1998). Linkage of ATM to cell cycle regulation by the Chk2 protein kinase. Science *282*, 1893-1897.

Mayer, B.J. (2001). SH3 domains: complexity in moderation. J Cell Sci *114*, 1253-1263.

McGlincy, N.J., Tan, L.Y., Paul, N., Zavolan, M., Lilley, K.S., and Smith, C.W. (2010). Expression proteomics of UPF1 knockdown in HeLa cells reveals autoregulation of hnRNP A2/B1 mediated by alternative splicing resulting in nonsense-mediated mRNA decay. BMC Genomics *11*, 565.

McIlwain, D.R., Pan, Q., Reilly, P.T., Elia, A.J., McCracken, S., Wakeham, A.C., Itie-Youten, A., Blencowe, B.J., and Mak, T.W. (2010). Smg1 is required for embryogenesis and regulates diverse genes via alternative splicing coupled to nonsense-mediated mRNA decay. Proc Natl Acad Sci U S A *107*, 12186-12191.

McIvor, E.I., Polak, U., and Napierala, M. (2010). New insights into repeat instability: role of RNA*DNA hybrids. RNA Biol *7*, 551-558.

Medghalchi, S.M., Frischmeyer, P.A., Mendell, J.T., Kelly, A.G., Lawler, A.M., and Dietz, H.C. (2001). Rent1, a trans-effector of nonsense-mediated mRNA decay, is essential for mammalian embryonic viability. Hum Mol Genet *10*, 99-105.

Meeks-Wagner, D., and Hartwell, L.H. (1986). Normal stoichiometry of histone dimer sets is necessary for high fidelity of mitotic chromosome transmission. Cell *44*, 43-52.

Mendell, J.T., ap Rhys, C.M., and Dietz, H.C. (2002). Separable roles for rent1/hUpf1 in altered splicing and decay of nonsense transcripts. Science *298*, 419-422.

Mendell, J.T., Sharifi, N.A., Meyers, J.L., Martinez-Murillo, F., and Dietz, H.C. (2004). Nonsense surveillance regulates expression of diverse classes of mammalian transcripts and mutes genomic noise. Nat Genet *36*, 1073-1078.

Mendez, J., and Stillman, B. (2000). Chromatin association of human origin recognition complex, cdc6, and minichromosome maintenance proteins during the cell cycle: assembly of prereplication complexes in late mitosis. Mol Cell Biol *20*, 8602-8612.

Metzstein, M.M., and Krasnow, M.A. (2006). Functions of the nonsense-mediated mRNA decay pathway in Drosophila development. PLoS Genet *2*, e180.

Michel, F., Schumperli, D., and Muller, B. (2000). Specificities of Caenorhabditis elegans and human hairpin binding proteins for the first nucleotide in the histone mRNA hairpin loop. RNA *6*, 1539-1550.

Mignon-Ravix, C., Depetris, D., Delobel, B., Croquette, M.F., and Mattei, M.G. (2002). A human interstitial telomere associates in vivo with specific TRF2 and TIN2 proteins. Eur J Hum Genet *10*, 107-112.

Miki, Y., Swensen, J., Shattuck-Eidens, D., Futreal, P.A., Harshman, K., Tavtigian, S., Liu, Q., Cochran, C., Bennett, L.M., Ding, W.*, et al.* (1994). A strong candidate for the breast and ovarian cancer susceptibility gene BRCA1. Science *266*, 66-71.

Miller, J.H. (1972). Experiments in Molecular Genetics (Cold Spring Harbor Laboratory Press).

Monnat, R.J., Jr., and Saintigny, Y. (2004). Werner syndrome protein--unwinding function to explain disease. Sci Aging Knowledge Environ *2004*, re3.

Mordes, D.A., and Cortez, D. (2008). Activation of ATR and related PIKKs. Cell Cycle *7*, 2809-2812.

Moriarty, P.M., Reddy, C.C., and Maquat, L.E. (1998). Selenium deficiency reduces the abundance of mRNA for Se-dependent glutathione peroxidase 1 by a UGA-dependent mechanism likely to be nonsense codon-mediated decay of cytoplasmic mRNA. Mol Cell Biol *18*, 2932-2939.

Moriniere, M., Delhommeau, F., Calender, A., Ribeiro, L., Delaunay, J., and Baklouti, F. (2010). Nonsense-mediated mRNA decay (NMD) blockage promotes nonsense mRNA stabilization in protein 4.1R deficient cells carrying the 4.1R Coimbra variant of hereditary elliptocytosis. Blood Cells Mol Dis *45*, 284-288.

Moser, B.A., Subramanian, L., Chang, Y.T., Noguchi, C., Noguchi, E., and Nakamura, T.M. (2009). Differential arrival of leading and lagging strand DNA polymerases at fission yeast telomeres. EMBO J *28*, 810-820.

Moyzis, R.K., Buckingham, J.M., Cram, L.S., Dani, M., Deaven, L.L., Jones, M.D., Meyne, J., Ratliff, R.L., and Wu, J.R. (1988). A highly conserved repetitive DNA sequence, (TTAGGG)n, present at the telomeres of human chromosomes. Proc Natl Acad Sci U S A *85*, 6622-6626.

Mueller, D.L., Jenkins, M.K., and Schwartz, R.H. (1989). Clonal expansion versus functional clonal inactivation: a costimulatory signalling pathway determines the outcome of T cell antigen receptor occupancy. Annu Rev Immunol *7*, 445-480.

Mullen, T.E., and Marzluff, W.F. (2008). Degradation of histone mRNA requires oligouridylation followed by decapping and simultaneous degradation of the mRNA both 5' to 3' and 3' to 5'. Genes Dev *22*, 50-65.

Muller, B., Blackburn, J., Feijoo, C., Zhao, X., and Smythe, C. (2007a). Are multiple checkpoint mediators involved in a checkpoint linking histone gene expression with DNA replication? Biochem Soc Trans *35*, 1369-1371.

Muller, B., Blackburn, J., Feijoo, C., Zhao, X., and Smythe, C. (2007b). DNA-activated protein kinase functions in a newly observed S phase checkpoint that links histone mRNA abundance with DNA replication. J Cell Biol *179*, 1385-1398.

Nagy, E., and Maquat, L.E. (1998). A rule for termination-codon position within intron-containing genes: when nonsense affects RNA abundance. Trends Biochem Sci *23*, 198-199.

Nakamura, A.J., Chiang, Y.J., Hathcock, K.S., Horikawa, I., Sedelnikova, O.A., Hodes, R.J., and Bonner, W.M. (2008). Both telomeric and non-telomeric DNA damage are determinants of mammalian cellular senescence. Epigenetics Chromatin *1*, 6.

Nandakumar, J., and Cech, T.R. (2013). Finding the end: recruitment of telomerase to telomeres. Nat Rev Mol Cell Biol *14*, 69-82.

Negrini, S., Gorgoulis, V.G., and Halazonetis, T.D. (2010). Genomic instability--an evolving hallmark of cancer. Nat Rev Mol Cell Biol *11*, 220-228.

Nishino, M., Ashiku, S.K., Kocher, O.N., Thurer, R.L., Boiselle, P.M., and Hatabu, H. (2006). The thymus: a comprehensive review. Radiographics *26*, 335-348.

Ohnishi, T., Yamashita, A., Kashima, I., Schell, T., Anders, K.R., Grimson, A., Hachiya, T., Hentze, M.W., Anderson, P., and Ohno, S. (2003). Phosphorylation of hUPF1 induces formation of mRNA surveillance complexes containing hSMG-5 and hSMG-7. Mol Cell *12*, 1187-1200.

Okada-Katsuhata, Y., Yamashita, A., Kutsuzawa, K., Izumi, N., Hirahara, F., and Ohno, S. (2012). N- and C-terminal Upf1 phosphorylations create binding platforms for SMG-6 and SMG-5:SMG-7 during NMD. Nucleic Acids Res *40*, 1251-1266.

Olovnikov, A.M. (1973). A theory of marginotomy. The incomplete copying of template margin in enzymic synthesis of polynucleotides and biological significance of the phenomenon. J Theor Biol *41*, 181-190.

Pal, M., Ishigaki, Y., Nagy, E., and Maquat, L.E. (2001). Evidence that phosphorylation of human Upfl protein varies with intracellular location and is mediated by a wortmannin-sensitive and rapamycin-sensitive PI 3-kinase-related kinase signaling pathway. RNA *7*, 5-15.

Park, E., Gleghorn, M.L., and Maquat, L.E. (2012). Staufen2 functions in Staufen1-mediated mRNA decay by binding to itself and its paralog and promoting UPF1 helicase but not ATPase activity. Proc Natl Acad Sci U S A.

Peltz, S.W., Morsy, M., Welch, E.M., and Jacobson, A. (2013). Ataluren as an agent for therapeutic nonsense suppression. Annu Rev Med *64*, 407-425.

Perlick, H.A., Medghalchi, S.M., Spencer, F.A., Kendzior, R.J., Jr., and Dietz, H.C. (1996). Mammalian orthologues of a yeast regulator of nonsense transcript stability. Proc Natl Acad Sci U S A *93*, 10928-10932.

Pettitt, J., Crombie, C., Schumperli, D., and Muller, B. (2002). The Caenorhabditis elegans histone hairpin-binding protein is required for core histone gene expression and is essential for embryonic and postembryonic cell division. J Cell Sci *115*, 857-866.

Pines, J. (1995). Cyclins and cyclin-dependent kinases: a biochemical view. Biochem J *308 (Pt 3)*, 697-711.

Pirzio, L.M., Pichierri, P., Bignami, M., and Franchitto, A. (2008). Werner syndrome helicase activity is essential in maintaining fragile site stability. J Cell Biol *180*, 305-314.

Podust, V.N., Podust, L.M., Muller, F., and Hubscher, U. (1995). DNA polymerase delta holoenzyme: action on single-stranded DNA and on double-stranded DNA in the presence of replicative DNA helicases. Biochemistry *34*, 5003-5010.

Pohler, J.R., Otterlei, M., and Warbrick, E. (2005). An in vivo analysis of the localisation and interactions of human p66 DNA polymerase delta subunit. BMC Mol Biol *6*, 17.

Porro, A., Feuerhahn, S., Reichenbach, P., and Lingner, J. (2010). Molecular dissection of telomeric repeat-containing RNA biogenesis unveils the presence of distinct and multiple regulatory pathways. Mol Cell Biol *30*, 4808-4817.

Pulak, R., and Anderson, P. (1993). mRNA surveillance by the Caenorhabditis elegans smg genes. Genes Dev *7*, 1885-1897.

Randall, A., and Griffith, J.D. (2009). Structure of long telomeric RNA transcripts: the G-rich RNA forms a compact repeating structure containing G-quartets. J Biol Chem *284*, 13980-13986.

Rattray, A.M., Nicholson, P., and Muller, B. (2013). Replication stress-induced alternative mRNA splicing alters properties of the histone RNA-binding protein HBP/SLBP: a key factor in the control of histone gene expression. Biosci Rep *33*.

Redon, S., Reichenbach, P., and Lingner, J. (2007). Protein RNA and protein protein interactions mediate association of human EST1A/SMG6 with telomerase. Nucleic Acids Res *35*, 7011-7022.

Redon, S., Reichenbach, P., and Lingner, J. (2010). The non-coding RNA TERRA is a natural ligand and direct inhibitor of human telomerase. Nucleic Acids Res *38*, 5797-5806.

Redon, S., Zemp, I., and Lingner, J. (2013). A three-state model for the regulation of telomerase by TERRA and hnRNPA1. Nucleic Acids Res *41*, 9117-9128.

Reichenbach, P., Hoss, M., Azzalin, C.M., Nabholz, M., Bucher, P., and Lingner, J. (2003). A human homolog of yeast Est1 associates with telomerase and uncaps chromosome ends when overexpressed. Curr Biol *13*, 568-574.

Rieder, C.L., and Palazzo, R.E. (1992). Colcemid and the mitotic cycle. J Cell Sci *102 (Pt 3)*, 387-392.

Rizzo, A., Salvati, E., Porru, M., D'Angelo, C., Stevens, M.F., D'Incalci, M., Leonetti, C., Gilson, E., Zupi, G., and Biroccio, A. (2009). Stabilization of quadruplex DNA perturbs telomere replication leading to the activation of an ATR-dependent ATM signaling pathway. Nucleic Acids Res *37*, 5353-5364.

Roy, A., Kucukural, A., and Zhang, Y. (2010). I-TASSER: a unified platform for automated protein structure and function prediction. Nat Protoc *5*, 725-738.

Roy, A., Yang, J., and Zhang, Y. (2012). COFACTOR: an accurate comparative algorithm for structure-based protein function annotation. Nucleic Acids Res *40*, W471-477.

Rufener, S.C., and Muhlemann, O. (2013). eIF4E-bound mRNPs are substrates for nonsense-mediated mRNA decay in mammalian cells. Nat Struct Mol Biol *20*, 710-717.

Sadhu, K., Reed, S.I., Richardson, H., and Russell, P. (1990). Human homolog of fission yeast cdc25 mitotic inducer is predominantly expressed in G2. Proc Natl Acad Sci U S A *87*, 5139-5143.

Sancar, A., Lindsey-Boltz, L.A., Unsal-Kacmaz, K., and Linn, S. (2004). Molecular mechanisms of mammalian DNA repair and the DNA damage checkpoints. Annu Rev Biochem *73*, 39-85.

Sato, N., Arai, K., and Masai, H. (1997). Human and Xenopus cDNAs encoding budding yeast Cdc7-related kinases: in vitro phosphorylation of MCM subunits by a putative human homologue of Cdc7. EMBO J *16*, 4340-4351.

Savitsky, K., Bar-Shira, A., Gilad, S., Rotman, G., Ziv, Y., Vanagaite, L., Tagle, D.A., Smith, S., Uziel, T., Sfez, S*., et al.* (1995). A single ataxia telangiectasia gene with a product similar to PI-3 kinase. Science *268*, 1749-1753.

Schoeftner, S., and Blasco, M.A. (2008). Developmentally regulated transcription of mammalian telomeres by DNA-dependent RNA polymerase II. Nat Cell Biol *10*, 228-236.

Schweingruber, C., Rufener, S.C., Zund, D., Yamashita, A., and Muhlemann, O. (2013). Nonsense-mediated mRNA decay - mechanisms of substrate mRNA recognition and degradation in mammalian cells. Biochim Biophys Acta *1829*, 612-623.

Serquina, A.K., Das, S.R., Popova, E., Ojelabi, O.A., Roy, C.K., and Gottlinger, H.G. (2013). UPF1 Is Crucial for the Infectivity of Human Immunodeficiency Virus Type 1 Progeny Virions. J Virol *87*, 8853-8861.

Sfeir, A., Kosiyatrakul, S.T., Hockemeyer, D., MacRae, S.L., Karlseder, J., Schildkraut, C.L., and de Lange, T. (2009). Mammalian telomeres resemble fragile sites and require TRF1 for efficient replication. Cell *138*, 90-103.

Shay, J.W., and Wright, W.E. (2004). Telomeres are double-strand DNA breaks hidden from DNA damage responses. Mol Cell *14*, 420-421.

Shay, J.W., and Wright, W.E. (2005). Senescence and immortalization: role of telomeres and telomerase. Carcinogenesis *26*, 867-874.

Singh, G., Jakob, S., Kleedehn, M.G., and Lykke-Andersen, J. (2007). Communication with the exon-junction complex and activation of nonsense-mediated decay by human Upf proteins occur in the cytoplasm. Mol Cell *27*, 780-792.

Sittman, D.B., Graves, R.A., and Marzluff, W.F. (1983). Histone mRNA concentrations are regulated at the level of transcription and mRNA degradation. Proc Natl Acad Sci U S A *80*, 1849-1853.

Smith, G.C., Cary, R.B., Lakin, N.D., Hann, B.C., Teo, S.H., Chen, D.J., and Jackson, S.P. (1999). Purification and DNA binding properties of the ataxia-telangiectasia gene product ATM. Proc Natl Acad Sci U S A *96*, 11134-11139.

Snow, B.E., Erdmann, N., Cruickshank, J., Goldman, H., Gill, R.M., Robinson, M.O., and Harrington, L. (2003). Functional conservation of the telomerase protein Est1p in humans. Curr Biol *13*, 698-704.

Speicher, M.R., Gwyn Ballard, S., and Ward, D.C. (1996). Karyotyping human chromosomes by combinatorial multi-fluor FISH. Nat Genet *12*, 368-375.

Stalder, L., and Muhlemann, O. (2009). Processing bodies are not required for mammalian nonsense-mediated mRNA decay. RNA *15*, 1265-1273.

Steinert, P.M., Mack, J.W., Korge, B.P., Gan, S.Q., Haynes, S.R., and Steven, A.C. (1991). Glycine loops in proteins: their occurrence in certain intermediate filament chains, loricrins and single-stranded RNA binding proteins. Int J Biol Macromol *13*, 130-139.

Stewart, G.S., Wang, B., Bignell, C.R., Taylor, A.M., and Elledge, S.J. (2003). MDC1 is a mediator of the mammalian DNA damage checkpoint. Nature *421*, 961-966.

Su, W., Slepenkov, S.V., Slevin, M.K., Lyons, S.M., Ziemniak, M., Kowalska, J., Darzynkiewicz, E., Jemielity, J., Marzluff, W.F., and Rhoads, R.E. (2013). mRNAs containing the histone 3' stem-loop are degraded primarily by decapping mediated by oligouridylation of the 3' end. RNA *19*, 1-16.

Sullivan, K.D., Mullen, T.E., Marzluff, W.F., and Wagner, E.J. (2009). Knockdown of SLBP results in nuclear retention of histone mRNA. RNA *15*, 459-472.

Sun, X., Perlick, H.A., Dietz, H.C., and Maquat, L.E. (1998). A mutated human homologue to yeast Upf1 protein has a dominant-negative effect on the decay of nonsense-containing mRNAs in mammalian cells. Proc Natl Acad Sci U S A *95*, 10009-10014.

Suraweera, A., Lim, Y., Woods, R., Birrell, G.W., Nasim, T., Becherel, O.J., and Lavin, M.F. (2009). Functional role for senataxin, defective in ataxia oculomotor apraxia type 2, in transcriptional regulation. Hum Mol Genet *18*, 3384-3396.

Szabo, C.I., Worley, T., and Monteiro, A.N. (2004). Understanding germ-line mutations in BRCA1. Cancer Biol Ther *3*, 515-520.

Tarpey, P.S., Raymond, F.L., Nguyen, L.S., Rodriguez, J., Hackett, A., Vandeleur, L., Smith, R., Shoubridge, C., Edkins, S., Stevens, C.*, et al.* (2007). Mutations in UPF3B, a member of the nonsense-mediated mRNA decay complex, cause syndromic and nonsyndromic mental retardation. Nat Genet *39*, 1127-1133.

Trcek, T., Sato, H., Singer, R.H., and Maquat, L.E. (2013). Temporal and spatial characterization of nonsense-mediated mRNA decay. Genes Dev *27*, 541-551.

Ubersax, J.A., and Ferrell, J.E., Jr. (2007). Mechanisms of specificity in protein phosphorylation. Nat Rev Mol Cell Biol *8*, 530-541.

Unterholzner, L., and Izaurralde, E. (2004). SMG7 acts as a molecular link between mRNA surveillance and mRNA decay. Mol Cell *16*, 587-596.

Usuki, F., Yamashita, A., Higuchi, I., Ohnishi, T., Shiraishi, T., Osame, M., and Ohno, S. (2004). Inhibition of nonsense-mediated mRNA decay rescues the phenotype in Ullrich's disease. Ann Neurol *55*, 740-744.

Vallon-Christersson, J., Cayanan, C., Haraldsson, K., Loman, N., Bergthorsson, J.T., Brondum-Nielsen, K., Gerdes, A.M., Moller, P., Kristoffersson, U., Olsson, H.*, et al.* (2001). Functional analysis of BRCA1 C-terminal missense mutations identified in breast and ovarian cancer families. Hum Mol Genet *10*, 353-360.

Verdun, R.E., Crabbe, L., Haggblom, C., and Karlseder, J. (2005). Functional human telomeres are recognized as DNA damage in G2 of the cell cycle. Mol Cell *20*, 551-561.

Verdun, R.E., and Karlseder, J. (2006). The DNA damage machinery and homologous recombination pathway act consecutively to protect human telomeres. Cell *127*, 709-720.

Wang, D., Zavadil, J., Martin, L., Parisi, F., Friedman, E., Levy, D., Harding, H., Ron, D., and Gardner, L.B. (2011). Inhibition of nonsense-mediated RNA decay by the tumor microenvironment promotes tumorigenesis. Mol Cell Biol *31*, 3670-3680.

Wang, Z.F., Whitfield, M.L., Ingledue, T.C., 3rd, Dominski, Z., and Marzluff, W.F. (1996). The protein that binds the 3' end of histone mRNA: a novel RNA-binding protein required for histone pre-mRNA processing. Genes Dev *10*, 3028-3040.

Weischenfeldt, J., Damgaard, I., Bryder, D., Theilgaard-Monch, K., Thoren, L.A., Nielsen, F.C., Jacobsen, S.E., Nerlov, C., and Porse, B.T. (2008). NMD is essential for hematopoietic stem and progenitor cells and for eliminating by-products of programmed DNA rearrangements. Genes Dev *22*, 1381-1396.

Wengrod, J., Martin, L., Wang, D., Frischmeyer-Guerrerio, P., Dietz, H.C., and Gardner, L.B. (2013). Inhibition of nonsense-mediated RNA decay activates autophagy. Mol Cell Biol *33*, 2128-2135.

Wittkopp, N., Huntzinger, E., Weiler, C., Sauliere, J., Schmidt, S., Sonawane, M., and Izaurralde, E. (2009). Nonsense-mediated mRNA decay effectors are essential for zebrafish embryonic development and survival. Mol Cell Biol *29*, 3517-3528.

Wittmann, J., Hol, E.M., and Jack, H.M. (2006). hUPF2 silencing identifies physiologic substrates of mammalian nonsense-mediated mRNA decay. Mol Cell Biol *26*, 1272-1287.

Wyatt, H.R., Liaw, H., Green, G.R., and Lustig, A.J. (2003). Multiple roles for Saccharomyces cerevisiae histone H2A in telomere position effect, Spt phenotypes and double-strand-break repair. Genetics *164*, 47-64.

Xu, W.Y., Gu, M.M., Sun, L.H., Guo, W.T., Zhu, H.B., Ma, J.F., Yuan, W.T., Kuang, Y., Ji, B.J., Wu, X.L*., et al.* (2012). A nonsense mutation in DHTKD1 causes Charcot-Marie-Tooth disease type 2 in a large Chinese pedigree. Am J Hum Genet *91*, 1088-1094.

Xu, Y., Kaminaga, K., and Komiyama, M. (2008a). G-quadruplex formation by human telomeric repeats-containing RNA in Na+ solution. J Am Chem Soc *130*, 11179-11184.

Xu, Y., Kimura, T., and Komiyama, M. (2008b). Human telomere RNA and DNA form an intermolecular G-quadruplex. Nucleic Acids Symp Ser (Oxf), 169-170.

Xu, Y., Suzuki, Y., Ito, K., and Komiyama, M. (2010). Telomeric repeat-containing RNA structure in living cells. Proc Natl Acad Sci U S A *107*, 14579-14584.

Yamashita, A., Izumi, N., Kashima, I., Ohnishi, T., Saari, B., Katsuhata, Y., Muramatsu, R., Morita, T., Iwamatsu, A., Hachiya, T*., et al.* (2009). SMG-8 and SMG-9, two novel subunits of the SMG-1 complex, regulate remodeling of the mRNA surveillance complex during nonsense-mediated mRNA decay. Genes Dev *23*, 1091-1105.

Yamashita, A., Ohnishi, T., Kashima, I., Taya, Y., and Ohno, S. (2001). Human SMG-1, a novel phosphatidylinositol 3-kinase-related protein kinase, associates with components of the mRNA surveillance complex and is involved in the regulation of nonsense-mediated mRNA decay. Genes Dev *15*, 2215-2228.

Yang, C., Strobel, P., Marx, A., and Hofmann, I. (2013). Plakophilin-associated RNA-binding proteins in prostate cancer and their implications in tumor progression and metastasis. Virchows Arch.

Yehezkel, S., Segev, Y., Viegas-Pequignot, E., Skorecki, K., and Selig, S. (2008). Hypomethylation of subtelomeric regions in ICF syndrome is associated with abnormally short telomeres and enhanced transcription from telomeric regions. Hum Mol Genet *17*, 2776-2789.

Yepiskoposyan, H., Aeschimann, F., Nilsson, D., Okoniewski, M., and Muhlemann, O. (2011). Autoregulation of the nonsense-mediated mRNA decay pathway in human cells. RNA *17*, 2108-2118.

Zakut-Houri, R., Bienz-Tadmor, B., Givol, D., and Oren, M. (1985). Human p53 cellular tumor antigen: cDNA sequence and expression in COS cells. EMBO J *4*, 1251-1255.

Zhang, Y. (2008). I-TASSER server for protein 3D structure prediction. BMC Bioinformatics *9*, 40.

Zhao, X., McKillop-Smith, S., and Muller, B. (2004). The human histone gene expression regulator HBP/SLBP is required for histone and DNA synthesis, cell cycle progression and cell proliferation in mitotic cells. J Cell Sci *117*, 6043-6051.

Zheng, L., Dominski, Z., Yang, X.C., Elms, P., Raska, C.S., Borchers, C.H., and Marzluff, W.F. (2003). Phosphorylation of stem-loop binding protein (SLBP) on two threonines triggers degradation of SLBP, the sole cell cycle-regulated factor required for regulation of histone mRNA processing, at the end of S phase. Mol Cell Biol *23*, 1590-1601.